River modeling for control tasks in water systems

Dissertation
Zur Erlangung des akademischen Grades
Doktor-Ingenieur (Dr.-Ing.)

vorgelegt der
Fakultät für Informatik und Automatisierung
der Technischen Universität Ilmenau

von

Msc. Long Duc Nguyen

Gutachter:

1. Prof. Dr.-Ing. habil. Thomas Rauschenbach
2. Prof. Dr.-Ing. habil. Pu Li
3. Prof. Dr.rer. nat. Lars Ribbe

Tag der Einreichung: 26.6.2017
Tag der wissenschaftlichen Aussprache: 14.2.2018
urn:nbn:de:gbv:ilm1-2018000056

Acknowledgments

First and foremost, I would like to send a special thank the Ministry of Agriculture and Rural Development (MARD) and the Deutscher Akademischer Austauschdienst (DAAD) for the scholarship that they provided to me, that offered the chance to expand my knowledge, broaden my mind and widen my personal horizon. I would also like to thank Fraunhofer Institute IOSB-AST for giving me a comfort working space and consistent support during three years of my study.

I would like to express my sincere gratitude to my supervisor Professor Thomas Rauschenbach for the support, guidance and inspiration throughout my research. Many thanks to Professor Pu Li and Professor Lars Ribbe for their time to review my dissertation and give me many advices to improve it. A special thank sends to Dr. Divas Karimanzira for thorough and effective debate during my research. I would also like to thank members in the Surface Water and Mobile System group for sharing knowledge and discussing on my research problems.

I dedicate my work express my biggest gratitude to my parents, for their love and continuous support. Many thanks to my parents in-law, who have continuously encouraged me and helped my wife for four years. I would specially like to thank my beloved wife, Le Thu Ha, for her unconditional love, her patience, and her constant trust in me over years of my study. I knew how hard and difficult you were when you alone look after and educate our children. You always stay behind all my successes and never leave me at the most difficult time. This thesis is devoted for you. Thanks to my beloved daughters, Nguyen Le Bao Han, Nguyen Le Vy and Nguyen Le Anh, for giving me happy time and many efforts to complete the dissertation. Many thanks to my friends (2013 to 2017) for sharing difficulties and joys with me at TU Ilmenau. We are a Ilmenau family. Also, I would like to express my thank to the families: Tung-Thu, Duong-Ha for their supports during my stay in Ilmenau.

Abstract

The Saint Venant Equations (SVEs) are frequently used to describe flow in open channel/river. On the one hand, models based on SVEs require huge data for parameterization as well as large computation time in order to simulate flow behavior. On the other hand, simplified models are an often-chosen technique for model based-control without eliminating the key dynamic attributes. The Adaptive Time Delay model (ATD) expands the application scope of the previous time delay models by simulating the flow using a prismatic trapezoidal geometry. In this approach, the mathematical derivation of the ATD model and the linearized Saint Venant model (SVEs) are defined. The transfer functions of the ATD model and the complex hydraulic model (SVEs) are derived by Laplace transformation. The Taylor expansion technique is used to find cumulants of the two transfer functions and the time constant and time delay of the ATD model as functions of the complex hydraulic model parameters. Another innovation is the coupling of the ATD model with the reservoir model in order to simulate the backwater effect. The reach is fundamentally separated into two parts: upstream uniform flow area and downstream backwater area. The length of both areas is relied on flow rate and downstream condition. The model parameters are thus the functions of both flow rate and the length of the areas. The third contribution of the dissertation is a method to identify parameters of ATD model from a complex hydraulic model. Initially, the typical hydrograph of an extreme flood event is generated by the method of characteristic hydrograph analysis. Secondly, the typical outflow is simulated by the complex hydraulic model to determine the flow behavior. Then those data are used to estimate parameters of ATD model by a optimization technique. The application of the new method is presented by the case study of optimal control of a hydropower plant cascade. The advantage of this is that the ATD model is able to describe the system dynam-

ics. All of extensions are then integrated in the 'WaterLib' tool box by MATLAB SIMULINK for water system simulation.

Zusammenfassung

Die Saint Venant Gleichungen (Englisch: Saint Venant Equations; SVEs) werden sehr häutig eingesetzt, um das Fließverhalten im offenen Kanal / Fluss zu beschreiben. Einerseits benötigen Modelle, die auf den SVEs basieren, sehr viele Daten für die Parametrierung und auch große Rechenzeiten, um das Fließverhalten zu simulieren. Andererseits sind vereinfachte Modelle eine oft angewandte Technik, um komplexe hydrodynamische Modelle für die modellbasierte Steuerung einzusetzen ohne die wichtigsten dynamischen Attribute zu vernachlässigen. Das adaptive Zeitverzögerungsmodell (Englisch: Adaptive Time Delay; ATD) erweitert den Anwendungsbereich des bisher eingesetzten Zeitverzögerungsmodells durch Simulation des Durchflusses mit einer prismatischen Trapezgeometrie. In dieser Arbeit wird die mathematische Herleitung des ATD-Modells aus dem linearisierten Saint Venant-Modell (SVEs) dargestellt. Die Übertragungsfunktionen des ATD-Modells und des komplexen hydraulischen Modells (SVEs) werden mittels Laplace-Transformation abgeleitet. Es wird die Taylor-Reihen-Entwicklung verwendet, um die Kumulanten der beiden Übertragungsfunktionen zu finden, und um daraus die Zeitkonstante und Totzeit des ATD-Modells als Funktionen der komplexen hydraulischen Modellparameter abzuleiten.

Eine weitere Neuerung ist die Kopplung des ATD-Modells mit dem Reservoir-Modell, um den Effekt des Rückstaus zu simulieren. Das Gerinne ist dabei grundsätzlich in zwei Teile unterteilt: der stromaufwärtige gleichförmige Durchflussbereich und der stromabwärtige Rückstaubereich. Die Länge ist abhängig von der Fließgeschwindigkeit und dem stromabwärtigen Zustand. Die Modellparameter sind damit Funktionen sowohl der Fließgeschwindigkeit als auch der Länge der genannten Bereiche. Der dritte Beitrag in dieser Dissertation ist ein Verfahren, um Parameter des ATD-Modells anhand eines komplexen hydraulischen Modells zu identifizieren.

Zunächst wird die typische Hydrographie eines extremen Hochwasserereignisses durch das Verfahren der medianen Hydrographanalyse erzeugt. Zweitens wird der typische Abfluss durch das komplexe Hydraulikmodell simuliert, um das Abflussverhalten zu bestimmen. Dann werden diese Daten verwendet, um Parameter des ATD-Modells durch ein Optimierungsverfahren zu ermitteln. Die Anwendung der neu entwickelten Verfahren wird am Beispiel der optimale Steuerung einer Staustufenkaskade gezeigt. Der Vorteil ist, dass das ATD-Modell die Systemdynamik sehr gut beschreiben kann. Alle Modellerweiterungen, die in dieser Arbeit vorgestellt werden, wurden in die WaterLib Toolbox von der MATLAB SIMULINK zur Simulation von Wassersystemen integriert.

Keywords

Time delay, time constant, flow rate, water level, small hydropower plant, water storage, adaptive time delay model, simulation, optimization

Contents

List of Figures

List of Tables

Nomenclature

Q	flow rate
A	wetted cross sectional area
q	lateral flow per unit length
Δx	spatial interval
Δx	temporal interval
S_f	friction slope
τ	mean shear stress
P	wetted perimeter
V	mean velocity of flow in cross-sectional area
Y	water depth
n	Manning coefficient
S_b	bottom slope
g	gravitational acceleration
L	length of river reach
t	time
x	abscissa
C	celerity
D	diffusion

ϑ	storage
y_c	vertical distance below the free surface to the center of wetted area
ξ	the momentum flux correction factor
υ_{x}	the unit velocity of flow in direction x
υ_{L}	the unit velocity of lateral flow
Γ	complete gamma function
ς	dummy variable
Φ	the angle of the later flow direction and the x direction
Q_0	flow rate at steady uniform condition
$Y_0(x)$	water level at steady uniform condition
f_Q, f_Y	partial derivative of the SVEs equations against Q, Y
ζ	the high order terms
B	the surface width
K	the geometry factor
G	gain
T_c	time constant determining attenuation of flow
T_d	time delay determining lag of flow
Q_{in}	inflow at upstream end
Q_{sim}	simulated flow
Fr	Froude number
λ_1	wave toward upstream
λ_2	wave toward downstream
b	bottom width

m	side slope
y_{sim}	simulated water level
S_L	deviation of the line tangent of the backwater curve to it
y_n	normal depth
T_M	travel time
Z	crest elevation
ZD	dead water level
ZF	flood waring water level
L_u	length of uniform part
L_b	length of backwater part
α, β	coefficients defined in chapter 4
E	energy generated in a duration t
P_t	power generation
ρ	density of water
H	water head
η	overall efficiency of hydropower plant
ψ	reduction factor from difference of water head
F	Force
Mom	Momentum

Abbreviations

ATD	Adaptive Time Delay
ARX	Auto Regressive with Exogenous Input
ANN	Artificial Neural Network
DP	Dynamic Programming
DLCM	Discrete Linear Cascade Model
FDM	Finite Different Method
FEM	Finite Element Method
FVM	Finite Volume Method
ID	Integrator Delay
IDZ	Integrator Delay Zero
IR	Integrator Resonance
LP	Linear Programming
LQ	Linear Quadratic
LQR	Linear Quadratic Regulator
LPA	Linear Parabolic Approximation
LPV	Linear Parameter Varying
LBLR	Linear Backwater Lag and Route
MPC	Model Predictive Control

MDLC	Multi Discrete Linear Cascade
NLP	Nonlinear Programming
NSE	Nash-Sutcliffe Efficiency
TD	Time Delay
PDE	Partial Differential Equations
POD	Proper Orthogonal Decomposition
PBIAS	Percent bias
GA	Genetic Algorithm
SVEs	Saint Venant Equations
SISO	Singe Input Single Output
ODE	Ordinary Differential Equations

Chapter 1

Introduction

1.1 Motivation of the study

River flow modeling plays an important role to solve a variety of problems, for example in water allocation. Rivers do not only supply water for agriculture, domestic use, and industry but also to preserve wildlife environment. Surplus water in rivers causes flood. This natural disaster critically impacts on a large part of the population on earth causing loss of human lives and damage to properties. While, deficiency of water over a long period of time, normally a season or a year, results in drought which has severe affects on agriculture, life expectancy, and the economic performance of countries. Furthermore, the occurrence of the phenomenon are more frequent over the years due to climate change. Hence, a fact is that water source has to be stored and allocated effectively.

The efficient management of a water system brings numerous benefits, such as reliability and resiliency. In terms of navigation, water level monitoring and control are necessary. The lowest water depth must be maintained so that boats can navigate safely. On the other hand, the water level is not allowed to exceed the maximum value so that boats can pass under the bridges. Another type of water system management is reservoir cascade control which is performed to reach multi-objectives: electricity production, flood protection, and so on. Therefore, it is crucial to investigate and simulate the flow dynamics of the distribution system.

Water flow propagation is very significant for hydraulic engineers to develop several methods for its analysis and simulation. The characteristics of physical

phenomena including river morphology, initial condition and flow can be spatially and temporally described by a function of flow rate and water level. In his research, Saint Venant derives a hyperbolic system expressed by partial differential equations to describe the one dimensional flow in open channels (Saint-Venant, 1871). Because of the inexistence of analytical solutions, a wide range of numerical approaches to solve these equations have been developed, such as the method of characteristics, finite difference schemes, finite element schemes, finite volumes schemes, and spectral (finite) volume schemes. Base on this, several software solutions that simulate the flow dynamics exists such as HECRAS, MIKE 11, and SOBEK. These software solutions are able to describe the flow behavior in complex river system with high accuracy, but require an enormous input data as well as huge computation effort.

For practical purposes, numerous efforts have been made to simplify the full SVEs in order to reduce computation time and data demand while ensuring a reasonable result. These include the well-known classical methods such as the Hayami model (Hayami, 1951), Muskingum model (Cunge, 1969), Kalinin-Milyukov method (Apollov et al, 1964) which are usually used to simulate the outflow of a certain river reach quickly. Particularly, reduced models for control purposes are increasingly required and developed in recent years. A few typical models include the Integrator Delay Method (ID) by (Schuurmans et al, 1995, 1999b), Integration Delay Zero (IDZ) by (Litrico and Fromion, 2004a), and the Integrator resonance model (IR) (van Overloop et al, 2010, 2014). Automatic control then is simply implemented based on the model.

The potentials in advancement and applications of the simplified model for modeling water flow in rivers as well as in open channels for controller design propel the work of this dissertation.

1.2 Objectives

This research aims at improving the existing time delay based model so that the model can be used to simulate all hydraulic situations applied in optimal control and a number of improvements includes:

1. Extend the adaptive time delay (ATD) model for prismatic trapezoidal cross

section of channel to simulate narrow natural streams.

2. Develop a new flow routing model with backwater effect by coupling the ATD model with a reservoir model. Then, the ATD model is able to simulate a river with different downstream boundary conditions.

3. Develop a method to determine parameters of the ATD model for a river reach with arbitrary river characteristics. River geometry and geology significantly influences the flow through the roughness coefficient, which consequently influence the time delay and time constant.

4. Prove the applicability of ATD model in optimal control of a water system by carrying out optimal control of a hydropower cascade

5. Supplement the existing WaterLib toolbox with newly developed dynamic flow routing models.

1.3 Thesis contribution

The scientific contributions of this research leans directly to the objectives and are remarked as follows:

- An advancement of a simplified flow routing model is proposed. It is an Adaptive Time Delay model that expands the application scope of the available time delay model (TD) by simulating the flow using a prismatic trapezoidal geometry.

- A new method for routing flow with backwater effect is introduced. It is a coupling of ATD model and reservoir model which is able to simulate the unsteady non-uniform flow.

- A complex hydraulic model based on the discretized SVEs can simulate flow and water level accurately, however, the discretization requires an enormous computation time, hence is not applicable for using controller design. This thesis suggests an approach to simplify a complex hydrodynamic model without eliminating the key dynamic attributes, and is inevitable for model-based control.

- Another contribution is presented to improve the operation regimes of coordinated reservoir cascades by applying the ATD model in simulating and optimizing the system. It is actually a replacement for the complex hydraulic model by an adaptive time delay (ATD) model. The cutting- edge point is that the ATD model is able to quickly predict the system dynamics both in simulation and optimization.

1.4 Outline of the thesis

Each consecutive chapter is systematically dedicated to one of the mentioned topics. For each problem, a method will be proposed and rigorously examined. In chapter 2, a general picture of hydraulic models for open channel flows is given. At first, the chapter is devoted to the establishment of the Saint Venant Equation (SVEs) for flow dynamics. A number of key assumptions are made to simplify the complexities of nature of flow in a open channel. Flow is then analyzed by applying theory of Reynold transport theorem and control volume approach (Crowe, 2009) according to the law of conservation of mass and momentum. The mathematical description of the SVEs are obtained from the analysis afterwards. The initial and boundary condition to limit the system are also introduced. The available solutions of the SVEs are mentioned in two categories: numerical approaches and reduced model approaches. The advancements of time delay model as a simplified model for the SVEs are addressed in chapter 3. In chapter 4, the reduced model is further developed in order to describe the flow behavior with the downstream backwater effect. Chapter 5 introduces a procedure for estimating the parameters of ATD model from complex hydrodynamic model is described. The advancement of the method is rigorously proved by a case study. An utilization of ATD model for optimal control strategy of a hydropower cascade is introduced in chapter 6. Firstly, the system including two hydropower plants and a transition river reach is mathematically illustrated by two reservoirs models and a ATD model for the reach. Using the method in chapter 5, parameters of ATD model are estimated. Secondly, the energy production of the cascade is maximized by optimization. The nonlinear programming is applied to optimize the energy production of the system. A case study is used to prove the

method and demonstrated promising results. In chapter 7, the implementation of the newly developed tools into WaterLib toolbox is described. Finally, main achievements and some limitations and outlooks for future developments are summarized in the conclusions.

Chapter 2

State of the art

2.1 The Saint Venant equation

2.1.1 Assumption of the model

The channel flow is basically a free surface fluid dynamics driven by gravitational force. According to principles of fluid mechanics, the flow is attributed as: a fluid element on which all the forces affecting balanced to the pressure on the stream flow of atmospheric pressure; flow boundaries can adapt to the given flow conditions; flow extreme variability caused by geometrical shape and resistance (Sturm, 2010). Those characteristics make the flow unsteady and non uniform. To describe this issue, the principle of continuity and momentum represented by two partial differential equations is applied, in which the continuity equation is used when the flow variable is continuous while the momentum equation is required for discontinuities, such as surges or tides. To derive these governing equations, the following assumption are introduced (Sturm, 2010; Chaudhry, 2007):

- Water in river is shallow with hydrostatic vertical pressure distribution;
- The channel bottom slope is small so that the longitudinal profile of river bed is relative to the horizontal;
- The channel is prismatic, as a result, the cross section and channel bottom do not change spatially;
- The bottom elevation is stable and unchanged with time;

- The flow is described as one dimensional resulting in (a) the water level is horizontal across any cross section such that the transverse velocity is ignored; (b) the velocity and the shear stress take average value for a whole cross section;

- The bed friction is unchanged in unsteady flow as well as steady flow and calculated by Manning or Chezy equations.

2.1.2 Continuity equation

On the basis of the conservation of mass, the general continuity equation (Crowe, 2009) is a result of analyzing a mass transition of a matter by the Reynold transport theorem and control volume approach. It states that the accumulation rate of mass in the control volume is balanced with the net outflow rate of mass through the control surface. Applying the theory to a moving fluid particle in open channel whose fixed volume has depth y, and length Δx as in figure 2.1,

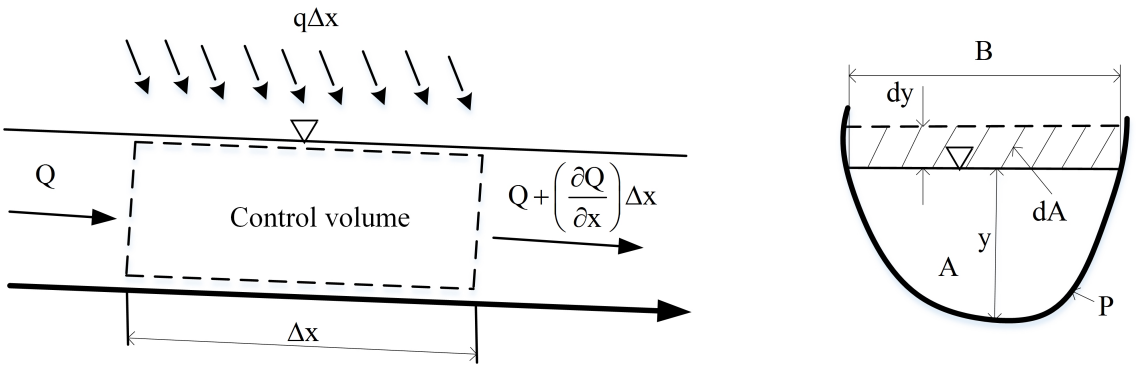

Figure 2.1: Control volume for derivation of continuity equation

the continuity equation is expressed that the net volume out of control surface in a time interval Δt is balanced to change of volume in that time step (Sturm, 2010):

$$\frac{\partial Q}{\partial x}\Delta x\Delta t - q\Delta x\Delta t = -\frac{\partial A}{\partial t}\Delta x\Delta t \tag{2.1}$$

By dividing $\Delta t\Delta x$, and $\Delta t \to 0$, $\Delta x \to 0$, the differential form of the equation is presented

$$\frac{\partial \mathrm{A}}{\partial \mathrm{t}} + \frac{\partial \mathrm{Q}}{\partial \mathrm{x}} = \mathrm{q} \tag{2.2}$$

It is denoted that Q is the flow rate, A is the cross sectional area, q is the lateral flow, B is the top width, q is the lateral flow distributed along the length of control volume Δx.

2.1.3 Momentum equation

Derivation of the momentum equation for a fluid particle is also based on the Reynolds transport theorem and control volume approach following the conservation of momentum. In stead of mass of matter, the force of motion which is described by the second law of Newton is used. The principle is that the rate of change of momentum in a control volume of the particle, and the outflow net momentum through control surface must be equal to the resultant force acting on it (Crowe, 2009). As in figure 2.2 adopted from (Sturm, 2010), the control volume of flowing fluid matter with acting forces is presented.

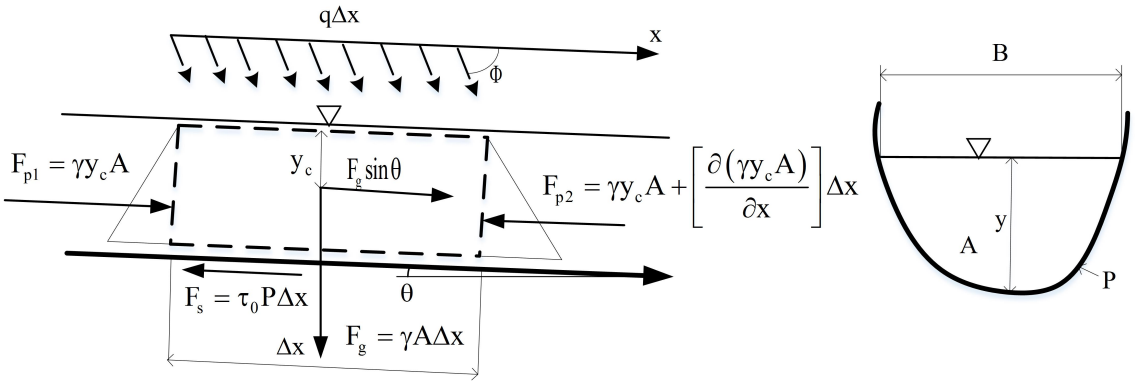

Figure 2.2: Control volume approach for derivation of momentum equation

From that, the momentum equation is formulated as in (Sturm, 2010):

$$F_{px} + F_{gx} - F_{sx} = Mom_{cv} + Mom_{cs} - Mom_{extra} \tag{2.3}$$

The the left side of equation 2.3 is summation of forces acting on the fluid particle:

- the resultant force of hydrostatic pressure at both sides of the control volume in the x direction

$$F_{px} = F_{p1} - F_{p2} = -\frac{\partial}{\partial x}\left[\gamma y_c A\right]\Delta x = -\frac{\partial y}{\partial x}\gamma A \Delta x \tag{2.4}$$

- the gravitational force F_{gx} in the x direction. The terms $sin\theta$ is approximated by a bed slope $\tan\theta \approx S_0$ due to a small value of slope.

$$F_{gx} = \gamma A \Delta x S_0 \tag{2.5}$$

- the boundary shear force between water and cross section surface in the x direction.

$$F_{sx} = \tau_0 P \Delta x \tag{2.6}$$

The right side of the equation 2.3 is the summation of momentum of the particle:

- the time rate of change of momentum in control volume

$$Mom_{cv} = \frac{\partial}{\partial x}\left[\int_A \rho v_x dA\right]\Delta x = \frac{\partial}{\partial x}\left[VA\right]\rho\Delta x \tag{2.7}$$

- the net outflow rate of momentum through surface of the control volume

$$Mom_{cs} = \frac{\partial}{\partial x}\left[\int_A \rho v_x^2 dA\right]\Delta x = \frac{\partial}{\partial x}\left[\xi\rho V^2 A\right]\Delta x \tag{2.8}$$

- the extra momentum flux from lateral flow in control volume

$$Mom_{extra} = \rho q v_L \Delta x \cos\Phi \tag{2.9}$$

Replace equations 2.4 to 2.9 for 2.3, and dividing by $\rho\Delta x$, for $\Delta x \to 0$ to obtain

$$\frac{\partial Q}{\partial t} + \frac{\partial}{\partial x}\left(\xi\frac{Q^2}{A}\right) + \frac{\partial}{\partial x}\left(g y_c A\right) = gA\left(S_0 - S_f\right) + qv\cos\Phi \tag{2.10}$$

The momentum equation 2.10 is built according to the conversation rule for an prismatic open channel, in which, $Q = AV$ is the flow rate; S_f=$\tau_0/(\gamma R)$ is the friction slope; τ_0 is the mean shear stress; A is the wetted area; P is the wetted perimeter; $R = A/P$ is the hydraulic radius; $\xi = 1$ is the momentum correction coefficient; q is the lateral flow per unit length, and the direction of q is at the angle of ϕ with respect to x direction; v_x is the velocity of a flow particle in direction x. Both equations 2.2 and 2.10 are 2 components of the Saint Venant Equations. In

case, the lateral flow $q = 0$, the representation of the SVEs are obtained (Saint-Venant, 1871)

$$\frac{\partial \mathrm{A}}{\partial \mathrm{t}} + \frac{\partial \mathrm{Q}}{\partial \mathrm{x}} = 0 \tag{2.11}$$

$$\frac{\partial \mathrm{Q}}{\partial \mathrm{t}} + \frac{\partial Q^2/A}{\partial \mathrm{x}} + \mathrm{gA}\frac{\partial Y}{\partial x} + \mathrm{gA}\left(S_f - S_b\right) = 0 \tag{2.12}$$

$$S_f = \frac{Q^2 n^2}{A^2 R^{4/3}} \tag{2.13}$$

It is denoted that V is the mean velocity of a whole cross sectional area; Y is the water depth; n is the Manning coefficient; S_b is the bed slope; and g is gravitational acceleration, L is length of the river reach. The solutions of those equation is discussed in the next section

2.1.4 Initial and Boundary condition

Initial condition

In the computation of flow dynamics in open channels, a specified time for beginning the simulation is essential. The flow condition at the starting time is defined as an initial condition, i.e, flow rate Q_0 and water level Y_0 at time step $t = 0$ are referred to as initial conditions.

Boundary condition

The boundary condition must be specified at all of the open ends of the river system in order to limit the studied physical system. There are different categories of the conditions as follows: a given flow data (discharge or water level), a rating curve, a junction, or a hydraulic structure (Brunner, 1995). These boundary conditions are illustrated in figure 2.3, and discussed in detail.

1. A given flow data: consists of the flow hydrograph, the stage hydrograph, the flow and stage hydrograph at upstream or downstream end of river which are used to model river flow.

2. A rating curve: presents a relationship between water level and discharge at a cross section: $Q = f(y)$.

3. A junction is the place where confluence and effluence of flow exists. If energy loss is minor and the difference in velocity head is small, the water level of reaches at junction must be equal, and sum of discharge entering the junction should be equal to the sum of discharge leaving the junction.

4. A hydraulic structure: a weir or gate is installed on a river in order to control the flow to respond with a specific purpose.

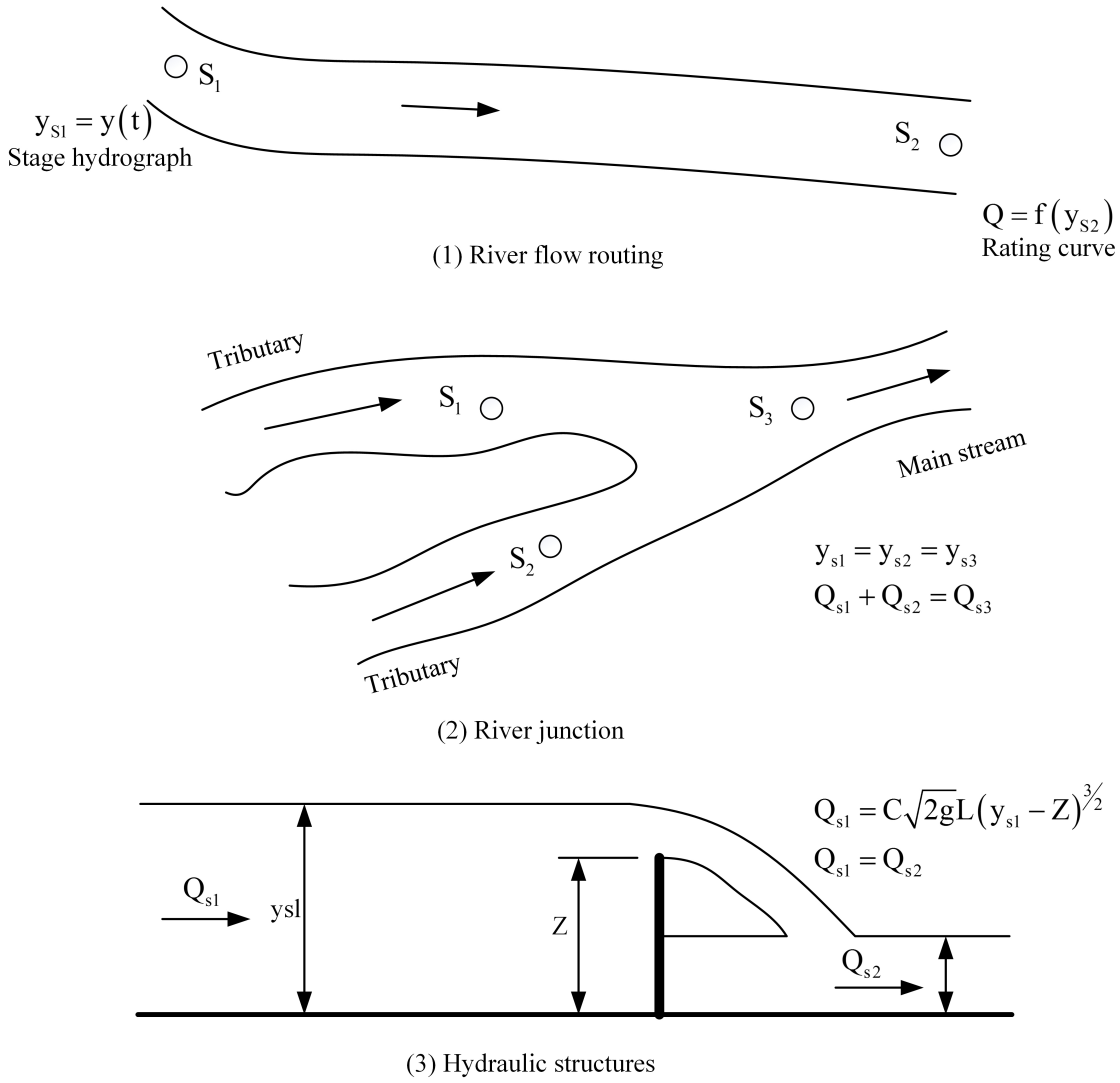

Figure 2.3: Boundary conditions for flow simulation

2.2 Solutions for the Saint Venant Equation

2.2.1 Numerical methods

Method of characteristics

The approach is fundamentally a graphical procedure to integrate parial differential equations (PDE). The SVEss equations are transformed into a set of 4 ordinary differential equations (ODE) which are then expressed in its characteristic plane $(x - t)$. The ODEs are only valid along characteristic curves consisting of positive curve C^+ and negative curve C^- as shown in the plots of equation 2.14 in figure 2.4. Physical meaning of flow is well explained based on these characteristic curves. The equations are numerically solved by the method of intervals and characteristic grid. In spite of several published applications to open channel flows such as (Stoker, 2011; Abbott, 1966, 1979; Lai, 1986), the approach is more helpful in understanding the wave propagation and the determination of boundary conditions than in deriving solutions (Chaudhry, 2007).

$$\frac{dx}{dt} = V \pm c \tag{2.14}$$

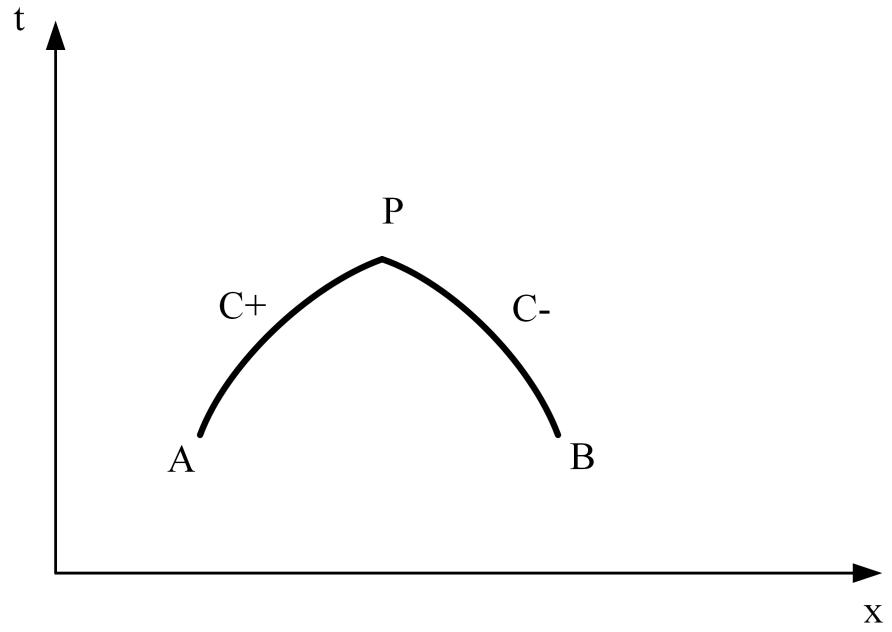

Figure 2.4: Positive and negative characteristics curves

Finite difference method

The finite difference method (FDM) has been extensively used to solve the nonlinear partial differential equation such as the SVEs (Abbott, 1979; Harley, 1967; Fread, 1985; Garcia and Kahawita, 1986; Stoker, 1957). Considering a function $f(x,t)$ with two dependent variables: x as spatial variable, and t as temporal variable. The function is then described by the curve on the $x-t$ plane in figure 2.5a. Also, the geometry calculation of basic approaches including forward, backward and central FDM are shown in the figure (Chaudhry, 2007). The finite difference grid is indicated in figure 2.5b which is divided along the x axis and t axis with interval Δx and Δt. Based on the initial conditions and boundary conditions, the solution of the f is derived. The method is categorized as explicit FDM and implicit FDM.

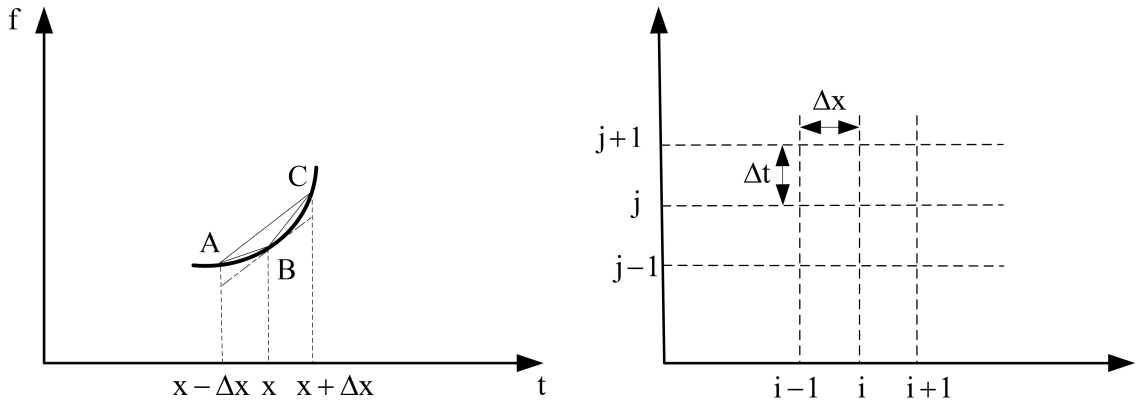

Figure 2.5: Finite different approximation

In terms of the explicit FDM, the spatial partial derivatives (variables) depend explicitly on those at the known time step. Many schemes have been introduced for the solution of SVEs due to its simplicity and fast computation, however, the method encounters instability when the size grid spacing goes beyond the satisfaction of the Courant condition (Courant et al, 1967). To improve this weakness, sort of typical schemes are presented such as Lax Diffusive scheme, Leapfrog scheme, Lax Wendroff scheme, Predictor Corrector methods, Flux-Splitting scheme (Sturm, 2010). Three forms in executing explicit FDM are follow:

- Backward: $\frac{\partial f}{\partial x} = \frac{f_i^k - f_{i-1}^k}{\Delta x}$
- Forward: $\frac{\partial f}{\partial x} = \frac{f_{i+1}^k - f_i^k}{\Delta x}$
- Central: $\frac{\partial f}{\partial x} = \frac{f_{i+1}^k - f_{i-1}^k}{\Delta x}$

Regarding the implicit FDM, the spatial partial derivatives are evaluated at the new time step. The method is not restricted by time step condition so that it is suitable for simulating a large scale system. Typical schemes have been utilized in analysis of open channel flow: Preismann scheme, Beam and Warming scheme, and Vasilive scheme. Three ways to implement implicit FDM are as follow:

- Backward: $\frac{\partial f}{\partial x} = \frac{f_i^{k+1} - f_{i-1}^{k+1}}{\Delta x}$
- Forward: $\frac{\partial f}{\partial x} = \frac{f_{i+1}^{k+1} - f_i^{k+1}}{\Delta x}$
- Central: $\frac{\partial f}{\partial x} = \frac{f_{i+1}^{k+1} - f_{i-1}^{k+1}}{\Delta x}$

Other numerical approaches

Although a finite element method (FEM) is usually applied to two or three dimensional simulation, a few researches proved that it can effectively approximate the solution of SVEs. At first, the FEM based on the Galerkin method is introduced in (Cooley and Moin, 1976) in order to approximate the unsteady flow in open channel. The scheme returns a stable and convergent result as well as the stability is also validated. Other applications include: (Szymkiewicz, 1991; Hughes et al, 1989; Versteeg and Malalasekera, 2007). However, it still is not commonly used in river flow simulation because the model encounters many difficulties when dealing with low stability of the model (Chaudhry, 2007).

A finite volume method (FVM) based on the application of Riemann solvers have also been used to solve the SVEs numerically. As in (Crossley et al, 2003), local time stepping strategies are executed in FVM to approximate the solution of SVEs. The reduction in computational time, error of control and increase accuracy of the solution in a certain range are considered as benefits of the method. The feasibility of the scheme for flow propagation in open channel with downstream boundary condition is demonstrated by (Cozzolino et al, 2011, 2014a,b). Application of FVM to debris flow transportation is recently published in (D'Aniello et al, 2015; Cozzolino et al, 2016).

Regarding the spectral method, it is viewed as a significant advancement of types of discretization methods for partial differential equations (Canuto et al, 2012; Wang, 2002). An application to model surface water bodies, such as rivers, lakes

are common (Cozzolino et al, 2012). Nevertheless, problems arise in the application if the boundary conditions are non-periodic (Chaudhry, 2007).

An alternative has been introduced as smoothed particle hydrodynamics (SPH) which is a numerical mesh-free method based on Lagrangian formulation, which approximate the free surface flow (Monaghan, 1992; Liu and Liu, 2010). The performance of SPH is well presented and validated by several case studies: dam-break flow(Zhou et al, 2004) and turbulent flow simulation (Violeau and Issa, 2007; Violeau and Rogers, 2016).

The boundary-element method has been more commonly used in the areas of solid mechanics and acoustics problem than the fluid mechanics (Liggett, 1984; Brebbia and Dominguez, 1994; Camacho and Barbosa, 2005). The approach successfully approximate the flow dynamics by using the representation of the Navier Stokes equations according to velocity and making use of the penalty function method. Even though the workability and validity of the approach is shown in several studies (Camacho and Barbosa, 2005; Tosaka et al, 1985), it is not effective if applied to time dependent systems Chaudhry (2007).

In summary, approaches of numerical scheme are applied to solve a discretized one dimensional SVEs in space and time. Most of numerical algorithm used for 1D hydrodynamic model has to satisfy the stability condition which is known as the Courant requirement (Courant et al, 1967). Applying an explicit scheme for flow simulation needs a small time step which consumes large computation effort. Others use implicit or semi-implicit schemes which ensure the stability with a large time step. Some schemes result in unconditionally stable solutions such as Preismann method and Runge Kutta method. The major advantages are the applicability to several kinds of channels, and maintaining the nonlinear attribute of the system. In addition, these scheme can be used for real time control purposes, where the control time step is much larger than the simulation time step (Xu, 2013). The main limitations are large computation time. In case of using this implicit or semi-implicit scheme, the wave damping is also a drawback, although it needs to be eliminated in real-time control (Catalano et al, 2003; Xu, 2013).

2.2.2 Simplified methods for flow routing

Whilst the fully dynamic SVEs are numerically solved in the previous section, this section introduces simplified approaches in which a few terms are ignored, or different representations are used in order to derive an acceptable result and save computational effort as well as serve for other purposes. These models includes as follows:

Firstly, reservoir routing technique only utilizes the continuity equation to propagate flow from storage facilities (lake, reservoir, pond, detention basin) towards downstream (Chaudhry, 2007; Sturm, 2010). The water level in reservoir is assumed to be horizontal. The change between inflow I and outflow O is equal to the change of storage capacity ϑ as in equation 2.15. In order to route the flow through storage facilities, the equation is numerically integrated.

$$\frac{d\vartheta}{dt} = I - O \tag{2.15}$$

The second is a river routing model that is also known as the Muskingum model. Similar to the concept of reservoir routing, the storage capacity ϑ in a river reach is expressed as function of inflow I and outflow O accompanied with 2 additional coefficients: the storage constant or travel time of flood wave K, and the dimensionless weighting factor X ($0 \leq X \leq 1$). Both coefficient may be determined from recorded flow data; or may be estimated by optimization technique. In terms of the Muskingum-Cunge method, two coefficients K and X are determined by approximating the kinematic wave equation. For simplicity, this relation is assumed as linear shown in equation 2.16. In some circumstances, the nonlinear relationship in equation 2.17 is required to accurately account for the nonlinearity in storage and flow. The exponent factor m is determined during calculation. It has been commonly applied and innovated in river flow simulation, for instance, by (Bhuyan et al, 2015; Franchini et al, 2011; O'Sullivan et al, 2012).

$$\vartheta = KO + KX(I - O) \tag{2.16}$$

$$\vartheta = K[XI^m + (1 - X)O^m] \tag{2.17}$$

In terms of the kinematic wave model, the continuity equation and a reduced form of momentum equation are applied to simulate downstream flow. Due to the negligence of the inertia and pressure terms in momentum equation, the flow becomes unsteady and uniform by which the bed slope S_b is equal to the friction slope S_f, $S_b = S_f$. The model expressed in equation 2.18 describes the movement of the kinematic wave in river through the rate of change of discharge Q in response to t and x. The kinematic wave velocity is $C = dQ/dA$ (Seddon, 1900). The attenuation of outflow purely relies on the characteristic of numerical method and does not the reflects physical phenomenon of the wave. Extensive applications have been published for flow routing in channel networks (Haltas and Kavvas, 2009), solution of kinematic wave for overland flow (Cundy and Tento, 1985) and others.

$$\frac{\partial Q}{\partial t} + C\frac{\partial Q}{\partial x} = 0 \tag{2.18}$$

Another well known method is the diffusive wave routing which is also a combination of the continuity and a simplified momentum equation. In terms of simulation, the inertia term is excluded whereas the pressure term is taken into account. The model is described by equation 2.19. Two coefficients: diffusion $D = f(Q)$ and celerity $C = f(Q)$ which define physical behaviors of flow are obtained by observed hydrographs. The model is extended for several practical purposes, for example, simulation of river flow with uniform and concentrated lateral flow in (Fan and Li, 2006), approximating the parabolic wave accounting for downstream boundary condition and uniform flows in (Cimorelli et al, 2013, 2014). Moreover, the theory of Hayami is originally recognized as an analytical solution of diffusive wave model with an assumption of constant celerity and diffusivity, and without lateral flow. Since many years, improvement of Hayami model for simulating and controlling open channel flow has been presented, e.g., in (Bolea et al, 2010a; Moussa, 1996; Wang et al, 2014).

$$\frac{\partial Q}{\partial t} + D\frac{\partial Q}{\partial x} - C\frac{\partial^2 Q}{\partial x^2} = 0 \tag{2.19}$$

Last but not least, the Kalinin-Miliyukov method defines a characteristic river reach by assuming that a discharge at a cross section of a reach is not influenced by

lateral flow (Kalinin and Milyukov, 1957). Then, a whole river can be approximated by a series of characteristic reaches. The discharge is also a linear function of water storage within that reach. According to (Szilagyi, 2006), the outflow h is derived as in equations 2.20a-c.

$$h(t) = k\frac{(kt)^{I-1}}{\Gamma(I)}e^{-kt} \tag{2.20a}$$

$$Q(t) = k\vartheta(t) \tag{2.20b}$$

$$\Gamma(I) = \int_0^\infty \varsigma^{I-1}e^{-\varsigma}d\varsigma \tag{2.20c}$$

where h is a discharge of characteristic reach known as instantaneous unit hydrograph (IUH); k is a constant coefficient of linear relationship of discharge Q and storage ϑ; t is the time; I is the number of equal characteristic reach; Γ is the complete gamma function; and ς is the dummy variable. A further development by (Nash, 1957) is known as Kalinin-Miliyukov-Nash model (KMN). A linear reservoir model (equation 2.16) is defined as a characteristic reach that is connected in series to approximate the flow behavior. Each reach is characterized by equation 2.20b. Furthermore, the method is formulated in state space representation for forecasting stream flow (Szilagyi, 2003, 2006).

Empirical method for controller design

Methods apply previous knowledge of the system to build a hydrodynamic model for control purpose. Fundamentally, this approach is a selection between black box models and grey box models (Ljung and Glad, 1994).

In terms of black box models, the relationship of inflow and outflow of river system is achieved without the insight of physics. An illustration is that a stochastic model named Auto Regressive with Exogenous Input (ARX) is used to simulate downstream flow of river system by (Elfawal-Mansour et al, 1981; Sepulveda and Rodellar, 2005). The application of ARX is then presented and validated against measured data from Guira de Melena irrigation canal (Perez et al, 2008). Another approach use Linear Parameter Varying (LPV) for modeling irrigation and being validated by (Bolea et al, 2009, 2010b). A few researches in (Abdelmoumène Toudeft, 1996; Toudeft, 1995) use artificial neural network (ANN) for simulating canals or

rivers. In general, these types are costly and difficult for identification phase when the model of the system is at design stage.

Regarding the grey box models, they need some prior information of physical system to select the suitable model structures for simulation. The prior knowledge usually comes other from previous experience, or from experiment. As a research in (Weyer, 2001), a grey box model is developed for a irrigation canal system where input of the model is gate positions while output is water level over the gate. A channel stretch between two gates is considered as a pool. The prior information is known from measurements data: water level at upstream and downstream. To determine the model parameters, the procedure of system identification which consists of experimental design, model structure determination, parameter estimation, and model validation is introduced. The model is then obtained and validated for both high and low flow of Haughton Main Channel that presented a very good result. The model for combination of undershot and overshot gates is also developed by (Eurén and Weyer, 2007). An advancement is made by (Foo et al, 2010; Ooi and Weyer, 2008) that uses the linearized SVEs for modeling water level in canal pool or in river instead of executing experiments from measured data as previous researches. In addition, a combination of experiment design for defining time delay, and the SVEs have proved its advantage (Foo et al, 2014). In case of enough measured data, the experiment can return a very good results while the SVEs are helpful in situations of data shortage. The approach is validated in case studies such as Haughton Main Channel Weyer (2008), Broken River (Foo et al, 2014; Ooi et al, 2011) and applied for not only overshot gate but also undershot gates (Eurén and Weyer, 2007) and for a large scale modeling of irrigation area (Cantoni et al, 2007).

State space representation of SVEs

With a system representation in state space, the number of states and disturbances are significantly reduced whereas still ensuring the model accuracy. For that reason, the SVEs model can be used as internal model for controller design. The linear

finite state space model is (Malaterre and Baume, 1998)

$$\begin{cases} x(k+1) = Ax(k) + Bu(k) + B_p p(k) \\ y = Cx(k) \end{cases} \tag{2.21}$$

Where x is state vector, y is the controlled variable vector, u is input vector, p is vector of perturbation, A, B, B_p and C are constant matrices of appropriate dimensions, k is index. This expression in time domain broadens the applicability for many control approaches over former model in frequency domain. For instance, a linear quadratic (LQ) optimal control theory, or a model predictive control (MPC) need an internal model with state space presentation for optimization. In addition, the model can be formulated by aggregating different SISO transfer functions between inputs and outputs variables.

The SVEs are usually not used for controller design due to the expensive computation. Hence, the model must be simplified while maintaining the accurate prediction. Proper orthogonal decomposition (POD) is a powerful tool for deriving a low order model from dynamical process. The decomposition can be applied for temporal and spatial domain. Accompanied with POD, the snapshot technique is used to discretize the procedure of POD in temporal domain. Application of POD with a snapshot approach to obtain the simplified state space model of both linear SVEs and transport equation has been presented in (Xu, 2013). The method takes snapshots of an off-line simulation model and arranges a two point spatial correlation matrix. Each snapshot is a column of state vector in which consists of water level and solute concentration in a combined water quantity and quality model. As many snapshots are taken as more flow ranges are covered in the reduced model. In addition, taking more snapshots does not considerably increase the computation time.

An alternative approach of POD for simplifying hydraulic model is presented in (Breckpot et al, 2012a). The model aims at describing the flow of river with and without hydraulic structure at outlet. The idea is a combination of a linear SVEs model for simulating flow dynamic in a reach and nonlinear model for flow through gate (LN model) in order to produce a good result. This hybrid model is then simplified by using POD and Galerkin projection, in which the POD helps to obtain the

set of suitable orthonormal basis vectors from experimental data whereas Galerkin projection is applied to reduce the model order. In case of river network modeling, the supplement of reservoirs, junctions, and gates defines different boundaries for each river reach leading to distinct LN models. Afterwards, the whole system is then approximated with a linear state space model in order to serve for designing controller. In this case, it is noted that gate discharges are considered as controlled variables instead of the positions in order to save computation time. After the discharge is optimized, the conversion is made based on the gate equation. The technique is applied to serve for control technique as Linear Quadratic Regulator (LQR), and Model Predictive Control (MPC) in (Breckpot et al, 2012b; Breckpot and Moor, 2012).

A formulation of state space models for river networks using the SVEs and the constraint at junctions has been presented in (Rafiee Jahromi, 2012). The state variables: flow rate Q, and water level H. Firstly, the linearized SVEs are discretized by the Lax diffusive scheme for the internal grid points. The scheme must be stable according to the Courant condition (Courant et al, 1967). At the boundaries of the grid, the data must be also determined by the method of specified time intervals (Chaudhry, 2007). In which, the characteristic equation is established, the unknown variable at the boundary grid point are then predicted by using those equations. The method can be applied to a whole river network. However, it is essential to supplement the internal boundary conditions at a tributary of a river network as mentioned in figure 2.3. The model is used to estimate flow rate and stage for a river network (Hofleitner et al, 2013; Rafiee et al, 2009, 2011).

An updated research comes from (Szilagyi and Laurinyecz, 2012) named the discrete linear cascade model (DLCM). Fundamentally, the model is a state space description of a cascade of reservoir in rivers which are described by either the linear kinematic wave equation (Szilagyi et al, 2005; Szöllösi-Nagy, 1982) or diffusive wave equation (Szilágyi and Nagy, 2010). Flow propagation is thus able to be approximated spatially and temporally. This physically based flow routing method includes two parameters: number of sub reaches and their storage coefficient. The backwater effect is also accounted through relating the storage coefficient and flow rate.

Frequency representation of SVEs

The full SVEs equations are linearized and transformed into the frequency domain by Laplace transform. The transfer matrix is then obtained and addressed by several approaches. The frequency representation of the system is presented as follows (Baume et al, 1998).

In a case of finite and linear system, flow in the river with a downstream gate is assumed as uniform. The integrator model is then initially developed from transfer function of SVEs (Corriga et al, 1983, 1988; Ermolin, 1992; Papageorgiou and Messmer, 1985, 1989) that simulates the water movements. Afterwards, a research of (Schuurmans et al, 1995) which makes a significant improvement, describes channel flow more realistic than earlier versions. In addition, the description of the non-uniform flow of the channel through structures (gate, hydropower, culvert, and so on) is also modeled. The model considers the channel as a system where the water profile is separated into two parts: uniform and backwater part which are both simulated and connected together. Regarding the uniform part, the kinematic wave model is selected to approximate the wave deformation heading to downstream because of its simplicity and sufficient accuracy. On the other hand, the dynamic of backwater part is primarily influenced by reflection of waves so that it is suitable to be modeled by the reservoir model. Furthermore, the length of back water level toward upstream direction must be pointed out in order to join with the uniform part. The method is known as Integrator Delay Method (ID) which is validated in (Schuurmans et al, 1999b,a) and commonly used in modeling canal for controller design. The model only performs well for a long, steep, and shallow canal. Generally, the ID model is limited to the small flow changes because it is only stable in low frequency.

Despite ID has been popularly used to model a river in time domain, it may not be applicable to control design while the Integrator Delay Zero (IDZ) is a better solution. The reason is stated in (Litrico and Fromion, 2004a) that the time delay predicted by ID is much larger that the one derived by the IDZ model. This may result into poor controllers. Another improvement of IDZ (Litrico and Fromion, 2004a) is that a zero is supplemented to ID model in order to simulate the system in high frequency. Consequently, the IDZ has three parameters as integrator gain,

delay, and zeros that are explicitly functions of flow rate and water level. Even though (IDZ) compensates the weakness of the ID model, it still does not concern the resonance waves in modeling the relative short river reach.

An evolution that is called the integrator resonance model (IR) is composed of an integrator and a mode of long reflecting wave (Overloop van et al, 2014). The dynamics of short, flat, and deep open canal is approximated by the integrator resonance model. The integrator resonance (IR) model is built as an internal model for offline controller design. It has been tested in laboratory and proved applicability to offline controller design.

One of the most recent work by (Cimorelli et al, 2015) introduces a new model which can be used for real time forecasting and optimization. In which, the analytical solution for a cascade of diffusive channel has been derived in Laplace Transform domain accounting for downstream boundary conditions. In addition, other studies of (Cimorelli et al, 2013, 2014) introduce a reduced model of SVEs named Linear Parabolic Approximation (LPA) developed by ignoring inertial terms of SVEs. An analytical solution is then obtained in terms of discharge and water level variations, taking account of backwater effect and downstream lateral flow.

The time delay model

The reduced model for flow routing based on the lag time (or time delay) has been developed since years. Initially, the lag-and route method is introduced and recommended to use because it could alleviate deficiencies of conventional Muskingum model (Meijer, 1941). The method consists of two components: lag time and routing reservoir in which a relationship of discharge and storage in routing is linear. To obtain a better outcome, an upgrade is made by (Bentura and Michel, 1997) where the linear routing reservoir component is substituted by a quadratic routing reservoir. The model is calibrated for uniform flow in a wide rectangular channel and its advantages are demonstrated. However, the physical attributes of channel are not apparently related in both studies.

Another is the multilinear discrete lag cascade model (MDLC) proposed by (Camacho and Lees, 1999), which is an extension of two parameter multilinear discrete cascade model of (Perumal, 1994) by supplementing a time delay parameter. The

inclusion of time delay which varies against each element of inflow show a clear physical characteristic as well as provided explicit time transition of flood wave to downstream. Nevertheless a drawback is the occurrence of irregularities at peak regions of simulated hydrograph due to involvement of inappropriate time delay. This problem is then exposed by (Perumal et al, 2007) comprehensively. The study points out that a varied pure time delay of MDLC model obtained by multiplying an integer with routing time interval caused truncation errors in the routing process so that it returns discontinuities or sudden falls in the simulated hydrograph. An option of keeping a time delay constant during routing process is suggested and validated in order to overcome this weakness. However, the fixed constant lag value does not reflect an accurate physical manner of flow propagation. In addition, it is not considered to use for controller design.

The time delay model to describe flow movements in rivers has been developed by (Pfuetzenreuter and Rauschenbach, 2005; Rauschenbach, 2001). The model parameters time delay and time constant are determined by the least square method. Further advancement is a toolbox named WaterLib (Pfuetzenreuter and Rauschenbach, 2005), which is built up based on this approach to simulate a river system for controller design. It is also validated in many projects (Rauschenbach, 2005). Beside the flexibility in modeling a wide range of river network, the method is still simple because significant parameters of model: time constant and time delay cannot adapt with flow variation.

The similar method is also introduced by (Litrico and Georges, 1999) that derives transfer functions of the linear Hayami model, and a linear Ordinary Differential Equations (ODE). By applying moment matching method on both transfer functions, parameters of ODE are defined as functions of parameters of Hayami model. The ODE is then able to use for controller design. Moreover, this work is extended in (Litrico et al, 2010) that approximates a linearized SVEs and considers the change of time delay with flow variation. The study on Jacui River validated the model. In both cases, the cross section of the canal is rectangular, where the analytical derivation is not complicated.

The investigation with backwater effect is also conducted by (Munier et al, 2008). The model named Linear Backwater Lag and Route (LBLR) model transforms the

linearized SVEs in time domain into frequency domain in order to derive the transfer functions. Then, the downstream boundary conditions are introduced as local feedback between discharge and water depth. Afterwards, the first or second order time delay model is utilized to approximate the system in low frequencies. Consequently, either uniform flow or non-uniform flow can be computed by the model. While the advancement is that the model is able to give the discharge at any location in channel and dealing with non-uniformity of flow, the complexity of mathematical transformation is still an obstacle for users. Another disadvantage is that application of this model to unsteady flow is still an open question.

2.3 Conclusion

In summary, the SVEs are a system of the partial differential equations describing the one dimensional flow in channel/river. Due to no analytical solution, a number of typical methods have been studied to find their solution. A wide range of numerical approaches to solve these equations have been developed: method of characteristic, finite difference methods, finite element methods, finite volume methods, spectral methods, boundary element methods and many more. From these methods, several sophisticated hydrodynamic models have been built (HECRAS, MIKE 11, SOBEK, and many others). Moreover, model simplification aims at reducing system order or dimension while maintaining the model accuracy in flow routing, and using for controller design. On the one hand, for quick simulation, typical models consists of reservoir routing model, Muskingum model, kinematic model, diffusion model, Muskingum-Cunge model. On the other hand, empirical methods, transfer function of SVEs, state space representation of SVEs are often used for controller design. In modeling open channel flow, the SVEs are selected as a governing tool for describing flow dynamics because of high accuracy. It requires high computation time and, huge input demand. In contrast, a low order linear model is usually required for quick simulation and control (Camacho and Bordons, 2004). For that reason, studies on model reduction for different objectives have been continuously implemented (Holmes et al, 1998).

A primary work of the dissertation is to develop a simplified model for flow

routing and controller design of water system. The well known time delay model is selected. After investigating development of the time delay model through available researches of (Meijer, 1941; Perumal, 1994; Bentura and Michel, 1997; Camacho and Lees, 1999; Schuurmans et al, 1999b; Rauschenbach, 2001; Munier et al, 2008; Litrico et al, 2010), the time delay model is basically developed by using the first order time delay model to approximate the fully hydraulic model. Following the fundamental approach, significant advancements of the time delay model are presented in this research. The work will be thoroughly described in following chapters.

Chapter 3

Adaptive time delay model

3.1 Introduction

In this chapter a new contribution to the control models is introduced. It is known as the ATD model and tries to eliminate most of the limitations and drawbacks of the other models mentioned in chapter 2. The advancement of the ATD model is that it does not only approximate the full SVEs but also use both water level and the flow rate to calculate the model parameters, which has not been realized before. This can be considered as an upgrade of previous time delay models (Schuurmans et al, 1999b; Pfuetzenreuter and Rauschenbach, 2005; Litrico et al, 2010). Based on existing literature (Dooge et al, 1987, 1988; Litrico and Fromion, 2009) the study presents a methodology for a reduced model that is able to be applied to a river with prismatic trapezoidal cross, and a river with downstream backwater effect.

3.2 The fundamental method for derivation of the ATD model

The SVEs are linearized and transferred to frequency domain to obtain their transfer function. On the other side, a linear first order time delay model is selected to approximate the SVEs and its transfer function is also derived. By equating the cumulants of both transfer functions of the SVEs and first order time delay, the relationship between both models is established. In this way, the time delay model can describe the flow dynamics because its parameters are functions of parameters

of the SVEs. The approach illustrated in figure 3.1 includes the following steps:

- Definition the two physical models (linearized SVEs and ATD);
- Derivation the transfer functions of linearized SVEs and the adaptive time delay (ATD) model;
- Determination of the parameters of the ATD model from parameters of the linearized SVEs.

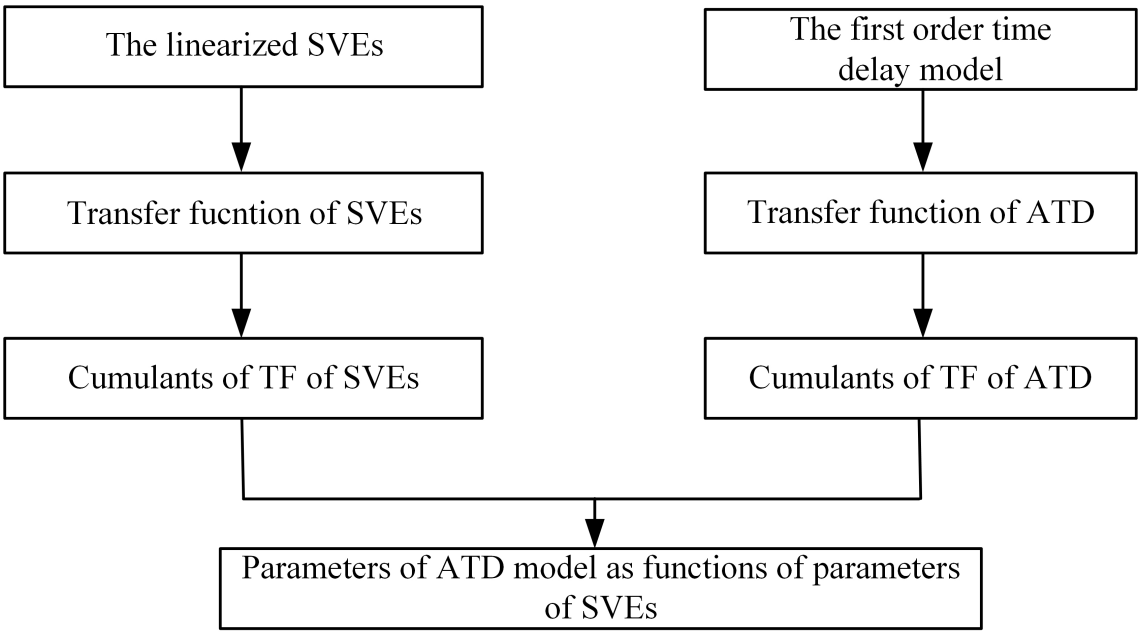

Figure 3.1: Approach of approximating the SVEs

3.2.1 Linearization of the Saint Venant Equation

The Saint Venant Equations analyze the movement of flood waves in open channel flow on the basis of a one dimension, hence, the independent variables are the elapsed time t and the single space dimension x in the flow direction. The characteristics of flow at downstream cross section is predicted by investigation of the characteristics of flow at upstream cross section and hydraulic attributes of the reach between two cross sections (Dooge et al, 1988; Cunge et al, 1980). As mentioned in the previous chapter, the hyperbolic system without impact of lateral flow is given by:

$$\frac{\partial \mathrm{A}}{\partial \mathrm{t}} + \frac{\partial \mathrm{Q}}{\partial \mathrm{x}} = 0 \tag{3.1}$$

$$\frac{\partial \mathrm{Q}}{\partial \mathrm{t}}+\frac{\partial Q^2/A}{\partial \mathrm{x}}+\mathrm{gA}\frac{\partial Y}{\partial x}+\mathrm{gA}\left(S_f-S_b\right)=0 \tag{3.2}$$

It is denoted that $A(x,t)$ is the wetted area; $Q(x,t)$ is the flow rate; $Y(x,t)$ is the water depth; $S_f(x,t)$ is the friction slope; S_b is the bed slope; and g is the gravitational acceleration, L is length of the river reach. The friction slope S_f which represents the friction law applied, the shape and roughness of cross section, and the flow attributes at studied section, is calculated by Manning-Strickler (Chow, 1959) as.

$$S_f=\frac{Q^2n^2}{A^2R^{4/3}} \tag{3.3}$$

where n is the Manning coefficient; R = A/P is the hydraulic radius; and P is the wetted perimeter.

It is essential to consider the unsteady flow as a perturbation from a steady flow condition. The total flow characteristic is then written accordingly (Dooge et al, 1988)

$$Q\left(x,t\right)=Q_0+q\left(x,t\right) \tag{3.4a}$$

$$Y\left(x,t\right)=Y_0+y\left(x,t\right) \tag{3.4b}$$

where Q_0, $Y_0(x)$ are the flow rate and water level at steady uniform condition; q, y are the first order of increments.

To linearize the SVEs, the equations 3.4 a and b are substituted into the equations 3.1, 3.2 and expanded in series by Taylor method (Litrico and Fromion, 2004b). Significantly, only the linear parts q, y will remain while higher order parts are neglected even though it is false for a large perturbations from the steady stage. The Taylor series as is written for each term of the SVEs as follows.

$$f\left(Q,Y\right)-f\left(Q_0,Y_0\right)=f_Q\left(Q_0,Y_0\right)q\left(x,t\right)+f_Y\left(Q_0,Y_0\right)y\left(x,t\right)+\zeta \tag{3.5}$$

where f_Q, f_Y are the partial derivative of the SVEs equations with respect to Q,

Y; ζ is the high order terms ignored in expansion.

In terms of the continuity equation 3.1, each term is denoted t_1, t_2 which are expanded as follows

- the linearization of the first term $t_1 = A$, $A = B_0 y$ is obtained as

$$t_1 - t_{1,0} = B_0 \frac{\partial y}{\partial t} \tag{3.6}$$

- the linearization of the second term $t_2 = Q, Q = Q_0 + q$ is obtained as

$$t_2 - t_{2,0} = \frac{\partial q}{\partial x} \tag{3.7}$$

The linearized version is derived by:

$$B_0 \frac{\partial y}{\partial \mathrm{t}} + \frac{\partial \mathrm{q}}{\partial \mathrm{x}} = 0 \tag{3.8}$$

Regarding the momentum equation 3.2, each term is denoted t_1, t_2, t_3, t_4 and expanded respectively.

- the linearization of the first term $t_1 = Q, Q = Q_0 + q$ is obtained

$$t_1 - t_{1,0} = \frac{\partial q}{\partial t} \tag{3.9}$$

- In case of the second term $t_2 = Q^2/A$. At first

$$\frac{Q^2}{A} - \frac{{Q_0}^2}{A_0} = 2\frac{Q_0}{A_0} q - \frac{Q_0^2}{A_0^2} \frac{\partial A_0}{\partial Y} y = 2V_0 q - V_0^2 B_0 y \tag{3.10}$$

  with $V_0 = Q_0/A_0$, and $\partial A_0/\partial Y = B_0$ Differentiating equation 3.10 with respect to x we have

$$t_2 - t_{2,0} = 2V_0 \frac{\partial q}{\partial x} + 2\frac{dV_0}{dx} q - V_0^2 B_0 \frac{\partial y}{\partial x} - \left(V_0^2 \frac{dB_0}{dx} + 2V_0 B_0 \frac{dV_0}{dx} \right) y \tag{3.11}$$

  Because of the unsteady condition in prismatic channel, it is given that $dQ_0/dx =$

0, $dA_0/dx = B_0 dY_0/dx$, therefore the derivative of V_0 against x:

$$\frac{dV_0}{dx} = -\frac{Q_0}{A_0^2}\frac{dA_0}{dx} \tag{3.12}$$

Putting equation 3.12 into equation 3.10, and arranging terms leads to

$$t_2 - t_{2,0} = 2V_0\frac{\partial q}{\partial x} + 2\frac{V_0 T_0}{A_0}\frac{dV_0}{dx}q - V_0^2 B_0\frac{\partial y}{\partial x} + \left(\frac{V_0^2 B_0^2}{A_0}\frac{dY_0}{dx} - 2V_0^2\frac{dB_0}{dx}\right)y \tag{3.13}$$

- The third item $t_3 = gAY$ is expanded as in equation 3.14

$$t_3 - t_{3,0} = gB_0\frac{dY_0}{dx}y + gA_0\frac{\partial y}{\partial x} \tag{3.14}$$

- The fourth item $t_4 = gA(S_f - S_b)$ is expanded to

$$t_4 - t_{4,0} = gA_0\frac{\partial S_f}{\partial Q}q + \left[gB_0\left(S_{f0} - S_b\right) + gA_0\frac{\partial S_f}{\partial Y}\right]y \tag{3.15}$$

in which the friction slope S_f at stationary point (Q_0, Y_0) is derived as

$$\frac{\partial S_f}{\partial Q}\left(Q_0, Y_0\right) = 2\frac{S_{f0}}{Q_0} \tag{3.16a}$$

$$\frac{\partial S_f}{\partial Y}\left(Q_0, Y_0\right) = -2\frac{S_{f0}}{A_0}\frac{\partial A_0}{\partial Y} - \frac{4}{3}\frac{S_{f0}}{R_0}\frac{\partial R_0}{\partial Y} \tag{3.16b}$$

with

$$\frac{\partial A_0}{\partial Y} = B_0 \tag{3.17a}$$

$$\frac{\partial R_0}{\partial Y} = \frac{B_0}{P_0} - \frac{A_0}{P_0^2}\frac{\partial P_0}{\partial Y} \tag{3.17b}$$

Substituting equations 3.17a and 3.17b into 3.16b returns

$$t_4 - t_{4,0} = gA_0 S_{f0}\left[2\frac{q}{Q_0} - \left(\left(\frac{7}{3} + \frac{S_b}{S_{f0}}\right)\frac{B_0}{A_0} - \frac{4}{3P_0}\frac{\partial P_0}{\partial Y}\right)y\right] \tag{3.18}$$

Arranging terms q, y, $\partial q/\partial x$, $\partial y/\partial x$, the linearized momentum equation is ob-

tained

$$\frac{\partial q}{\partial t} + 2V_0\frac{\partial q}{\partial x} - \beta_0 q + \left(C_0^2 - V_0^2\right) B_0\frac{\partial y}{\partial x} - \gamma_0 y = 0 \tag{3.19}$$

where

$$\gamma_0 = V_0^2\frac{dB_0}{dx} + gB_0\left[KS_{f0} + S_b - \left(1 + 2Fr_0^2\right)\frac{dY_0}{dx}\right] \tag{3.20a}$$

$$\beta_0 = \frac{2g}{V_0}\left(Fr_0^2\frac{dY_0}{dx} - S_{f0}\right) \tag{3.20b}$$

$$K = \frac{7}{3} - \frac{4A_0}{3B_0P_0}\frac{\partial P_0}{dY} \tag{3.20c}$$

In case of the uniform steady flow in a channel with prismatic cross section: $dY_0/dx = 0$, $dB_0/dx = 0$, and $S_{f0} = S_b$, we obtain

$$\gamma_0 = gB_0S_b\left(1 + K\right) \tag{3.21a}$$

$$\beta_0 = -\frac{2gS_b}{V_0} \tag{3.21b}$$

$$K = \frac{7}{3} - \frac{4A_0}{3B_0P_0}\frac{\partial P_0}{dY} \tag{3.21c}$$

Both equations 3.8 and 3.19 are components of linearized SVEs which are able to describe the uniform flow in open channel flow. It is denoted that q is the deviation of discharge from equilibrium value Q_0, $y(x,t)$ is the deviation of water level form equilibrium value Y_0 , C_0 is the celerity, V_0 is the mean velocity, B_0 is the surface width, K is the geometry factor.

3.2.2 Linearization of the nonlinear first order time delay system

It is obvious that the flow routing in open channel flow is a delay process which also has attenuation of the peak flow. The phenomenon can be accurately described by a rational transfer function with delay (Rauschenbach, 2001). Therefore, the first order of delay model is considered to fully simulate the flow dynamics. The structure

of time delay model is selected as a nonlinear system with delay:

$$\begin{cases} \dot{\mathrm{q}}(\mathrm{t}) = \mathrm{f}\left(\mathrm{q}(\mathrm{t}), \mathrm{Q_{in}}(\mathrm{t})\right) \\ \mathrm{Q_{sim}}(\mathrm{t}) = \mathrm{h}\left(\mathrm{q}(\mathrm{t}-\mathrm{T_d}(\mathrm{q}))\right) \end{cases} \tag{3.22}$$

According to the Lemma 1 (Litrico et al, 2010), study an equilibrium point $f\left(Q_0, Q_{in,0}\right) = 0$, and a stable time invariant linear system with delay

$$\delta\dot{q}\left(t\right) = A\delta q\left(t\right) + B\delta Q_{in}\left(t\right) \tag{3.23a}$$

$$\delta Q_{sim}\left(t\right) = C\delta q\left(t - T_d\left(Q_0\right)\right) \tag{3.23b}$$

with

$$A = \frac{\partial f}{\partial q}\left(Q_0, Q_{in,0}\right) \tag{3.24a}$$

$$B = \frac{\partial f}{\partial Q_{in}}\left(Q_0, \bar{Q}_{in,0}\right) \tag{3.24b}$$

$$C = \frac{\partial h}{\partial q}\left(Q_0\right) \tag{3.24c}$$

Then the output $Q_{sim}(t)$ of the nonlinear system 3.22 beginning at $q(0) = Q_0$ with input $t \to \bar{Q}_{in} + \delta Q_{in}\left(t\right)$ is given by

$$Q_{sim}\left(t\right) = h\left(Q_0\right) + \delta Q_{sim}\left(t\right) + \varepsilon\left(\delta q, \delta Q_{in}\right) \tag{3.25}$$

where $\delta Q_{sim}\left(t\right)$ of the output of the linear system 3.23 starting at $\delta q\left(0\right) = 0$ with input $\delta Q_{in}\left(t\right)$, and ε is omitted at order 1 against its two arguments.

Apparently, there are several solutions existing to satisfy the relation between a nonlinear system and a family of linear system. Each term of the approximation system of the nonlinear system 3.22 is calculated around equilibrium point $Q = Q_0$.

$$A\left(Q_0\right) = -\frac{1}{T_c\left(Q_0\right)}; B\left(Q_0\right) = \frac{1}{T_c\left(Q_0\right)}; C\left(Q_0\right) = G \tag{3.26}$$

Finally, the representation of the linear first order time delay system that satisfy

the nonlinear the system 3.22 is derived as follow

$$\begin{cases} T_c \frac{dq}{dt} + q(t) = Q_{in}(t) \\ Q_{sim}(t) = Gq(t - T_d) \end{cases} \tag{3.27}$$

Where G is the gain; T_c is the time constant; T_d is the time delay; Q_{in} is the inflow at upstream end; Q_{sim} is the simulated flow at downstream of uniform part; q is the system state.

3.2.3 Derivation of the system transfer functions

The transfer functions (TF) of the systems are derived from frequency domain that explicitly express the relation of upstream discharge to discharge along the river

$$\mathrm{q_x(s) = TF(x, s)q_o(s)} \tag{3.28}$$

This ordinary differential equations 3.28 which are obtained by applying Laplace transformation to both linearized system 3.8, 3.19, and 3.27 contains variable x and is parameterized by the Laplace operator s (Dooge et al, 1987; Litrico and Fromion, 2004b). A function $\mathrm{f(x, t), t \geq 0}$, the temporal Laplace form is defined as follows:

$$\mathcal{L}\left[f(x,t)\right] = F(x,s) = \int_0^\infty f(x,t)e^{-st}dt \tag{3.29}$$

Then we obtain

$$\mathcal{L}\left[\frac{\partial f(x,t)}{\partial t}\right] = sF\left(x,s\right) - f\left(0^-\right) \tag{3.30a}$$

$$\mathcal{L}\left[\frac{\partial f(x,t)}{\partial x}\right] = \frac{\partial F(x,s)}{\partial x} \tag{3.30b}$$

$$\mathcal{L}\left[\frac{\partial^2 f(x,t)}{\partial x^2}\right] = \frac{\partial^2 F(x,s)}{\partial x^2} \tag{3.30c}$$

The boundary 0^- is as pre-conditional value of f that is selected to prevent problem of discontinuity of f at the origin (Lundberg et al, 2007).

In terms of SVEs, applying the Laplace transform to equation 3.8, 3.19 and rearranging the components we obtain

$$\frac{\partial q}{\partial x} = -B_0 s y \tag{3.31a}$$

$$\frac{\partial y}{\partial x} = \frac{1}{B_0\left(C_0^2 - V_0^2\right)}\left[\left(-s + \beta_0\right) q + \left(2V_0 B_0 s + \gamma_0\right) y\right] \tag{3.31b}$$

A linear ODE is formulated from the equations 3.31 a and b as follows

$$\frac{d}{dx}\begin{pmatrix} q_s(x) \\ y_s(x) \end{pmatrix} = TM(x,s)\begin{pmatrix} q_s(x) \\ y_s(x) \end{pmatrix} \tag{3.32}$$

with

$$TMs = \begin{pmatrix} 0 & -B_0 s \\ \frac{-s+\beta_0}{B_0\left(C_0^2 - V_0^2\right)} & \frac{2V_0 B_0 s + \gamma_0}{B_0\left(C_0^2 - V_0^2\right)} \end{pmatrix} \tag{3.33}$$

Substituting the equations 3.21 into the transfer matrix 3.33, and Froude number $Fr_0 = C_0/V_0$, the transfer matrix is given as

$$TMs = \begin{pmatrix} 0 & -B_0 s \\ \frac{2gS_b - V_0 s}{B_0 V_0 C_0^2\left(1 - Fr_0^2\right)} & \frac{2V_0 s + gS_b(1+K)}{C_0^2\left(1 - Fr_0^2\right)} \end{pmatrix} \tag{3.34}$$

The above ODE is able to simulate the flow rate Q and the water level y at downstream location corresponding to inflow $q_0(s)$ and water level $y_0(s)$ at upstream. To address the equation, the matrix $TM(s)$ is diagonalized.

$$TM\left(s\right) = X_s D_s X_s^{-1} \tag{3.35}$$

where

$$X_s = \begin{pmatrix} \lambda_1\left(s\right) & 0 \\ 0 & \lambda_2\left(s\right) \end{pmatrix} \tag{3.36a}$$

$$D_s = \frac{1}{B_0 s}\begin{pmatrix} B_0 s & B_0 s \\ -\lambda_1\left(s\right) & -\lambda_2\left(s\right) \end{pmatrix} \tag{3.36b}$$

$$X_s^{-1} = \frac{1}{\lambda_1\left(s\right) - \lambda_2\left(s\right)}\begin{pmatrix} -\lambda_2\left(s\right) & -B_0 s \\ \lambda_1\left(s\right) & B_0 s \end{pmatrix} \tag{3.36c}$$

Take determinant of the matrix

$$\det\left(\lambda I - TM\left(s\right)\right) = 0 \tag{3.37}$$

The eigenvalues are derived as:

$$\lambda_{1,2} = as + b \pm \sqrt{cs^2 + ds + b^2} \tag{3.38}$$

with

$$a = \frac{Fr_0}{C_0\left(1 - Fr_0^2\right)} \tag{3.39a}$$

$$b = \frac{\left(1 + K\right) B_0 S_b}{2A_0\left(1 - Fr_0{}^2\right)} \tag{3.39b}$$

$$c = \frac{1}{C_0^2\left(1 - Fr_0{}^2\right)^2} \tag{3.39c}$$

$$d = \frac{S_b B_0}{V_0 A_0} \frac{\left(2 + \left(K - 1\right) Fr_0{}^2\right)}{\left(1 - Fr_0{}^2\right)^2} \tag{3.39d}$$

$$Fr_0 = \sqrt{\frac{q^2 B_0}{g A_0{}^3}} \tag{3.39e}$$

The flow condition is supercritical for the Froude number $Fr_0 < 1$, a and b are thus positive. Hence, the positive root λ_1 is illustrated for waves propagating upstream while the negative root λ_2 represent waves toward the downstream. By using an assumption of semi-infinite river $x \to \infty$, the upstream wave λ_1 can be neglected and the simplified transfer function of SVEs is given by

$$\mathrm{q}\left(\mathrm{x}, \mathrm{s}\right) = \mathrm{e}^{\lambda_2 \mathrm{x}} \mathrm{q}\left(0, \mathrm{s}\right) \tag{3.40}$$

$$TF_{SVEs}\left(s\right) = e^{\lambda_2 x}; \lambda_2 = as + b - \sqrt{cs^2 + ds + b^2} \tag{3.41}$$

It is denoted that $q(x, s)$ is the flow rate at location x, $q(0, s)$ is the flow rate at upstream of the reach; λ_2 is that eigenvalue of transfer matrix TM.

Regarding the adaptive time delay model, the transfer function of the system

3.27 is given by Laplace transformation as follows

$$\mathrm{q}\,(\mathrm{x},\mathrm{s}) = \frac{G(x)e^{-sT_d(x)}}{1+sT_c(x)}\mathrm{q}\,(0,\mathrm{s}) \tag{3.42}$$

$$TF_{ATD}\,(x,s) = \frac{G(x)e^{-sT_d(x)}}{1+sT_c(x)} \tag{3.43}$$

Where G is the gain; T_c is the time constant; T_d is the time delay

3.2.4 Determination of the ATD model parameters by moment matching

To compute outflow of the river, the TF of SVEs must be transferred to time domain, which is not that simple with this hyperbolic system. Hence, we apply the approach suggested in (Dooge et al, 1987; Litrico and Fromion, 2004a) approximating the TF of SVEs by TF of ATD model in which the cumulants of both transfer functions are equated. As the SVEs will be approximated by the first order delay model, the accuracy of the simulated discharge will be enough by determining the first three cumulants of both TFs as described in the following approach:

1. Firstly, the cumulants of both TFs are derived by using Taylor development for the base-e logarithm of TFs, $ln[TFs]$ around $s = 0$ up to the second order

$$ln[TF\,(x,s)] = M_0\,(x) + M_1\,(x)\,s + M_2\,(x)\,s^2 + 0\left(s^3\right) \tag{3.44}$$

where $0(s)$ is a function of s so that $\lim_{s\to 0}\frac{0(s)}{s} = 0$, and cumulants M_k

$$M_k = (-1)^k \frac{d^k}{ds^k}(\ln\left[TF\,(x,s)\right])_{s=0} \tag{3.45}$$

For $k = 0$ to 2 we obtain

$$M_0\left(TF_{ATD}\right) = \ln G \tag{3.46a}$$

$$M_1\left(TF_{ATD}\right) = T_c + T_d \tag{3.46b}$$

$$M_2\left(TF_{ATD}\right) = {T_c}^2 \tag{3.46c}$$

$$M_0\left(TF_{SVEs}\right) = 0 \tag{3.47a}$$

$$M_1\left(TF_{SVEs}\right) = \frac{2}{\left(1+K\right)V_0} \tag{3.47b}$$

$$M_2\left(TF_{SVEs}\right) = \frac{\left[4-\left(K-1\right)^2 Fr_0^2\right]}{gS_b(1+K)^3 Fr_0^2} \tag{3.47c}$$

2. Secondly, the cumulants of the TF of SVEs are equated to those of the ATD model and consequently the ATD parameters are defined as follows:

$$T_c = \sqrt{\frac{4-\left(K-1\right)^2 Fr_0^2}{gS_b Fr_0^2(1+K)^3}2L} \tag{3.48}$$

$$T_d = \frac{2L}{\left(1+K\right)V_0} - T_c \tag{3.49}$$

where $G = 1$ is the gain, K is the geometry factor. These parameters will be applied in the ATD model in order to simulate outflow of a river reach.

It is noted that determination of the geometry factor K is very important, the simplified cross section with assumption of prismatic channel with particular shape of section are widely accepted in flow routing studies. In which, rectangular and trapezoidal geometry are popular. Utilization of both types of sections must follow the instruction of Ven Te Chow (Chow, 1959) that the rectangular can be used for a very wide river while the trapezoid is recommended to apply to a river which has a width smaller than ten times of water depth. The factor K for rectangular cross section is presented by (Litrico et al, 2010). In terms of trapezoidal cross section, the factor K is introduced in the following section.

3.3 The ATD model for a river with trapezoidal cross section

3.3.1 Approach

Flash flood forecasting at in narrow rivers is very important in flood mitigation as well as reservoirs operation. It is vital to extend the model to prismatic trapezoidal channel cross sections in order to not only broaden the model's applicability, but also to improve its accuracy. The geometry coefficient K in equation 3.21c thus has to be defined by different manner from which K contains two variables: water level y and flow rate Q. With assumption of uniform river flow, y which is related to Q will be estimated by the method of section factor $AR^{2/3}$ for uniform flow computation (Chow, 1959).

$$AR^{2/}3 = \frac{nQ_{sim}}{\sqrt{S_b}}; A = (b + my)\, y; R = A/P; P = b + 2y\sqrt{1 + m^2} \tag{3.50}$$

substituting the equation 3.50 into the equation 3.21c and 3.39e, the K and Fr are derived

$$K = \frac{7}{3} - \frac{8}{3}\frac{(b + ym)\, y\sqrt{1 + m^2}}{\left(b^2 + 2yb\left(m + \sqrt{1 + m^2}\right) + 4my^2\sqrt{1 + m^2}\right)} \tag{3.51}$$

$$Fr^2 = \frac{Q^2\,(b + 2my)}{g(b + my)^3 y^3} \tag{3.52}$$

The left side of equation 3.50 is a section factor $AR^{2/3}$ depending on the geometry of the water area (water level y, side slope m, and bottom width b) whilst the right side is determined by Manning coefficient n, discharge Q, and bottom slope S_b. As water level y is a variable, all parameters are expressed according to y. The procedure to determine the ATD model parameters as functions of Q, n, S_b, and y is illustrated in figure 3.2. Two components are presented in the flowchart as follows:

The model calibration is basically a least square nonlinear optimization technique with constraint that minimizes a quadratic error of simulated and observed outflow Q or water level y. The two possible objective functions are expressed in 3.53. All

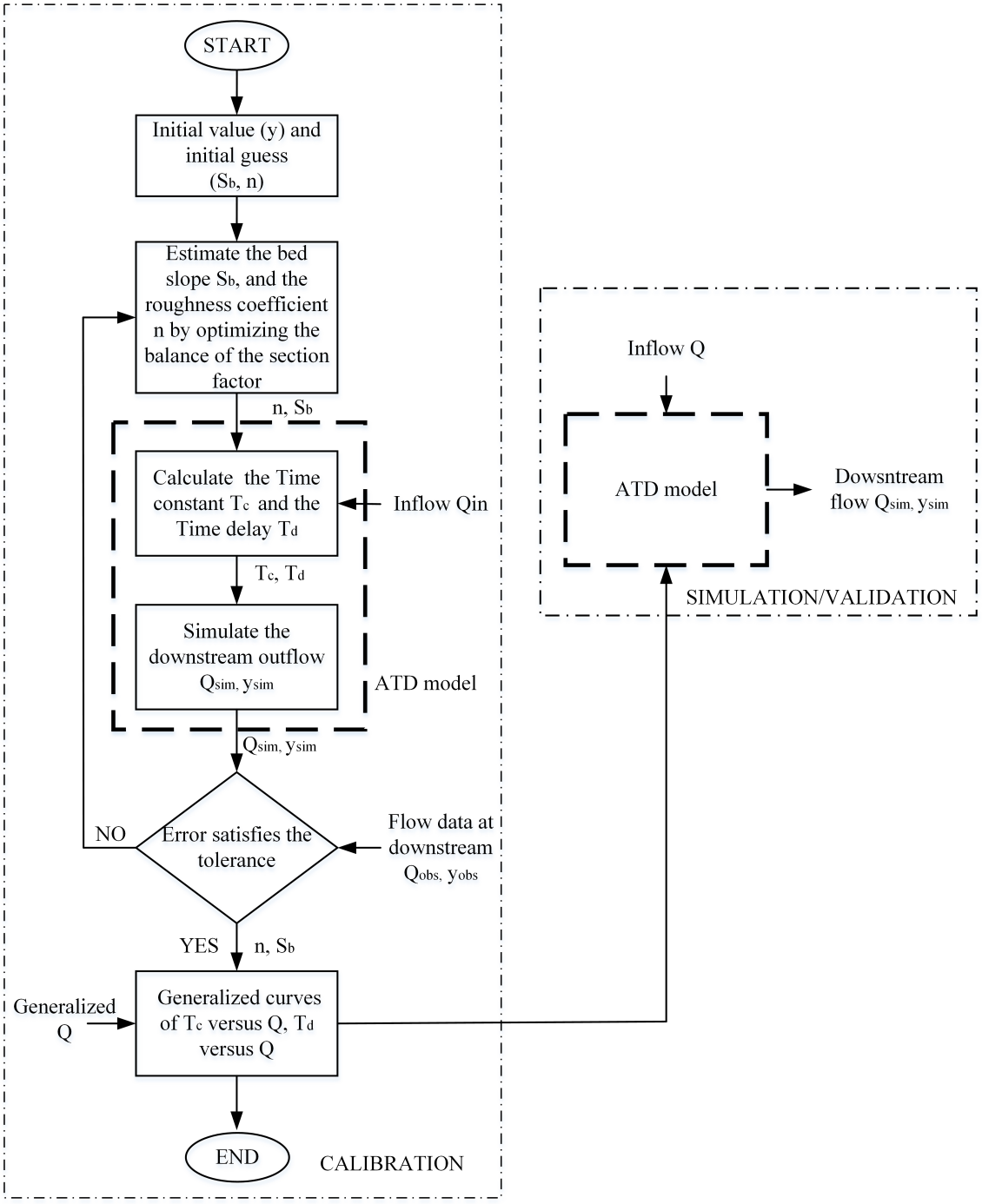

Figure 3.2: The flowchart for calibration and validation of an adaptive time delay model for river with prismatic trapezoidal cross section

of physical parameters such as the Manning coefficient n, and river bed slope S_b will be estimated in order to simulate outputs y_{sim} and Q_{sim}. According to the equation 3.54 and 3.55, the limitation of the roughness n and the bed slope S_b can be defined by the investigation of the previous studies of the research area as well as from the literature such as (Chaudhry, 2007; Sturm, 2010; Chow, 1959). At first, with the initial guess of S_b, n and initial value of y, an iterative process starts approximating the water level y. Subsequently, parameters Froude number Fr, geometry coefficient K, time constant T_c, and time delay T_d, are derived. The outflow of a reach is estimated by the fourth order Runge Kutta. The simulated flow is then compared to observed data. The iteration proceeds until the objective funtions are satisfied so that a best match between simulated and observed outputs is achieved as evaluated by the Nash-Sutcliffe Efficiency (NSE) (3.56) and Percent bias (PBIAS) (3.57). The outputs of calibration are the roughness n and the bed slope S_b.

$$\min \sum_{i=1}^{I} \left(Q_{obs,i} - Q_{sim,i}\left(S_b, n\right)\right)^2; \min \sum_{i=1}^{I} \left(y_{obs,i} - y_{sim,i}\left(S_b, n\right)\right)^2 \tag{3.53}$$

subject to

$$n_{\min} \leq n \leq n_{\max} \tag{3.54}$$

$$S_{b\min} \leq S_b \leq S_{b\max} \tag{3.55}$$

$$\text{NSE=1-}\left[\frac{\sum_{\text{i=1}}^{\text{I}}\left(\text{Q}_{\text{obs,i}}\text{-Q}_{\text{sim,i}}\right)^2}{\sum_{\text{i=1}}^{\text{I}}\left(\text{Q}_{\text{obs,i}}\text{-Q}_{\text{mean,i}}\right)^2}\right];\text{NSE=1-}\left[\frac{\sum_{\text{i=1}}^{\text{I}}\left(\text{y}_{\text{obs,i}}\text{-y}_{\text{sim,i}}\right)^2}{\sum_{\text{i=1}}^{\text{I}}\left(\text{y}_{\text{obs,i}}\text{-y}_{\text{mean,i}}\right)^2}\right] \tag{3.56}$$

$$\text{PBIAS=1-}\left[\frac{\sum_{\text{i=1}}^{\text{I}}\left(\text{Q}_{\text{obs,i}}\text{-Q}_{\text{sim,i}}\right)100}{\sum_{\text{i=1}}^{\text{I}}\text{Q}_{\text{obs,i}}}\right];\text{PBIAS=1-}\left[\frac{\sum_{\text{i=1}}^{\text{I}}\left(\text{y}_{\text{obs,i}}\text{-y}_{\text{sim,i}}\right)100}{\sum_{\text{i=1}}^{\text{I}}\text{y}_{\text{obs,i}}}\right] \tag{3.57}$$

After the calibration, the roughness n and the bed slope S_b are determined. The parameters T_c and T_d of the ATD model can be calculated in order to approximate the outflow of other flow. Nevertheless, it is proposed that the general relationship of T_c and T_d with Q are earlier developed and then are used to calculate the outflow of different scenarios by the linear interpolation. This method apparently reduces the computation time and maintains the simulation accuracy. However, the inflow must be in the valid range of the curves T_c vs Q and T_d vs Q so that the stability of the model is assured.

In terms of validation, the curves T_c versus Q and T_d versus Q which are used as parameters of ATD model for unknown flood event, and again evaluated by Nash-Sutcliffe Efficiency (NSE) (3.56) and Percent bias (PBIAS) (3.57). It is noted that maximum and minimum values of the flow of the unknown flood event must be within a valid range of the flow rate of the ATD model. Otherwise, the simulated hydrograph will be discontinued at the point where the inflow are not within the range.

3.3.2 Application of the ATD model (A case study)

To illustrate the performance of the ATD model, a small river reach located on an upstream part of Thu Bon River in central area of Vietnam is selected which is shown in figure 3.3. The reach starts from Nong Son gauge station and ends at Giao Thuy gauge station. The geometry data of the river reach is listed in table 3.1. 1-year-period upstream and downstream flow data at both gauge stations are considered as referenced data for the simulations. According to the collected data at Giao Thuy, water depth reaches from 5.0m to 8.0 m during main flood season. It is suggested that the ATD with trapezoidal geometry should be utilized to enhance good accuracy in estimating the flood peak in this narrow but deep stream. The idea is that the ATD model parameters will be calibrated using the referenced data

for 3 months of main flood season (October-December) to obtain the relation curves $Q \quad vs \quad T_c$ and $Q \quad vs \quad T_d$ for a wide range of discharge Q. After calibration the model is validated using reference data from the drought season (January-June) and compared to the model given in (Litrico et al, 2010). In addition, the estimated parameters must satisfy the constraints presented in table 3.2.

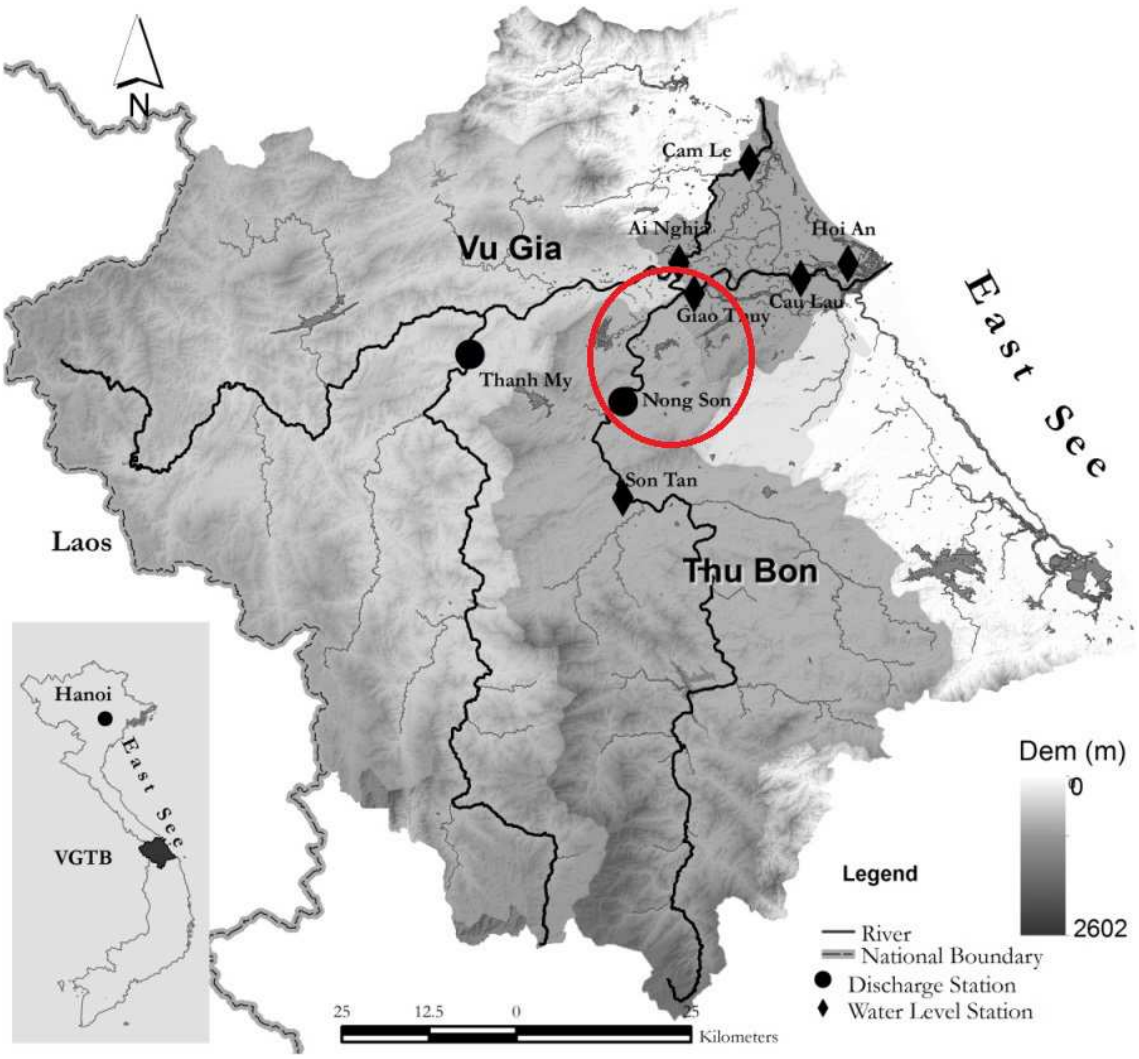

Figure 3.3: Location of the selected river reach at Vu Gia Thu Bon river basin in Central Vietnam

The ATD model calibration results are depicted in figure 3.4. The model uses geometry data in table 3.1 and 3 months of upstream main flood (see, figure 3.4a) to simulate the downstream flood of which returns both flow rate and water level. The time interval of flow data is 10 minutes. Figure 3.4b presents the simulated and observed discharge. For figure 3.4c shows the water level estimated by ATD model against the measured data. The accuracy of the model is quantified in the table

Table 3.1: Characteristic of studied river reach at upstream Vu Gia Thu Bon river basin

Geometry data			Flow data with dt = 10 minutes	
L (km)	b (m)	m	Upstream observed flow rate at Nong Son station	Downstream observed water level at Giao Thuy station
22	40	2	1 year period of 2010	1 year period of 2010

Table 3.2: Lower and upper limits on physical parameters

Parameter	Min value	Max value
Manning coefficient, n	0.01	0.07
Bed slope, Sb	0.00008	0.0025

3.3 which shows a NSE coefficient equals to 0.94 for both Q and y while PBIAS reaches -10.5 for Q and –6.5 for y. This indicates that the ATD model returns a very good result according to the guidelines of evaluating stream flow models in (Moriasi et al, 2007). During calibration, the roughness n and the bed slope S_b of the river reach are determined. In table 3.3, n and S_b are also shown as 0.035 and 0.0014, respectively.

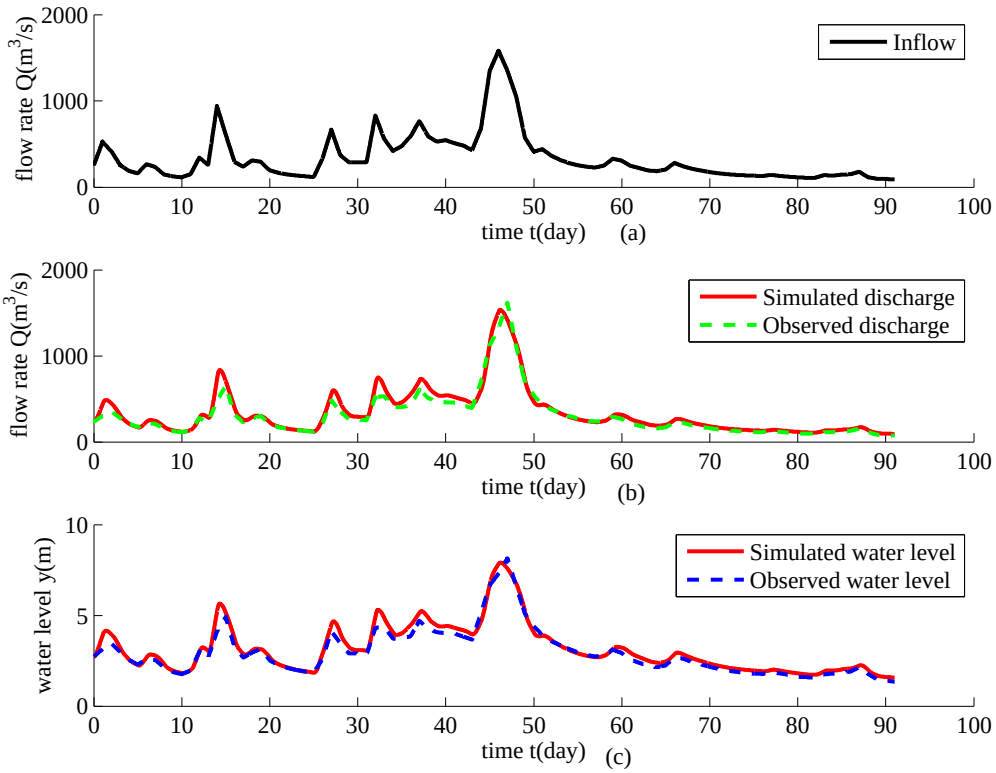

Figure 3.4: Model calibration results for the two objective functions for discharge and water level

After calibration, the generalized nonlinear relationships between the time constant T_c , the time delay T_d and the discharge Q are determined as depicted in figure 3.5. The time constant T_c varies from approximately 30 minutes to 40 minutes when flow rate changes between 5 m^3/s to 2000 m^3/s. Whereas, the time delay T_d varies from 60 minutes to almost 350 minutes in the same variation range of flow rates. The linearly interpolated parameters values from these curves are directly used by ATD model to simulate downstream flood in different upstream flood scenarios. This approach significantly reduces the computation time as well as raises feasibility for real time flood simulation application. Based on estimated parameters, it should be a deep river with stone and weeds at the bottom that is in accordance with attributes of the selected river reach located in mountainous area of Vu Gia Thu Bon basin at which agriculture and forest land exist (Mai, 2009).

The validation task is executed by applying the calibrated curves of T_c vs Q and T_d vs Q to simulate outflow for 6 months of drought period. The result is depicted in figure 3.6. Generally, the model shows a very good result presented by the NSE

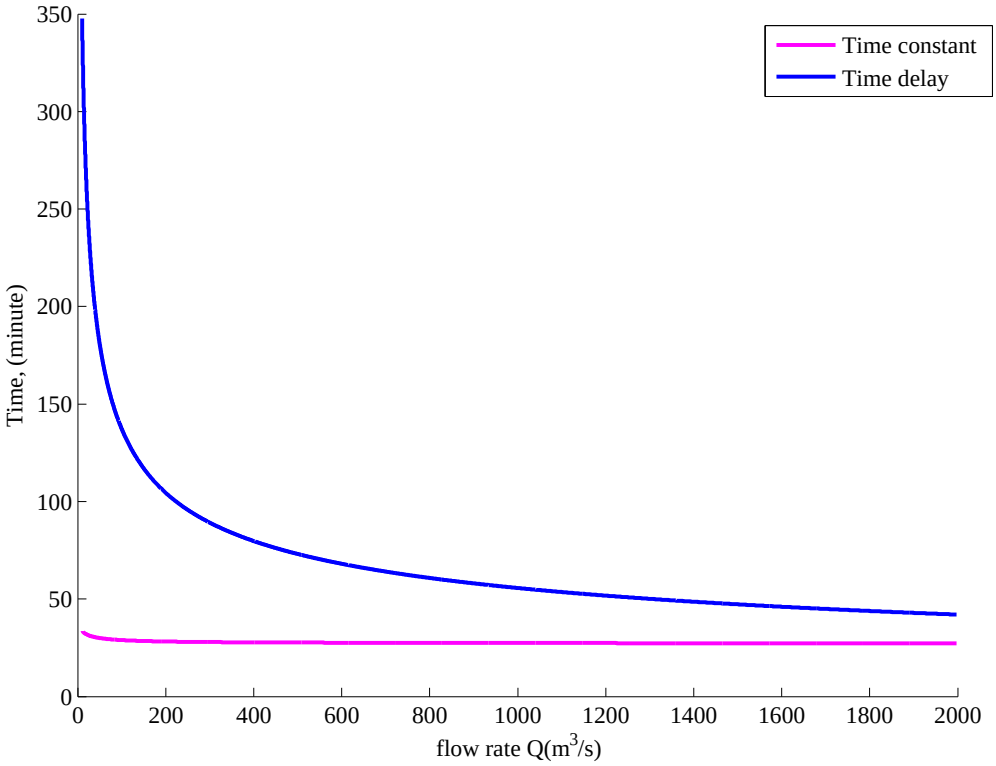

Figure 3.5: Time constant T_c and Time delay T_d versus inflow Q

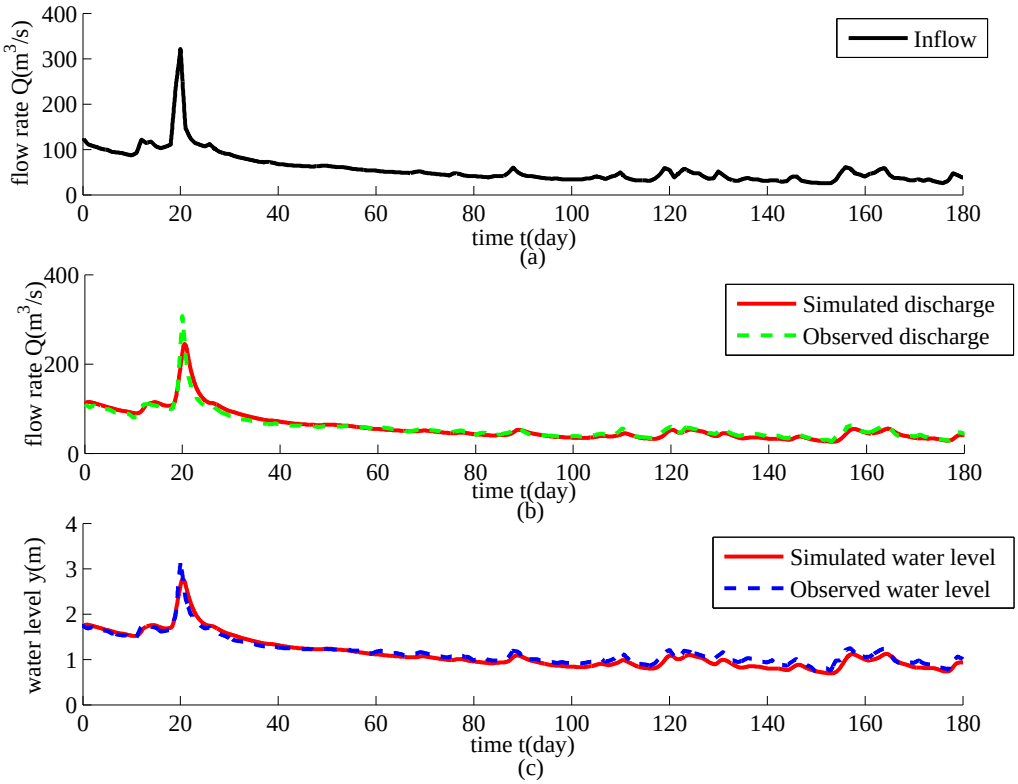

Figure 3.6: Model validation results

Table 3.3: Results of calibration, validation and estimated model parameter

Criteria	Calibration		Validation		Model parameter	
	Q	y	Q	y	n	Sb
NSE	0.94	0.94	0.91	0.9	0.035	0.0014
PBIAS	-10.5	-6.5	0.68	4.06		

of 0.91 for Q and 0.90 for y as well as by $PBIAS$ of 0.68 for Q and 4.06 for y, (see table 3.3). As in (Moriasi et al, 2007) this proves that the model is valid for application to flow routing of this river reach.

The performance of the ATD model in comparison to the model in (Litrico et al, 2010) based on rectangular profile is also evaluated for the main flood season. The measured water level is used to evaluate the goodness of both models. The technique for approximating water level from section factor (Chow, 1959) is applied to simulate the water level from the flow rate estimated by the model in (Litrico et al, 2010). The results are shown in figure 3.7 and table 3.4. It can be seen that the water level of the ATD model matches with observed stage better than the water level of the model in (Litrico et al, 2010). In terms of NSE, the accuracy of ATD model for this case study is 0.94 compared to 0.89 of the model in (Litrico et al, 2010). In figure 3.7, it is clear that assuming a rectangular profile overestimates the water level peak of 8.1 m in period time t from the day 45 to 47 by approximately 1.0 m compared to the ADT model which underestimates by only 0.2 m. Therefore, the ATD model returns more accurate results for the same hydrological conditions. This has very important role for decision maker who can determine an effective plan of flood prevention.

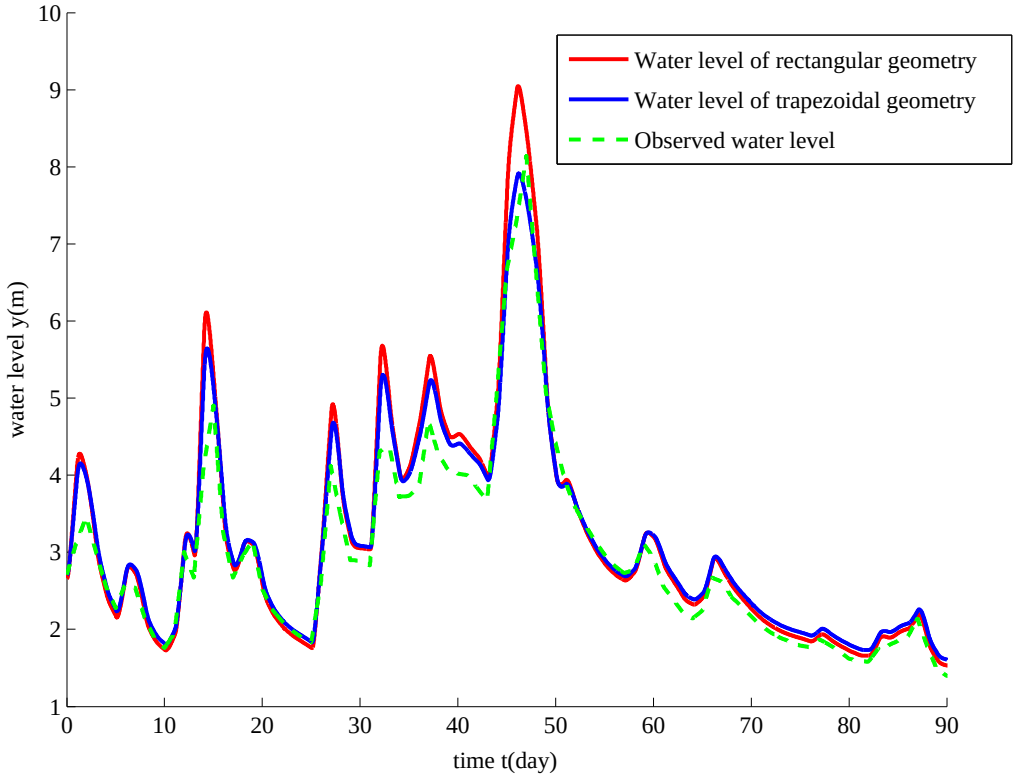

Figure 3.7: Comparison between ATD model with trapezoidal and rectangular geometry

Table 3.4: Result of 2 models comparison

Criteria	Trapezoid	Rectangular
NSE	0.94	0.89
Deviation (m)	0.2	1

3.4 Conclusion

In this chapter, a fundamental method for approximating the SVEs by an adaptive time delay model is presented. In addition, the ATD based on a prismatic trapezoidal geometry is introduced. The model is an extension of the river model developed in (Litrico et al, 2010) for very wide rectangular cross section channel. The method uses moment matching to derive the parameters of the model from linearized SVEs model. The application scope of the time delay models is also now opened for small deep rivers. After calibration of the model to obtain the nonlinear relation curves of T_c and T_d against Q, the outflow simulation for different scenarios

becomes very simple, fast and accurate. Therefore, this method can be utilized to simulate, and design control strategies for river systems. Although the application of the model in case study showed very promising results, further improvement with downstream boundary conditions may expand the applicability of the model. Hence, taking account of backwater effect caused by boundary condition in this ATD model would be beneficial and is going to be studied thoroughly in the next chapter.

Chapter 4

Adaptive time delay model with backwater effect

4.1 Introduction

The phenomena of backwater effect is a result of impact of downstream boundary condition (hydraulic structures, tide, river junctions) on the gradually varied flow that increases upstream depth. Typically, backwater is caused by downstream dam (weir, reservoir) which is significantly studied due to its impacts on upstream flood, energy production, and so on. When water starts flowing into reservoirs, the end point of backwater may shift either upstream or downstream depending on several factors, for instance, geometry characteristic of river (channel condition, cross sections, flood plains), or downstream boundary conditions (downstream water works, river tributaries). In field studies, the intersection point is considered as an approximate point of tangency of normal depth line to backwater curve. It may be specified by observation from drawing of flow profiles. The determined intersection point generally moves toward upstream when flow rate increases. According to previous researches, the restriction of upstream movement of backwater should be considerably defined to satisfy given requirement. The backwater profiles are commonly obtained by combining the differential equations of flow resistance and boundary conditions (Chanson, 2004). Neglecting backwater effects lead to large deviation in estimating the model parameters such as: time responses, peak time, and attenuation. Therefore, the chapter introduces an advancement that coupling

an adaptive time delay model and a reservoir model can be used for simulation of backwater effects. Firstly, the approximation of the backwater curve using a reservoir model is described, followed by the procedure for coupling the ATD model and the backwater model.

Figure 4.1 illustrates the backwater curve which defines the steady state water level for a given flow rate Q and a water depth y_L at downstream boundary. Obtained from reduced SVEs, the backwater can be approximated by the following reservoir model (Litrico and Fromion, 2009):

$$\frac{dy}{dx} = \frac{S_b - S_f}{1 - Fr^2} = S_L \tag{4.1}$$

In case of a river with infinite length, $x \to \infty$, then $\frac{dy}{dx} \to 0$, so $y \to y_n$, the uniform depth, S_L is the deviation of the line tangent of the backwater curve to it at downstream end, Fr is the Froude number. According to (Litrico and Fromion, 2004a; Schuurmans et al, 1999b) the backwater is described by 2 two pools connected together. The upstream part of the backwater curve corresponding to the uniform part is approximated by straight line parallel to bottom slope. The downstream part is approximated by the straight line tangent to the free surface at the downstream end. The intersection between to two lines exists at abscissa x_1

$$x = \begin{cases} \max\left(L - \frac{y_L - y_n}{S_L}, 0\right), S_L \neq 0 \\ L, S_L = 0 \end{cases} \tag{4.2}$$

The backwater curves is approximated as

$$y\left(x\right) = \begin{cases} y_1, x \in [0, x_1] \\ y_1 + (x - x_1)S_b, x \in [x_1, L] \end{cases} \tag{4.3}$$

with

$$y_1 = \begin{cases} y_n, x_1 \neq 0 \\ y_L - LS_L, x_1 = 0 \end{cases} \tag{4.4}$$

On the one hand, $x_1 \neq 0$, $y_1 = y_n$ is the part of channel effected by uniform flow and $y_1 = y_L - LS_L$ is the part of channel influenced by backwater. On the other hand, $x_1 = 0$, $y_1 = y_L - LS_L$, the whole channel reach is affected by backwater effect.

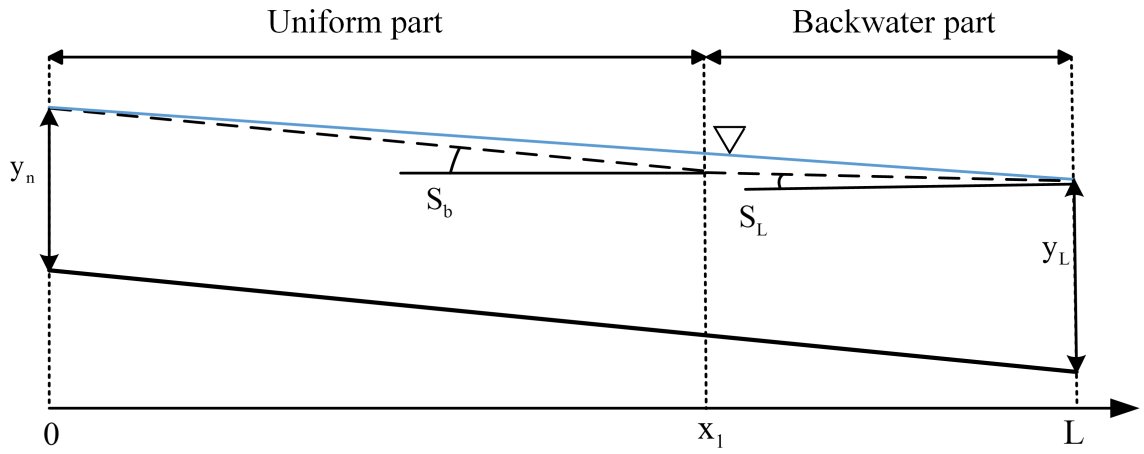

Figure 4.1: Backwater approximation approach

4.2 Coupling ATD model with backwater model

The author suggests the new approach that couples the ATD model with backwater model (reservoir model) taking into account for downstream feedback (see figure 4.2). The mathematical representation is shown in equations 4.5 and 4.6.

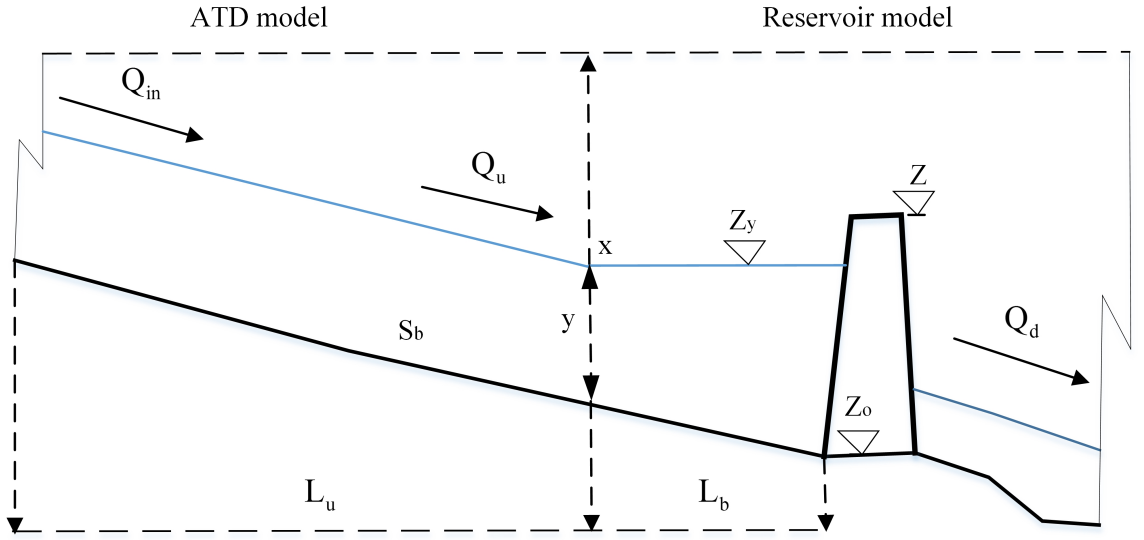

Figure 4.2: The selected river system

$$\begin{cases} T_c \frac{dq}{dt} + q(t) = Q_{in}(t) \\ Q_u(t) = q(t - T_d) \end{cases} \tag{4.5}$$

$$\frac{d\vartheta}{dt} = Q_u(t) - Q_d(t) \tag{4.6}$$

where Q_{in} is upstream flow, Q_u is flow into the reservoir, Q_d is downstream

discharge of the reservoir, $\vartheta(t)$ is storage of the reservoir, Z is the crest elevation; Z_o is the elevation of dam toe; Z_y is the water level elevation.

The model is then able to simulate dynamics of non-uniform flow. Differently with steady state modeling, the backwater part x_1 in this model changes against variation of discharges. It is apparent that due to the coupling, the parameters of T_c and T_d of the ATD model (uniform part) are now functions of flow rate Q and a uniform part of channel L_u. The upstream discharges will be transferred to downstream where its dynamic is altered by downstream boundary. Then, the water level of the pool is calculated, length of backwater curve L_b and uniform curve L_u are determined. Afterwards, these obtained information will be used for the next calculation. Figure 4.3 describes the procedure of calibration and simulation of the ATD model and the backwater effect model.

Fundamentally, the calibration task is similar to the one presented in the previous section. The objective function and the restrictions are shown in equations 4.7, 4.8. It is significant that because the water profile is close to horizontal in the backwater area (Schuurmans et al, 1995) and the water level in the reservoir is the same as the water level at the cross section where the intersection point is located. In particular, the process involves selecting the cross section at the intersection point and calibrating the coupled model to the measured water level y at the reservoir. According to the flowchart in the figure 4.3, the procedure firstly approximates the water level y with the initial values of L_u and y_o and initial guess of S_b, n. Then, parameters T_c and T_d of the ATD model are derived. The flow rate at the intersection point denoted by Q_u which is calculated by the fourth Runge Kutta is also the flow into the reservoir. It is different with the flow chart 3.2 that the water level is derived by the backwater model after calculating the water balance of the reservoir. The simulated water level is then compared to the measured data. The iteration process is ended when the objective function is satisfied. The model performance is evaluated by the NSE (3.56) and PBIAS (3.57). The outputs of calibration also consist of the roughness n and the bed slope S_b.

$$\min \sum_{\mathrm{i}=1}^{\mathrm{I}} \left(\mathrm{y_{obs,\,i}} - \mathrm{y_{sim,\,i}}(S_b, n)\right)^2 \tag{4.7}$$

the following equations show the minimum and maximum limit on roughness

coefficient n, bed slope S_b, and water level y

$$n_{\min} \leq n \leq n_{\max} \tag{4.8}$$

$$S_{b\min} \leq S_b \leq S_{b\max} \tag{4.9}$$

$$y_{\min} \leq y_i \leq y_{\max} \tag{4.10}$$

It is different with the ATD model in chapter 3 that the T_c and T_d are functions of both Q and L_u which are significantly impacted by the downstream boundary. Using the curves T_c vs Q and T_d vs Q to simulate the downstream flow of other simulation scenarios which have different downstream conditions is not possible.

Regarding validation or simulation task, the calibrated roughness n, and the bottom slope S_b are used to simulated the water level in the reservoir for random flood event, and again evaluated by Nash-Sutcliffe Efficiency (NSE) (3.56) and Percent bias (PBIAS) (3.57).

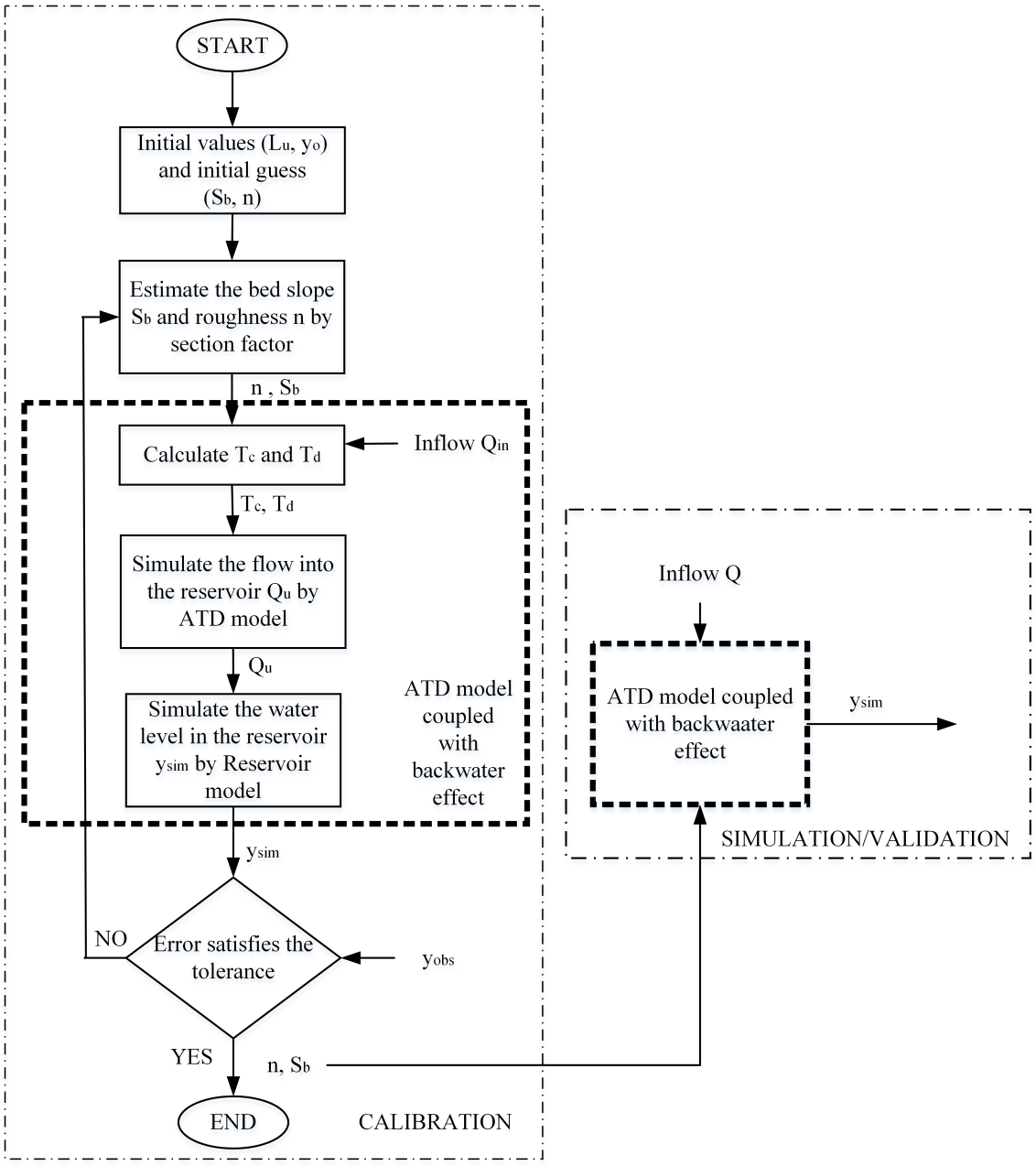

Figure 4.3: The flowchart for calibration and validation of a coupling of the ATD model and the backwater model

4.3 Application of backwater model (A case study)

The system includes two components: an upstream river reach and a weir at downstream end in the case study as illustrated in figure 4.2 and in table 4.1. The first component is the river reach whose parameters are calibrated in previous section is chosen for this application. The physical characteristics of the reach are presented in table 4.1. The second component is a weir which is located downstream of the

Giao Thuy station. The distance from the Giao Thuy station to the weir is assumed of 15.5 km approximately which can be considered as the upstream reservoir area created by the weir. The weir has a width $B = 40\ m$, the crest elevation at $Z = 20\ m$ and the dam toe at $Z_o = -5\ m$. The storage capacity of weir is determined by the curve of reservoir water level and storage as shown in figure 4.4. The 4-day data series of upstream flow rate is used to test the model. Time interval of data is 10.0 minutes. Because the upstream reach is well validated in previous section, its parameters can be directly used for simulation. It should note that the total length of upstream river reach which is the sum of the river reach length and the reservoir area, is 37.8 km. The impacts of the downstream boundary condition that the water flowing from upstream Q_{in} is accumulatively stored in downstream reservoir resulting in non-uniformity of water level in upstream channel is considerably analyzed. At the weir, the amount of water Q_d is also released to downstream due to demand of water users.

Table 4.1: Characteristic of the weir

Geometry data					Flow data with dt =10 minutes	
$Z(m)$	$Z_o(m)$	n	S_b	$L(km)$	$Q_{in}(m^3/s)$	$Q_d(m^3/s)$
20	-5	0.035	0.0014	37.8	4 day period	4 day period

The results of simulation using the model are illustrated in figures 4.5 and 4.6. Figure 4.5a shows the dynamic situation of the system. The blue line is used to show upstream flow which ranges from 2.93 to 42.47 m^3/s. The dash green line represents the hydrograph at the end of uniform part of channel which is propagated by the ATD model and reaches a peak value of 40.03 m^3/s. According to figure 4.5b, the red line shows amount of discharge preserved in the reservoir. After water balance calculation, the stored discharge rises from 1.93 m^3/s to 39.03 m^3/s. While, a constant amount of discharge of 1.0 m^3/s is continuously released to the downstream. According to figure 4.6, the situation is different for the black line representing the volume of flow stored in the reservoir. At the end of simulation period, the reservoir accumulates water volume up to 3730 $10^4 m^3/s$ and the reservoir water level reaches 17.37 m which is still under the reservoir restriction. This means that all of incoming water is hold by the reservoir.

Figure 4.7 shows the variation of the water surface and the channel bottom

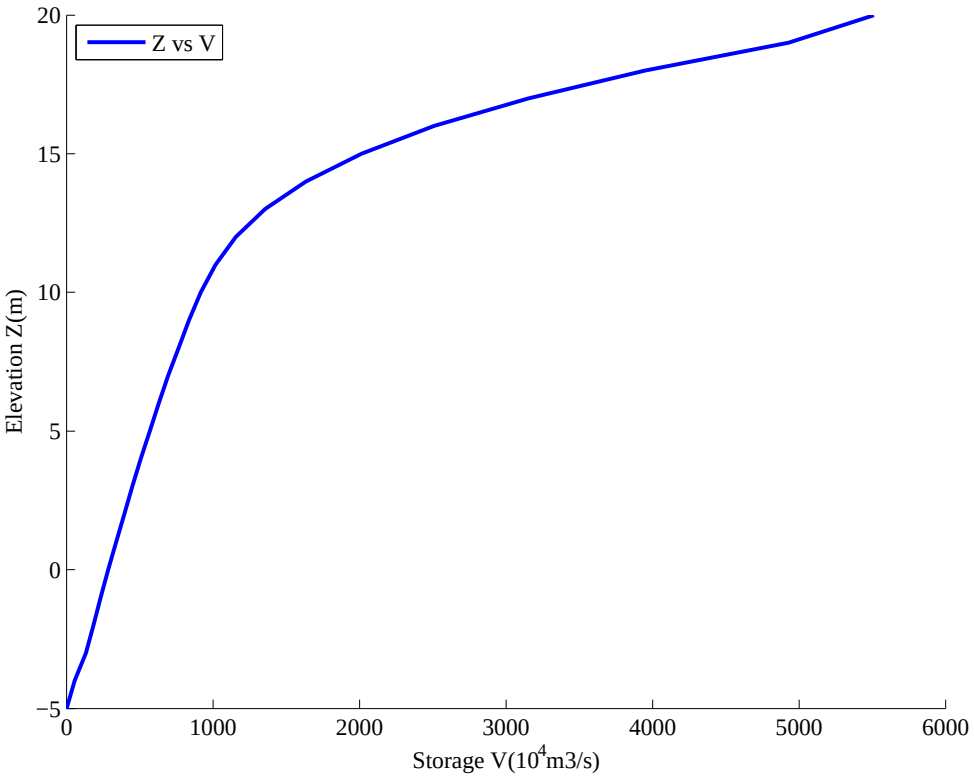

Figure 4.4: Characteristic curve of downstream reservoir

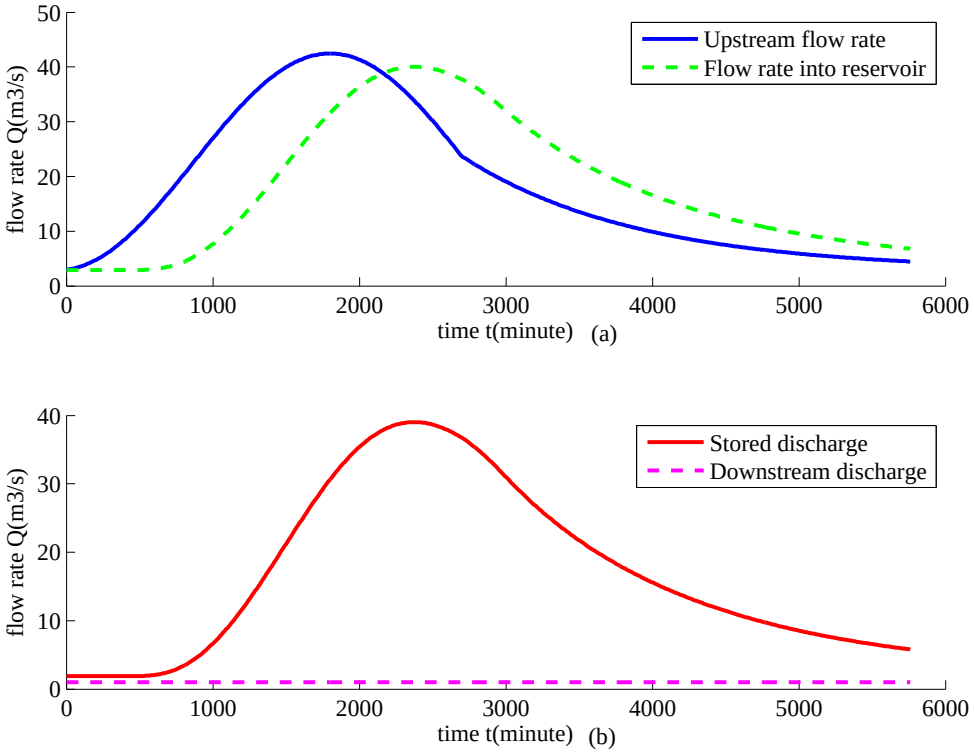

Figure 4.5: Discharge simulation

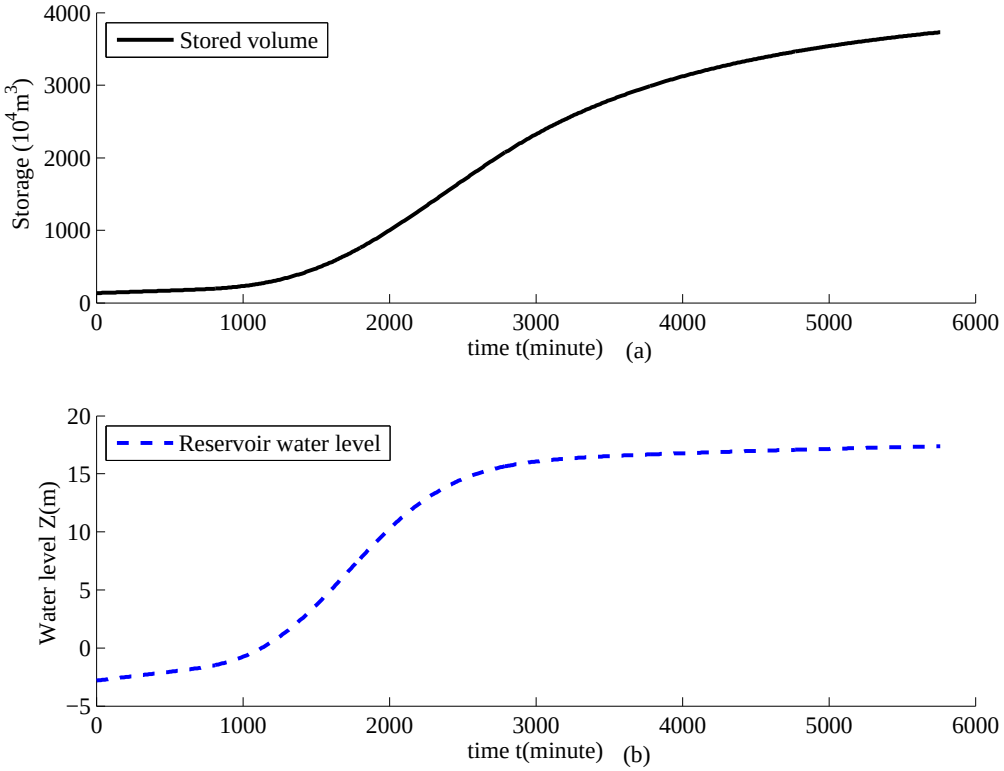

Figure 4.6: Simulation of volume and water level in the reservoir

according to the distance L and time t. The elevation of bottom channel which is calculated from the bottom slope S_b and elevation of dam toe Z_o change from -5.0 m to 47.9 m from upstream to downstream. The water surface consists of 2 parts: backwater part L_b and uniform part L_u which are separated at the intersection point x. The black line present changes of intersection point x which is determined by the change of L_b. L_b gradually rises from 1429 m to 15744 m while the L_u declines from 36371 m to 22056 m. Temporally, the water level in reservoir goes up from -2.81 m to 17.37 m and water depth in the uniform part fluctuates from 0.2 m to almost 1.0 m. Section A-A in figure 4.8 shows the stationary regime of the non uniform flow against a the time step $t = 2000$ minutes. The blue line is the water surface whose elevation is approximately 10 m in reservoir and goes up to 47.0 m in the channel upstream. The red line present the river bed.

Figure 4.9 shows the alternation of backwater pool and uniform pool through variables L_b, and L_u in response with water level in the reservoir Z and time t. Backwater part denoted by L_b is specified by the red line. The backwater expansion

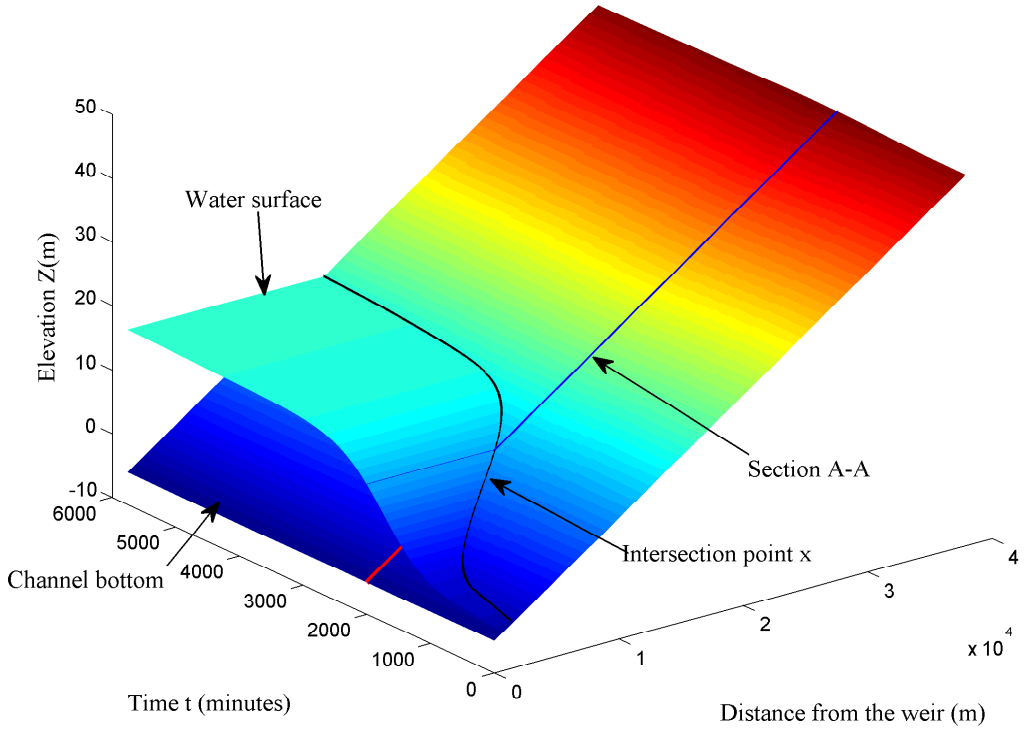

Figure 4.7: 3-D representation of non uniform flow

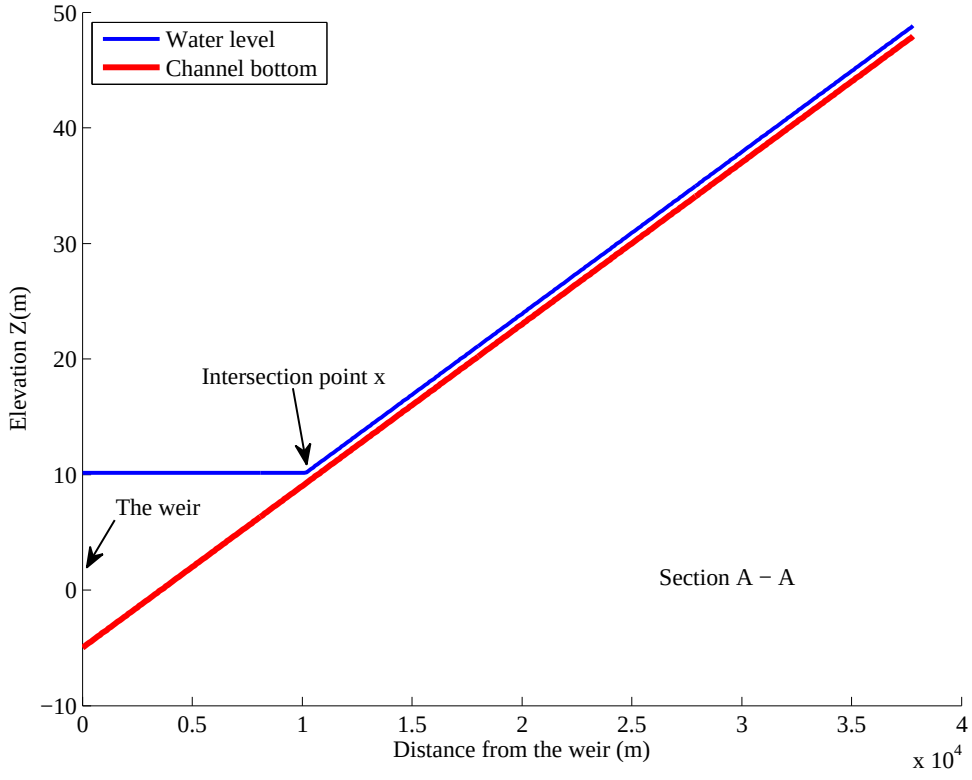

Figure 4.8: Section A-A: Non uniform flow

is directly proportional to change of water level Z and time t which is illustrated by an increase of L_b from 1429 m to 15744 m in response to the water level rising from -2.81 m to 17.37 m. Since the inflow reaches peak value, the maximum water level Z is at 17.37 m, the backwater pool L_b theoretically reaches a maximum value at 15744 m . On the other hand, the uniform pool denoted by a blue line is adversely proportional to variation of water level Z and time t. This pool area reduces from 36371 m to 22056 m. The reach length L is 37800 m described by the black curve. It is the sum of L_u and L_b.

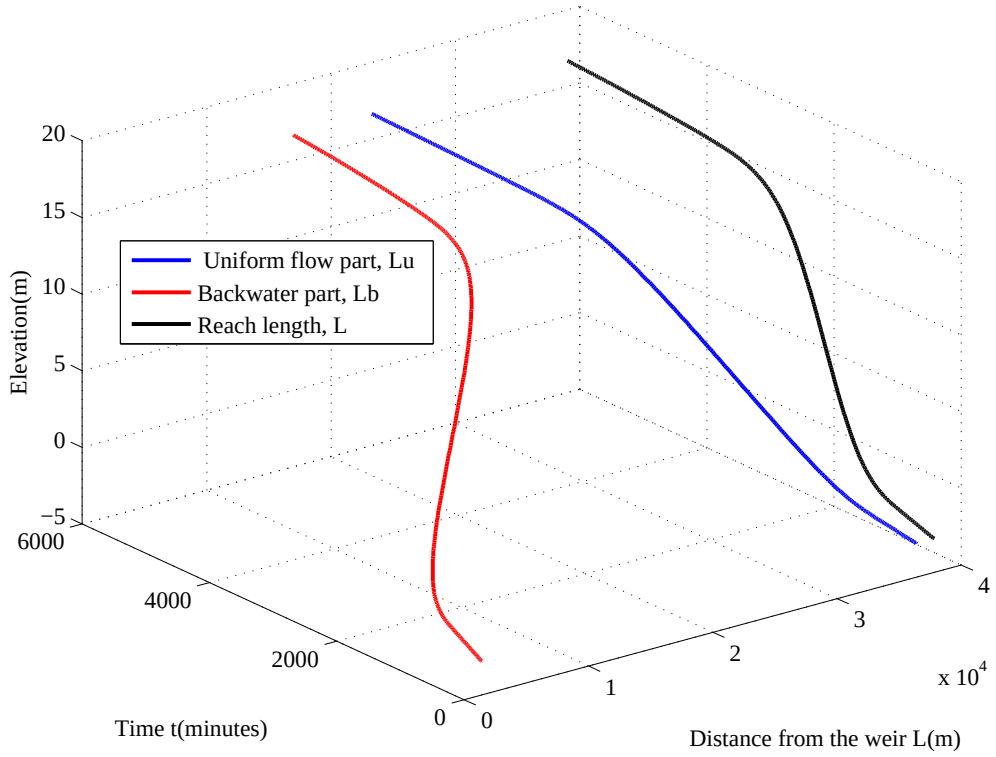

Figure 4.9: Variation of uniform part and backwater part of channel

Figure 4.10 presents parameters of ATD model: time constant T_c, and time delay T_d which are obtained from inflow Q_{in} and the length of uniform pool L_u for the first pool. The red curve shows the relationship of T_c versus Q and L_u while the blue one illustrates the behaviors of T_d versus Q and L_u. The attenuation of hydrograph is parameterized by time constant T_c. The first part of T_c ranging from 50 - 30 minutes which corresponds to the L_u from 36371 m to 29325 m determines the upward shape of the hydrograph Q from base flow $2.93m^3/s$ to peak value approximately

$42.47m^3/s$. The last part varying from 30 - 40 minutes with the change of L_u from 29325 m to 22056 m can forms the shape of downward side from peak to base value. Furthermore, the time delay is a determinant factor of the shift of the hydrograph. Similar to T_c, the first side of T_d: 960 - 250 minutes decides the delay time of rising curve of Q whereas the other side: 250 - 500 minutes is used for the transition of the recessing part. During the simulation, the reservoir continuously stores more water which leads to the gradual decrease of the L_u from 36371 m to 22056 m and the increase of the L_b from 1429 m to 15744 m. It is noted that the computation takes 10.30 seconds when using the computer with configuration: processor of Intel Core I7-4500U 1.8GHz and the random-accsess memory (RAM) of 8 Gigabytes.

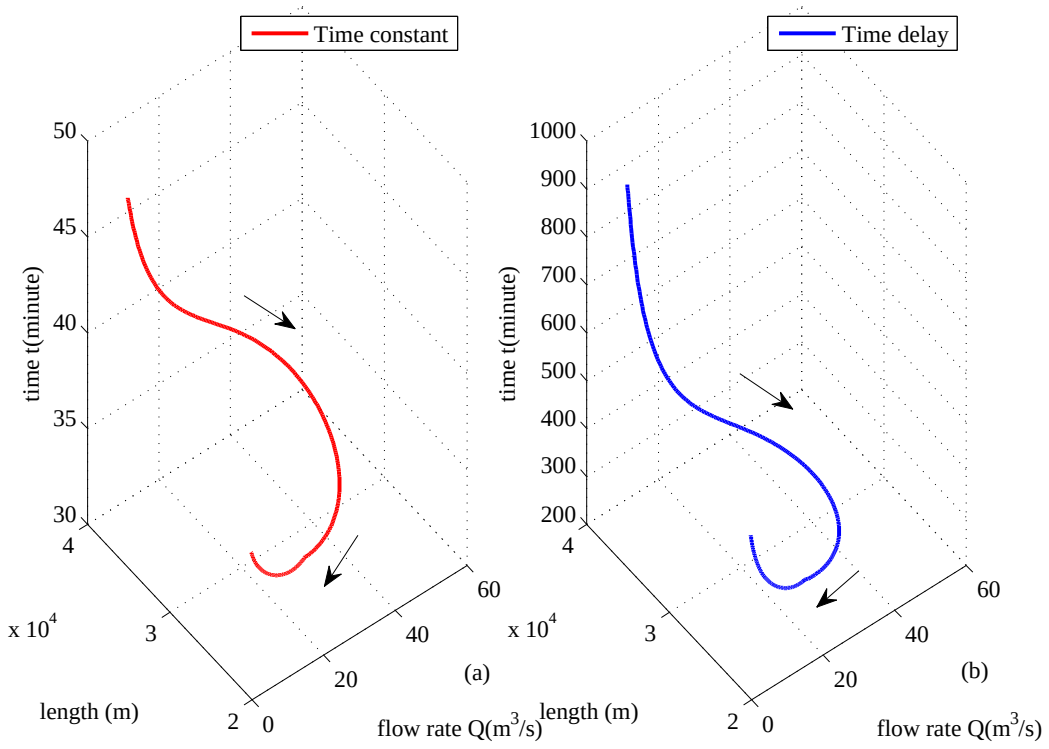

Figure 4.10: Relationship of T_c and T_d with flow rate Q

From the analysis, the simulation time of the coupled ATD model is quite a lot (10.30 seconds for 4 days). It is thus difficult to use it for quick simulation such as real time forecasting of flood in rivers. An improvement is suggested to simplify the model so that it can be used to simulate the flow dynamics of the water system quickly is presented in following section.

4.4 Simplified method of the coupled ATD model

The idea is to keep the intersection point of the two pools fixed so that the backwater area L_b and uniform area L_u remains unchanged despite of variation of downstream condition. Hence, the computation time of the model is reduced while still giving acceptable results. The method is described in detail as follow:

- The intersection point x is situated at the place where the backwater area L_b reaches maximum distance and the uniform area L_u is minimum. Therefore, the backwater flow does not have influence on the upstream uniform flow.
- For the upstream channel, the curves T_c vs Q, T_d vs Q can be determined for the uniform flow with normal depth at the downstream intersection point.
- Regarding the downstream weir, the water balance of the reservoir is calculated in order to determine the water level in the reservoir.

To compare with the previous method, the reservoir shown in previous section is used for simulation. The model is defined as follows:

- Based on the result of the previous simulation, the intersection point x is determined at the place where the largest backwater area L_b is equal to 15744 m while the minimum uniform flow area L_u is defined as 22056 m.
- The L_u is almost equal to the reach length L of the river reach between Nong Son station and Giao Thuy validated in the case study of the chapter 3. Hence, the curves T_c vs Q and T_d vs Q (see figure 3.5) can be used to generate discharge flowing into the reservoir
- Figure 4.11 shows the reservoir water level of both coupled models. On one hand, the dashed line Z_1 shows the results of the model with L_u and L_b changing in response to flow rate Q which is named the ATD model 1. The water level gradually rises up to 17.37 m. On the other hand, the solid line Z_2 shows the water level in the reservoir calculated by the coupled model fixed L_u and L_b known as the ATD model 2. Z_2 increases to 17.65 m. The mean deviation of both water levels is 0.54 m. The uniform part L_u in the ATD model 2 is selected as the minimum value of L_u so that the upstream

water flows in the reservoir earlier than the one of the ATD model 1. In this circumstance, the flow is less attenuated and an amount of the incoming water is larger than in the case of the ATD model 1. Nevertheless, there is a very good match between both models with NSE = 0.98 and PBIAS = 4.74 (see, table 4.2).

- Regarding computation time, the ATD model 2 is almost 10 times faster than the ATD model 1, 1.04 seconds in comparison to 10.3 seconds.

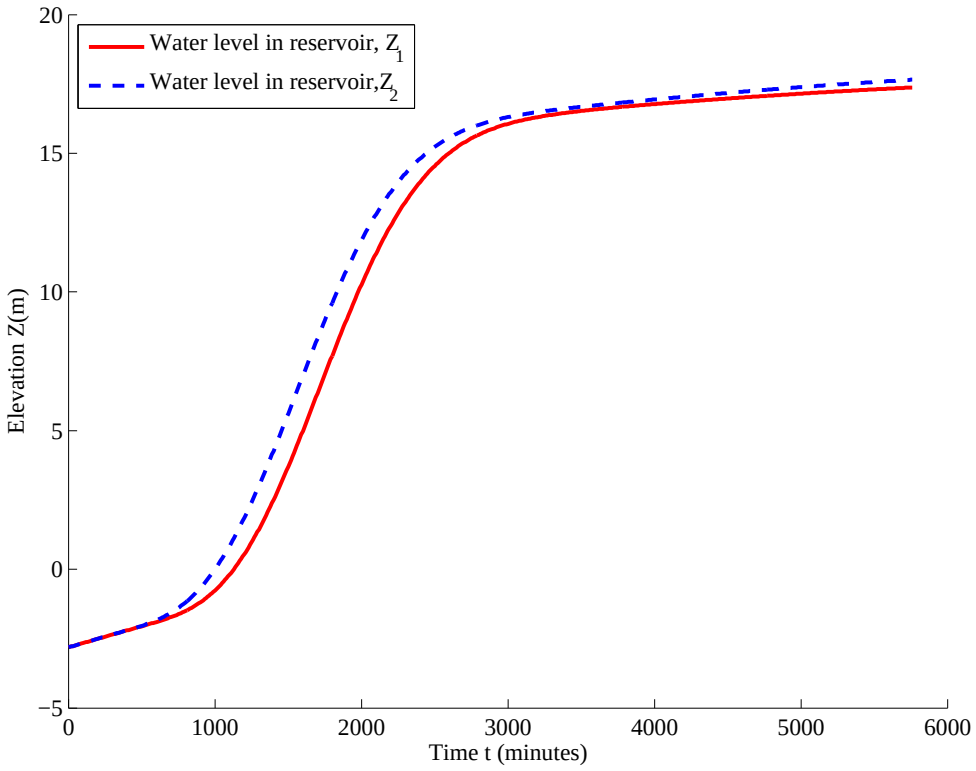

Figure 4.11: Comparison of 2 coupled ATD model

Table 4.2: Comparison of both coupled ATD models

Model	Computation time (s)	$\Delta Z(m)$	NSE	PBIAS
The coupled ATD model 1	10.3	0.54	0.98	4.74
The coupled ATD model 2	1.04			

4.5 Conclusion

The new approach that utilizes an ATD model coupling with the backwater model to illustrate the non-uniformity of flow in channel introduced. The advancement is that the uniform flow is considered in unsteady state for flow routing. Particularly, it is shown that the intersection point x of the 2 pools varies as the flow rate Q varies which is explicitly illustrated by interaction of backwater part L_b and uniform part L_u. By assuming a horizontal line for water level in reservoir, computation time is also declined. The approach compensates deficiencies of previous researches by taking into account the backwater effect in routing river flow.

The approach of determination of parameters of this ATD model is distinctive because T_c and T_d are now functions of Q and L_u. The uniform reach length L_u varies according to the upstream flow rate Q and the backwater part L_b. Indeed, the backwater part L_b is dynamically affected by downstream condition. For instance, if downstream boundary is a weir without discharging for water demand, the backwater length is affected only by the weir characteristics. If downstream water demand exists, the backwater length is not only influenced by the weir but also by the downstream demands. Hence, the concept that priorly designs the curves of T_c and T_d according to certain range of flow rate Q and apply then to simulate different scenarios encounters difficulties because of variation of downstream demands.

To overcome the difficulties, the simple coupled ATD model is introduced. In which, the intersection point is kept fixed so that the both pools remains constant according to variation of upstream and downstream flow. The model computes the outflow quickly and the results is well evaluated. Hence, the coupling ATD model is totally suitable to use for controller design.

Chapter 5

Parameter estimation of ATD model from a complex hydraulic model

5.1 Introduction

Using the parameter estimation method used in Chapter 3 and 4 to estimate the ATD parameters makes its application only for a narrow domain due to the valid assumption of simplified geometry (rectangular or trapezoidal). The obstacle comes from cross sectional irregularities in complex river systems. To solve this problem, a typical approach is to separate the river into small parallel rivers whose wetted areas are a fraction of the whole one. Afterwards, the parameters may be estimated for each parallel river and then be averaged to obtain the one for a whole cross section. This implementation for time delay model in case of irregular cross section is quite difficult and consumes a huge computation time. Moreover, it is not certain that the result is as accurate as the existing complex hydraulic programs (MIKE 11, HECRAS, and SOBEK). Therefore, this chapter presents a two step approach that may be considered as a remedy for the mentioned deficiencies. Furthermore, the approach can be considered as a model for control tasks from a complex hydraulic models like MIKE 11, HECRAS, and SOBEK.

5.2 Procedure

This approach is presented in figure 5.1 and is described step by step in the subsequent section. The main two steps are to model a complex river reach using a complex hydraulic model in the first step and to estimate the ATD model parameters based on the complex model in the second step. Afterwards, the estimated parameters are used to simulate a random flood events. What makes this approach so important is that most of the time such a complex model exists as it is required for other analysis problems.

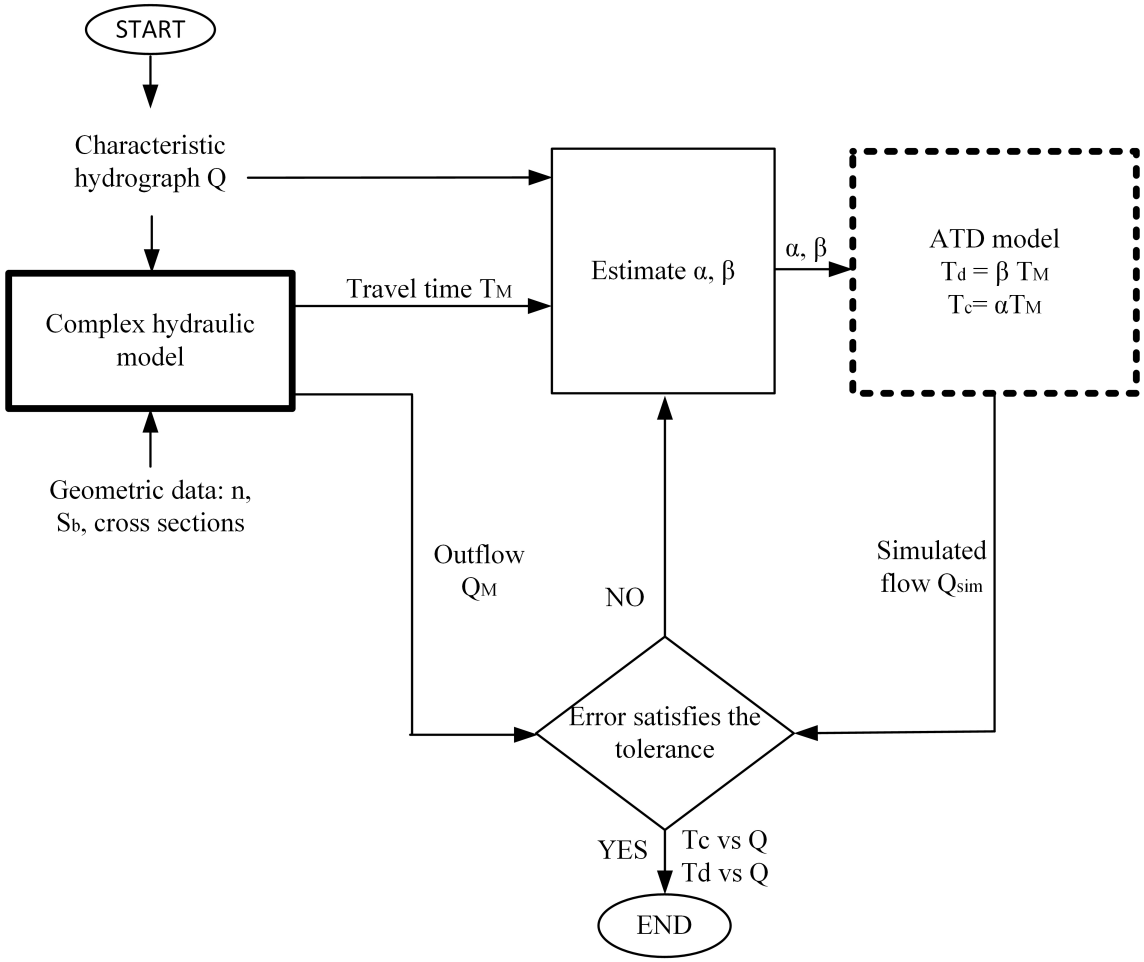

Figure 5.1: Approach for approximating a complex river reach

5.2.1 Set up a complex hydrodynamic model of a river reach

Commercial programs which are developed by prestigious organization such as Danish Hydraulics Institute, Delft University of Technology, US Army Corporation are usually selected to build the full hydrodynamic model of the reach. The one di-

mensional model which is composed by links and nodes to describe flow movement in open channel discretizes and numerically solves the SVE. The complex model of a river reach is built whose parameters must be carefully calibrated and validated with measured data. Then, the model can be used to determined ATD parameters as it will be described in the next steps.

5.2.2 ATD model parameter estimation from a complex model

Firstly, input data is prepared, which requires the determination of the characteristic hydropgraph. The hydrograph shape is not only a reflection of general attributes of successive periods of excessive rainfall leading to flood but is also moderated by features of river system. Therefore, deriving a simplified hydrograph that represents a catchment characteristic is significant for flood forecasting. This typical shape (see, figure 5.2) is derived based on analyzing the width of hydrograph corresponding to different flood waves, i.e, hydropgraph width analysis (Archer et al, 2000; O'Connor et al, 2014; O'Sullivan et al, 2012). Data should be adequate to derive a accurate characteristic hydrograph. The procedure is composed of steps as follows:

- Filtering of chosen hydrograph: a multi-peaks flood which represents the catchment responding to different rainfall periods. However, a broadly single-peaked flood is only preferred to use for extracting a characteristic hydrograph. To overcome this difficulty, all of complex parts of the hydrograph is discarded whereas maintaining a typical component. In addition, the base flow is essentially supplemented to the selected component.

- Standardizing the hydrograph of predefined flood event: the ordinates of filtered hydrograph are normalized to the peak value while the time scale of hydrograph remains unchanged. This peak value of 1.0 corresponds to the 100 percentage of the peak flow. Then, the new ordinates are defined as percentage of peak flow and they are identified at each interval of 5 percent of the peak (95, 90, 85...5) in order to extend this particular hydrograph. The result is a standardized hydrograph.

- Calculating the hydrograph width at particular predefined ordinates: the hydrograph width at predefined percentage of the peak is the duration before

and after the occurrence of the peak. The coordinates of filtered hydrograph is considered as a reference table from which the time period is calculated by linear interpolation. The width is separated into two parts: one is the rising limb and another is the receding limb. The combination of flow percentages and corresponded widths are coordinates for sketching the unit characteristic hydrograph, see figure 5.2.

- Median unit characteristic hydrograph: This method is repetitive for others annual maximum flood event in order to derive the unit characteristic hydrograph of the year. Afterwards, the median unit characteristic hydrograph is developed based on the annual unit characteristic hydrographs.

- Lastly, the characteristic hydrograph for a designed flood event is generated. From the flood frequency analysis, a peak flow of designed return period is calculated. By scaling up the median unit characteristic hydrograph for the peak value, the characteristic hydrograph of the designed year flood event is obtained. This hydrograph serves as inflow of hydraulic model of a river reach to simulate the outflow.

Secondly, the model parameters are estimated. A complex hydraulic model of a river reach with several cross sections is fully developed to simulate the designed flood dynamics. As a byproduct, a travel time of the flow is also determined during simulation. The travel time denoted T_M is used to estimate parameters of ATD model. From previous research for the upgraded Muskingum model (O'Sullivan et al, 2012), the travel time is directly used as constant storage parameter representing attenuation and lag time of peak. In terms of ATD model, the time constant is responsible for attenuation of peak whilst a pure time delay is the duration of the flow signal to appear at downstream of a reach. Hence, the author assumes that the travel time may be a combination of time constant and time delay of ATD model and two coefficient α and β. The suggestion is expressed by equation 5.2 where α and β are both coefficients determining proportion of T_c, and T_d of travel time T_M .

Parameters of ATD model in equation 3.27 are estimated by constrained non-linear programming technique (NLP). The objective function given by equation 5.1 aims at minimizing the sum of quadratic errors between discharges simulated by

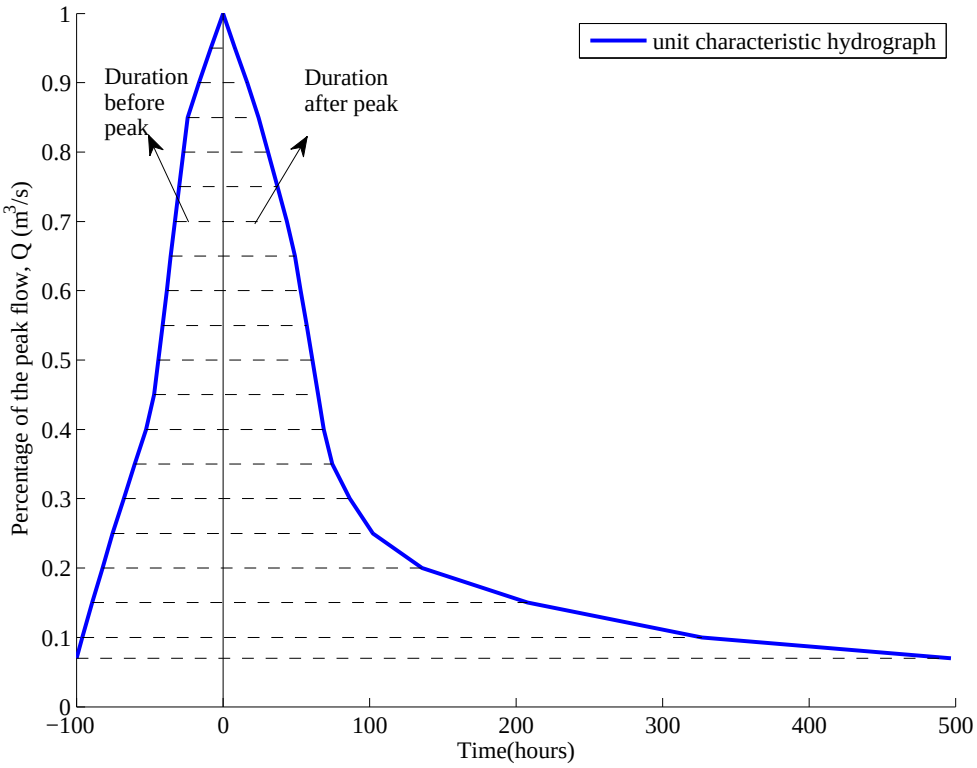

Figure 5.2: Definition diagram for derivation of duration of exceedence of percentiles of peak flow.

ATD model and the ones from complex model. During the optimization process, time constant and time delay are estimated to obtain the best match between Q_M and Q_{ATD}.

$$\min \sum_{\mathrm{i}=1}^{\mathrm{I}} \left(\mathrm{Q}_M^{\mathrm{i}} - \mathrm{Q}_{ATD}^{\mathrm{i}}\right)^2 \tag{5.1}$$

subject to

$$\begin{aligned} & T_c = \alpha T_M; T_d = \beta T_M \\ & \alpha + \beta \leq 1 \\ & \alpha > 0, \beta > 0 \\ & \alpha_o = \beta_o = 0.5 \end{aligned} \tag{5.2}$$

Further calculation of water level y, the relationship of y versus Q at downstream station is generated by the complex model during the procedure of estimating the parameters of the ATD model. This relationship is then used by the ATD model to calculate the water level y.

The model performance is evaluated by using the estimated T_c and T_d to approximate discharge for another flood event. Firstly, the outflow is computed by the complex model and by ATD model in parallel. Subsequently, output of ATD model is compared to the output of the model. The goodness of model is evaluated by NSE. With the parameters, the ATD model is valid for application to flow routing of this river reach corresponding to a designed range of flow rate from the lowest flow rate value to the highest peak

5.3 Application of the method (A case study)

The data of the river reach shown in chapter 3 is used for simulation in this case study. To illustrate the procedure of simplifying the complex hydraulic model by the ATD model, a case study of previous section is used. The program HECRAS is used to build the fully dynamic model of the reach. The characteristic hydrograph is derived from the statistical data by hydrograph width analysis as described before. The results are shown in figure 5.3. Then, it serves as inflow for the model of the river reach developed in HECRAS to obtain the simulated hydrograph at Giao Thuy station. The result is considered as reference for calibration of the ATD

model. Through adjusting parameters of the ATD model to reach the best fit with the reference data, its optimal parameters are derived. The model is calibrated with measured flow rate from November to December and early stopping through validation with data of October.

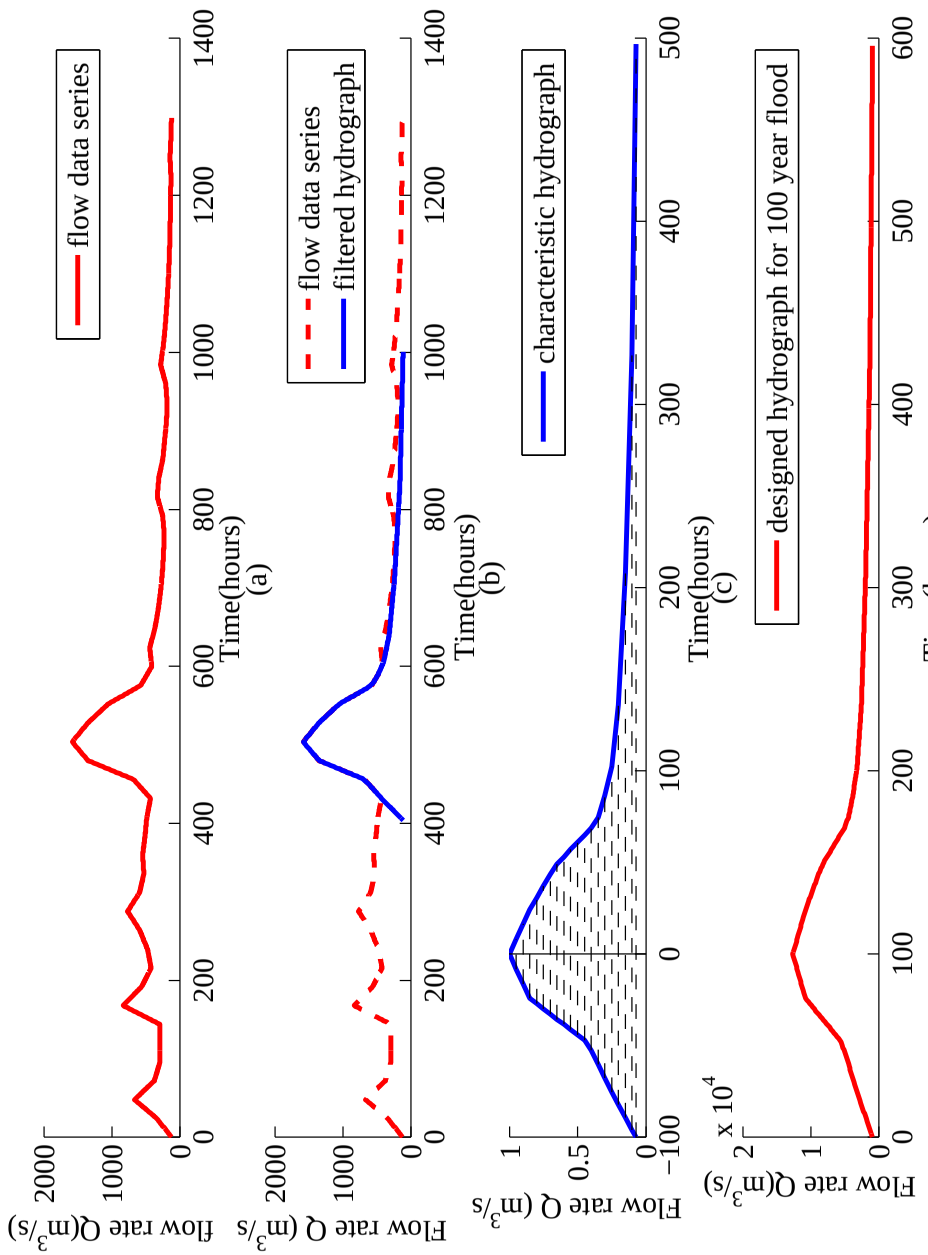

Figure 5.3: Procedure for defining characteristic hydrograph

Figure 5.4a presents the characteristic flow for the river reach obtained from figure 5.3d. The outflow shown by the blue curves in figure 5.4b is then calculated by HECRAS as response to the inflow. The highest flow rate at downstream reaches 11600 m^3/s while the minimum discharge is slightly over 18 m^3/s. As a byproduct, HECRAS generates a travel time of the flood wave, a black line denoted T_M in figure 5.4c, which is selected to estimate parameters of ATD model. The travel time fluctuates in between 7.0 hours to 29 hours. From which, the upward side of the graph is for the rising part of the characteristic hydrograph and the downward side is for the recession part of the graph.

Parameters of ATD model T_c and T_d are estimated by constrained nonlinear programming technique (NLP) based on the the objective function in equation 5.1 with constraint 5.2. The performance is evaluated by NSE and PBIAS during optimization for early stopping to avoid over-fitting. The outcome is shown in figure 5.5. Check on figure 5.5a, the hydrographs modeled by HECRAS (blue line) and by the ATD model (red curve) are almost indistinguishable. It proves that the reduced model can efficiently return a result as good as the one from the complex model. This is also confirmed by NSE and PBIAS of 0.99, and -0.92 respectively (see table 5.1). Figures 5.5b and 5.5c show the curves of T_c and T_d. The red line reflects the relationship between flow rate versus time constant which varies from 5.0 hours to 20 hours. On the other hand, the blue line reflects the relationship of flow rate and time delay which changes from 2.0 hours to 9.0 hours. Due to the size of the extreme flood event, the flood wave propagate quickly toward downstream. Hence, the time delay T_d in this case is smaller than the time constant T_c. The coefficient α reaches 0.7, and β is 0.3. These parameters are used by ATD model to estimate downstream flow of different upstream flood scenarios.

Table 5.1: Result of estimating parameters of ATD model

Criteria	Calibration	α	β
NSE	0.99	0.7	0.3
PBIAS	-0.92		

For validation, the model performance is evaluated by using the estimated T_c and T_d to approximate discharge for a set of real data of 25 days in October. The hourly data is the flow rate measured at Nong Son station. The results is depicted

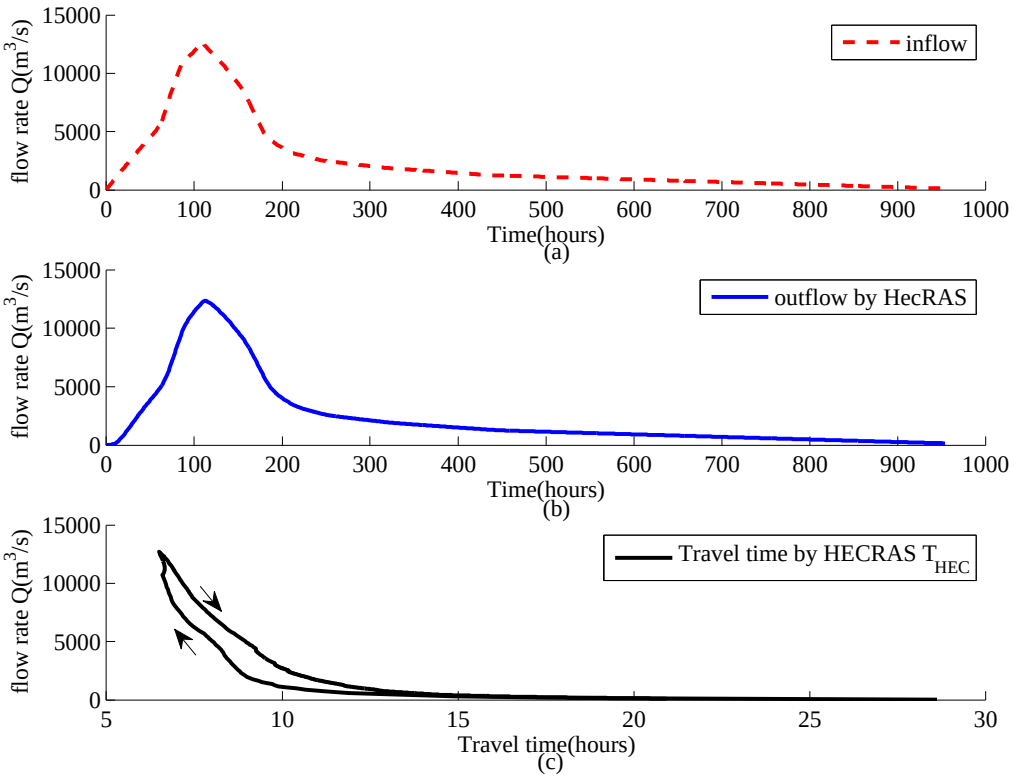

Figure 5.4: Outflow and travel time derived from HECRAS model

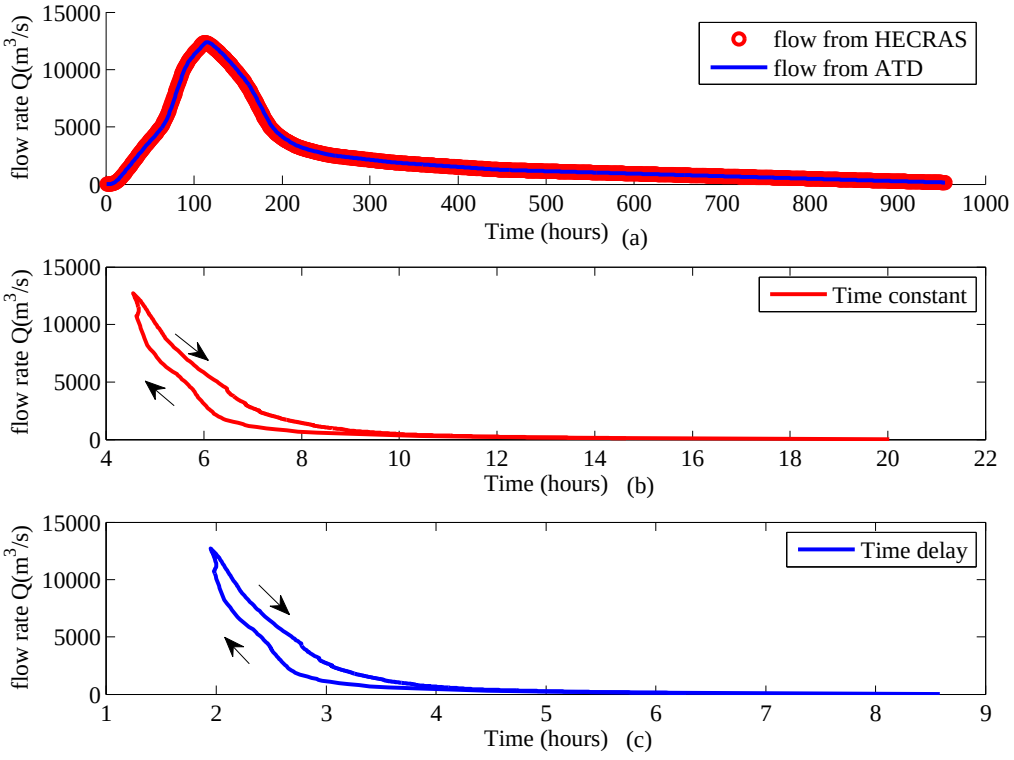

Figure 5.5: Time constant and time delay obtained from NLP

in figure 5.6. The flow data is shown in the dashed pink curve with highest flow of 950 m^3/s. The outflow of HECRAS is the red curve and the simulated flow of ATD model is the blue curve, and are nearly overlapping. A fact is that both hydrograph reaches almost 800 m^3/s of maximum value as well as 130 m^3/s of minimum point. Indeed, the model shows a good result presented in table 5.2 by NSE of 0.99 and PBIAS of -1.99. In particular, the simulation time of the ATD is much faster than the HECRAS programm, 0.15 seconds of ATD in comparison to 7.27 seconds of HECRAS. All of the simulations is implemented by the the computer used in the chapter 4. With the parameters, the ATD model is valid for application to flow routing of this river reach corresponding to the designed range of flow rate from the lowest flow rate value of 18 m^3/s to the highest peak of 11600 m^3/s .

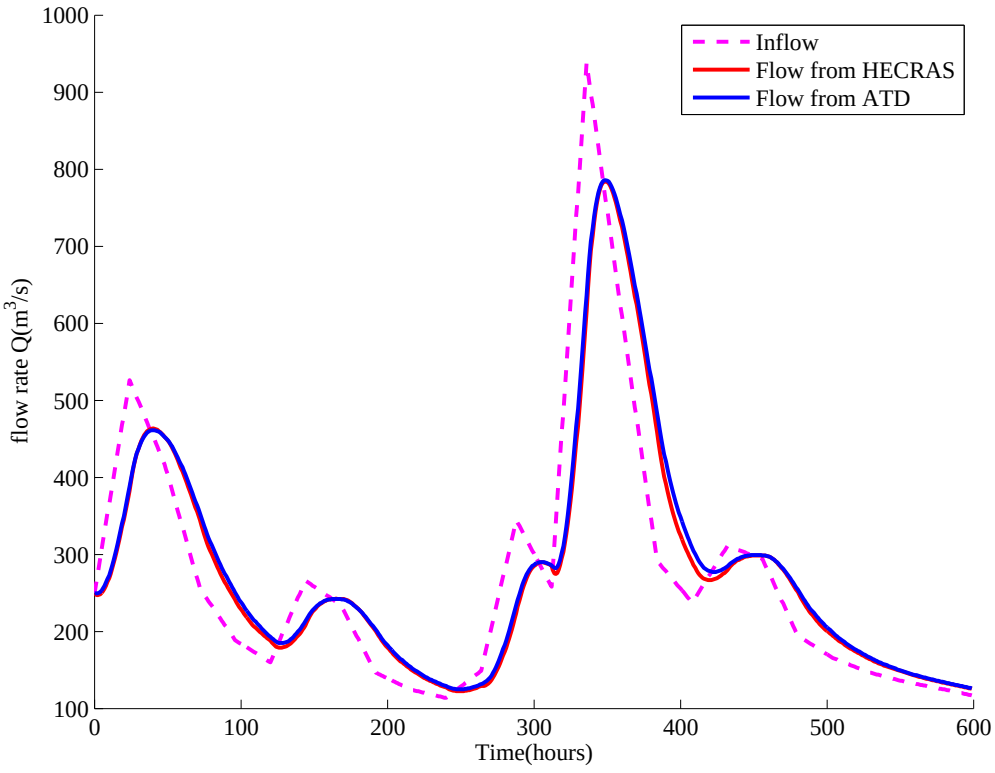

Figure 5.6: Validation of ATD model for flood in October

Table 5.2: Results of validation

Validation		Computation time (second)	
NSE	PBIAS	HECRAS	ATD
0.99	-0.49	7.27	0.15

5.4 Conclusion

In conclusion, this work presents an advancement of adaptive time delay model that can estimate river flow for irregular geometry. It is an upgrade of river model developed in (Litrico et al, 2010; Nguyen et al, 2016b). The NLP approach is utilized to achieve the curves of time constant T_c, and time delay T_d versus Q by minimizing the difference between the outflow generated by HECRAS and the one by the ATD model. The parameters are validated by a flood scenario of October and proved that the model is very fast and accurate. Hence, this ATD model is able to use for real time flood forecasting and design control policies for water systems.

Chapter 6

Application of ATD model in optimal control of hydropower cascade

6.1 Introduction

The main purpose of the ATD model with respect to controller design has been mentioned several times in the previous chapters. Therefore, it is essential to test its applicability in such an environment. Such an environment is the control of a reservoir cascade which is inevitable in water management.

Over the past decade, a tendency for supplementing and replacing conventional fossil sources for electricity generation by renewable sources has been substantially exerted because of the scarcity and limitation of fossil energy. Although the natural replenishment of these sources for renewable electricity is well known, an efficient manner in using this energy is always essential. Hydropower is one of the viable option for sustainable energy production. However, operation and management of hydropower systems is a challenging issue for decision makers and operators. The reasons are conflicts among stakeholders (electricity, flood protection, agriculture, industry, and others) as well as the uncertain nature of reservoir inflow that adds considerably to the complexity of the system (Karimanzira et al, 2014; Sattari et al, 2009; Schwanenberg et al, 2014). Popular powerful techniques for hydropower analysis are simulation and optimization. Models represent the system attributes and

predict the system responses under different conditions. A set of operating rules are developed and continuously improved in order to determine an acceptable release of reservoirs. On the other hand, the optimization that focuses on identifying optimal decision variables is based on mathematical formulation for maximizing or minimizing an objective function subject to constraints (Fayaed et al, 2013). In fact, the optimization models for hydropower systems are applied for different operation period such as seasonal operation, daily, hourly, or event-based real-time regulation. Moreover, its applicability is not only for an individual hydropower plant, but also for cascade of hydropower plants that improves significantly electrical productivity. A large number of optimization approaches for dam optimal control exists, e.g., linear programming (LP), nonlinear programming (NLP), dynamic programming (DP), genetic algorithm (GA), and have been applied since years (Hamann and Hug, 2014; Karamouz and Houck, 1987; Neelakantan and Pundarikanthan, 2000; Waltz et al, 2006; Yang et al, 2013).

This section introduces a new approach that combines an adaptive time delay model and backwater model for simulation of a reservoir system. Nonlinear constrainted programming is applied to the system to achieve an optimal regulation for enhancing the electricity generation of a cascade of hydropower plants. The integration of adaptive time delay river dynamics into the optimization is considered as a new in this filed as most of the time a simple travel time is assumed between the reservoirs.

6.2 Methodology

The method consists of two components: simulation and optimization. In terms of simulation, the dynamics of system are represented by the backwater model and flow routing model (ATD) (see figure 6.1). In which, the ATD model transfers water from upstream reservoir to downstream reservoir while backwater model simulates the behavior of dams. Regarding optimization, nonlinear programming technique is applied to determine the best release of the cascade by which the electricity production will meet the objective. For illustration, a case study of a cascade of two hydropower plants is selected in order to compare an energy production of an

optimized operation and existing operation. The objective of this study is to present a new method that may be applied to improve the operational policies of hydropower cascades through which electricity production is maximized, and flood or drought is mitigated, and so forth.

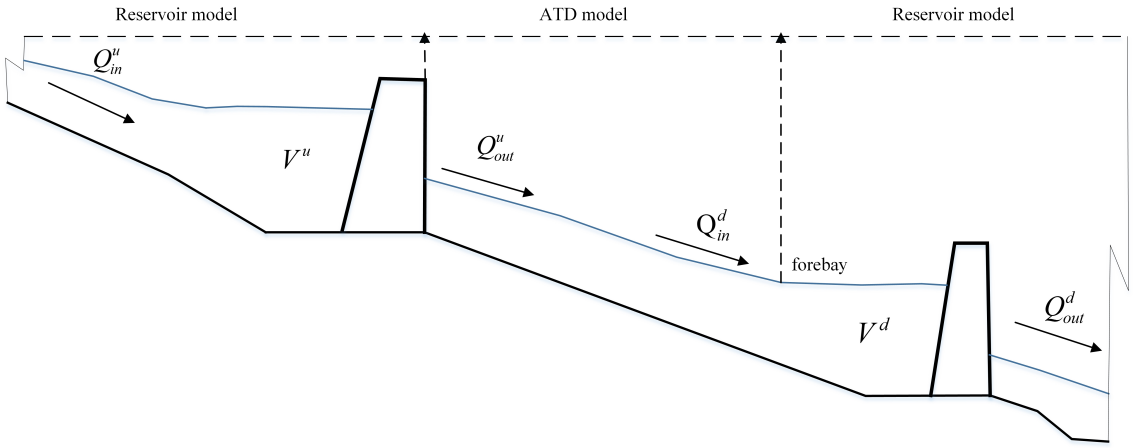

Figure 6.1: Hydropower cascade model

The coupled system is described by the following equation 6.1, 6.2, and 6.3. The equations 6.1 and 6.3 are the reservoir models that ensure mass balance of dams while the ATD model in equation 6.2 transfers discharges from upstream reservoir to downstream reservoir through a river reach between two dams. Particularly, the approach presented in chapter 5 will be used to define the ATD model, hence, the backwater effect is also taken into account. This concept considers the dynamics of flow transfer in optimization that increase accuracy of the optimal result.

$$\frac{\mathrm{d}\vartheta^{\mathrm{u}}}{\mathrm{dt}} = \mathrm{Q}^{\mathrm{u}}_{\mathrm{in}} - \mathrm{Q}^{\mathrm{u}}_{\mathrm{out}} \tag{6.1}$$

$$\begin{cases} \mathrm{T_c}\frac{\mathrm{dq}}{\mathrm{dt}} + \mathrm{q(t)} = \mathrm{Q}^{\mathrm{u}}_{\mathrm{out}}(\mathrm{t}) \\ \mathrm{Q}^{\mathrm{d}}_{\mathrm{in}}(\mathrm{t}) = \mathrm{q(t - T_d)} \end{cases} \tag{6.2}$$

$$\frac{\mathrm{d}\vartheta^{\mathrm{d}}}{\mathrm{dt}} = \mathrm{Q}^{\mathrm{d}}_{\mathrm{in}} - \mathrm{Q}^{\mathrm{d}}_{\mathrm{out}} \tag{6.3}$$

where $Q^u_{u,in}(t)$ is inflow of upstream reservoir, $Q^u_{out}(t)$ is discharge of upstream reservoir, $Q^d_{in}(t)$ is inflow of downstream reservoir, $Q^d_{out}(t)$ is discharge of downstream reservoir, $\vartheta^u(t)$ is storage of upstream reservoir, $\vartheta^d(t)$ is storage of downstream reservoir, $T_c(t)$ is the time constant, $T_d(t)$ is the time delay.

Regarding optimization, the objective function expressed by equation 6.4 to maximize electricity production.

$$\max \sum_{i=1}^{I} \sum_{j=1}^{J} E\left(Q\right) = \max \sum_{i=1}^{I} \sum_{j=1}^{J} P_t\left(Q\right) \Delta t \tag{6.4}$$

Subject to the constraints:

Water balance of dam:

$$\vartheta_{i,j} = \vartheta_{i,j-1} + \left(I_{i,j} - Q_{i,j}\right) \Delta t \tag{6.5}$$

Constraints of reservoir water level, outflow as, (further information in table 6.4):

$$\mathrm{ZD_{i,j}} \leq \mathrm{Z_{i,j}} \leq \mathrm{ZF_{i,j}} \tag{6.6}$$

$$\mathrm{Qmin_{i,j}} \leq \mathrm{Q_{i,j}} \leq \mathrm{Qmax_{i,j}} \tag{6.7}$$

Where I is number of dams; J number of hour; $E_{o,i,j}$ is the sum of optimal energy of reservoir i at hour j; $\vartheta_{i,j}$ storage of reservoir i at hour j; $I_{i,j}$ inflow to reservoir i at hour j is determined by ATD model; $Q_{i,j}$ is the outflow through turbine of reservoir i at hour j; Δt is the time interval; $Z_{i,j}$ is the water level of reservoir i at hour j; $ZD_{i,j}$ is the dead water level of reservoir i at hour j; $ZF_{i,j}$ is the flood warning water level of reservoir i at hour j; $Q_{min,i,j}$ is the minimum flow through turbine i an hour j; $Q_{max,i,j}$ is the maximum flow through turbine i at hour j.

The energy generation in a time period T is calculated as in equation 6.8

$$\mathrm{E} = \sum_{\mathrm{t=1}}^{\mathrm{T}} \mathrm{P_t} \Delta \mathrm{t}, \mathrm{P_t} = \sum_{\mathrm{j=1}}^{\mathrm{J}} \rho \mathrm{g} \eta \mathrm{HQ} \tag{6.8}$$

where E is the energy generated in a duration Δt; P_t is the power generation; ρ is the density of water; g is the gravitational acceleration; H is the water head; Q is the turbines discharge; η is the overall efficiency of hydropower plant.

The water head H is a deviation of water level in reservoir and downstream tail water. The general equation 6.9 which is used to estimate the tail water Z_{tw} is developed from the statistical data: the water level of the forebay of downstream

dam Z_{fb}, the tail water level of the dam Z_{tw}, and the downstream release Q.

$$Z_{tw} = \alpha_1 + \alpha_2 Z_{fb} + \alpha_3 Q^{\alpha_4} \tag{6.9}$$

Those coefficients α_1, α_2, α_3, α_4 are derived based on the least square non linear approach which minimize the quadratic errors between simulated $Z_{tw,sim}$ and the measured data $Z_{tw,data}$. The objective functions is subsequently introduced 6.10

$$\min \sum_{j=1}^{J} \left(Z_{tw,sim} - Z_{tw,data}\right)^2 \tag{6.10}$$

6.3 Application of the system (A case study)

The study area is the Wuyang river, which is situated in the eastern part of Guizhou province in China and has a long and narrow basin, (see figure 6.2). There are 16 hydropower stations constructed along the river mainstream. Among them are two reservoirs: Guanyinyan and Hongqi which are selected in order to demonstrate the applicability of proposed method. In terms of Guanyinyan station, the dead water is 577 m while the flood checking water level is 600.5 m. The maximum release of turbine is approximately 70 m^3/s. Regarding Hongqi station, the dead water level is 499 m, the flood checking water level is about 521.7 m. In addition, the maximum discharge of turbine also reaches 70 m^3/s. The collected data of flow rate, water level, and current energy production of January, 2011 are used as input for this work. The step size of the statistical data is 1.0 hour. Both reservoir responses are described by the backwater model while the river reach in between is simulated by the ATD model with backwater effect. Optimization is implemented to maximized energy product on the system.

6.3.1 Determination of parameters of ATD model

The ATD model is a simplified model of the existing complex hydraulic model which is built in a commercial software, HECRAS. According to the method already introduced in previous in chapter 5 (Nguyen et al, 2016c), the parameters T_c, T_d are derived by investigating the inflow and outflow of a river reach computed by HECRAS. Nonlinear programming (NLP) technique is used as a tool to determine

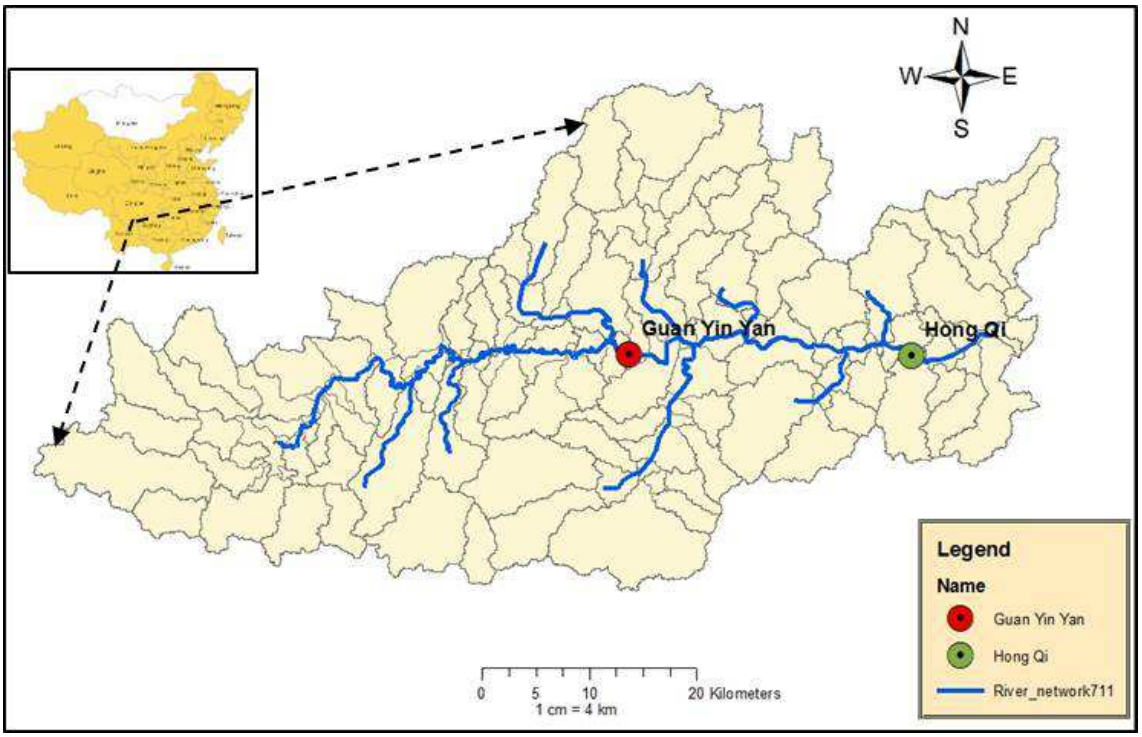

Figure 6.2: Geography of study area

the parameters.

The characteristic hydograph is obtained based on the method described in chapter 5. Due to data shortage, one year data is used for deriving the characteristic hydrograph. The time interval is 1.0 hour. Although this is a limitation, it is sufficient to show the applicability of the ATD model for optimization. The data series that show the river reach characteristics are illustrated in figure 6.3a. The flow reaches max value at 35 m^3/s, and minimum flow at 0.5 m^3/s. The highest single peaked flood is selected as a typical hydrograph that is illustrated by the blue curve in figure 6.3a and c. Other complex parts are discarded, and the base flow value 0.5 m^3/s is added to the graph. The gradient of upside and downside parts are maintained to ensure the attributes of flow.

To simulate a 100 year flood event. The designed flood hydrograph illustrated in red color (figure 6.3d) is derived by multiplying the peak value to ordinates of the unity hydrograph. The peak value is now nearly 380 m^3/s while the base flow is needed to be maintained at 0.5 m^3/s.

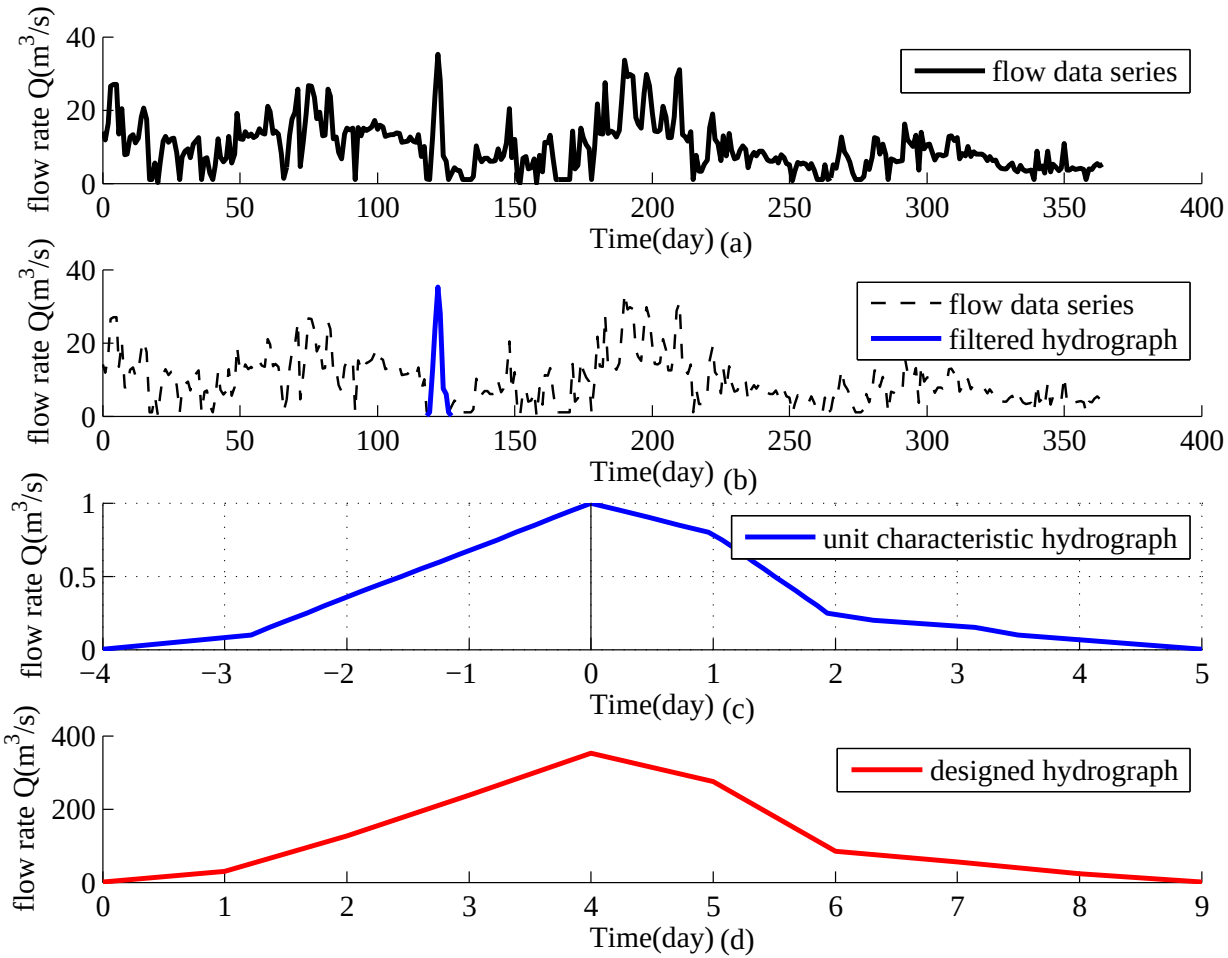

Figure 6.3: Procedure for deriving characteristic hydrograph

Model parameter estimation

The travel time T_M is also derived by HECRAS. This travel time obtained from HECRAS is used to derive the parameters of the ATD model based on NLP.

The results of calibration process are shown in table 5.2. They illustrate a very good result with NSE = 0.99 and PBIAS = -0.50. The coefficients for extracting T_c and T_d from T_M, α and β are determined as 0.285 and 0.10, respectively. In the figure 6.5a, the Q_M in red curve and Q_{ATD} in blue curve are almost identical. Besides, the curves of time constant T_c and time delay T_d versus discharge Q are also illustrated in figure 6.5b, 6.5c. The red line is for the time constant changing between 5.0 hours to 38 hours while the blue line is time delay which varies from 2.0 hours to 13 hours. ATD model uses these curves to estimate the inflow of downstream reservoir.

Regarding validation process, 1-year-data of flow is used as inflow of the ATD model and the outflow compared to the result of the HECRAS model. Table 6.2 indicates an acceptable accuracy with NSE = 0.87 and PBIAS = -3.65. As can be seen in figure 6.6, the 2 graphs are almost identical. The blue graph shows the simulated flow by ATD model whereas the red one represents the output of the HECRAS model. In terms of simulation time, the ATD model takes 3.0 seconds to derive the result while HECRAS needs 85.0 seconds for the same task and with the same computer. Therefore, it is more advantageous when using ATD model as substitution of the HECRAS model for developing control strategies of the system.

Table 6.1: Result of estimating parameters of ATD model

Criteria	Calibration	α	β
NSE	0.99	0.285	0.10
PBIAS	-0.5		

Table 6.2: Results of validation

Validation		Computation time (second)	
NSE	PBIAS	HECRAS	ATD
0.87	-3.65	85.0	3.0

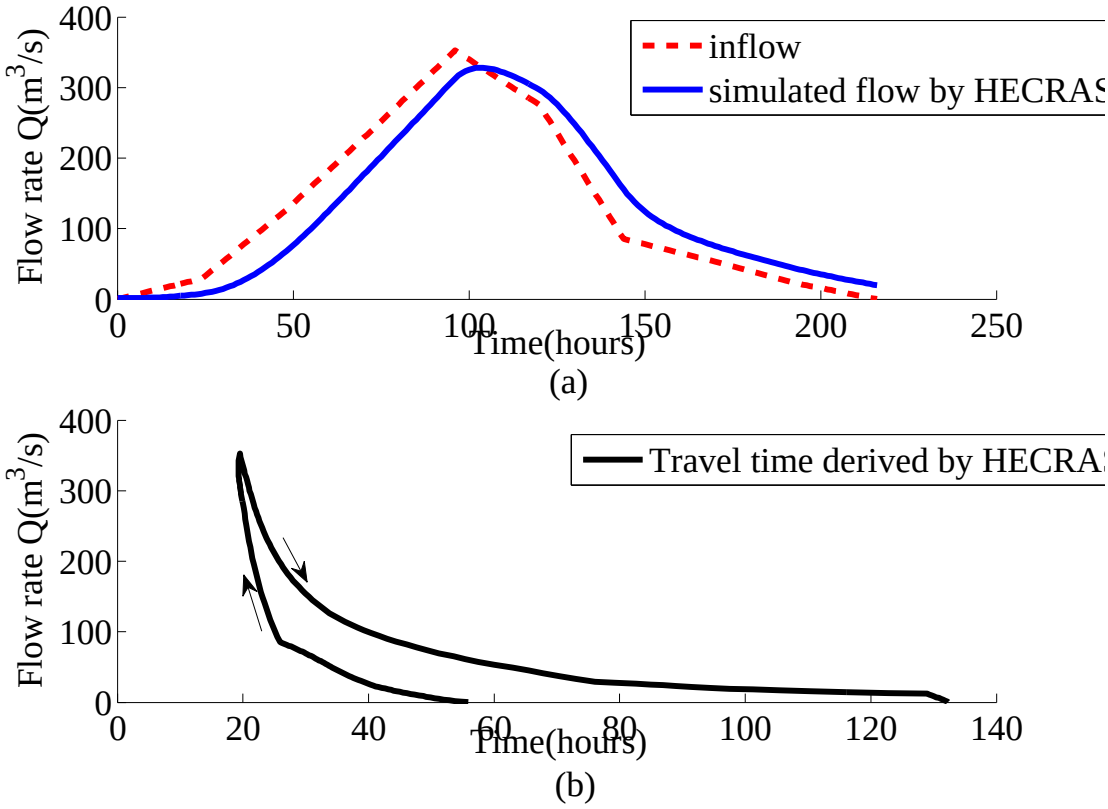

Figure 6.4: Travel time derived from HECRAS

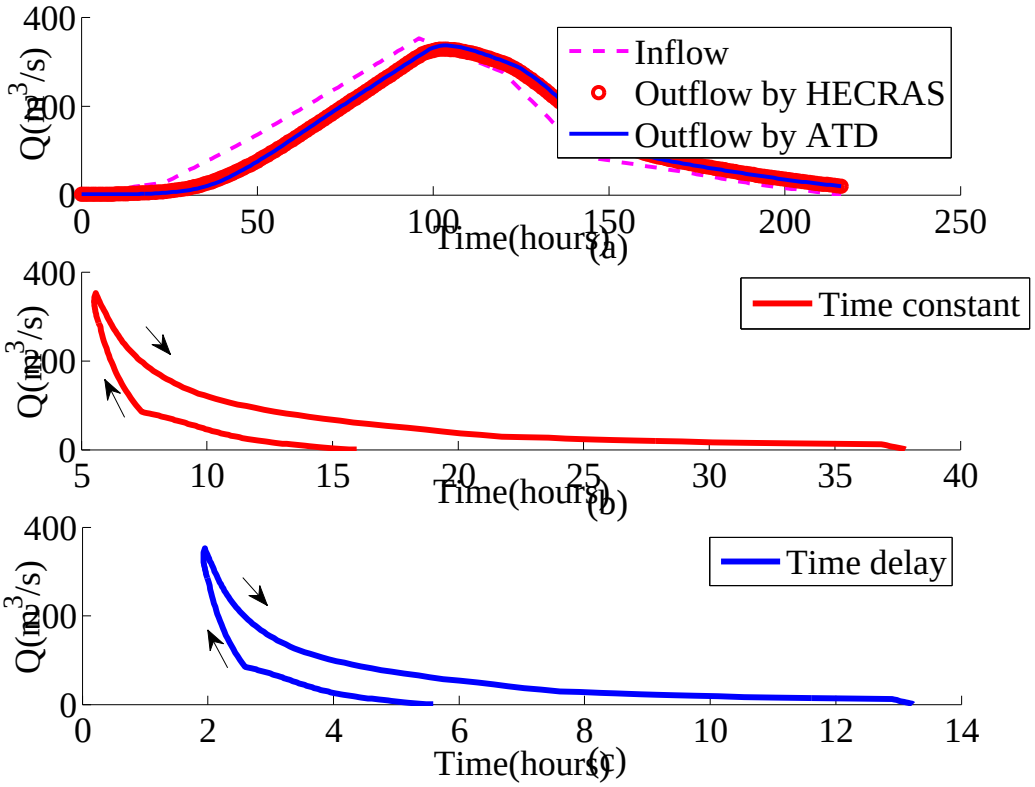

Figure 6.5: Time constant and time delay derived from HECRAS model

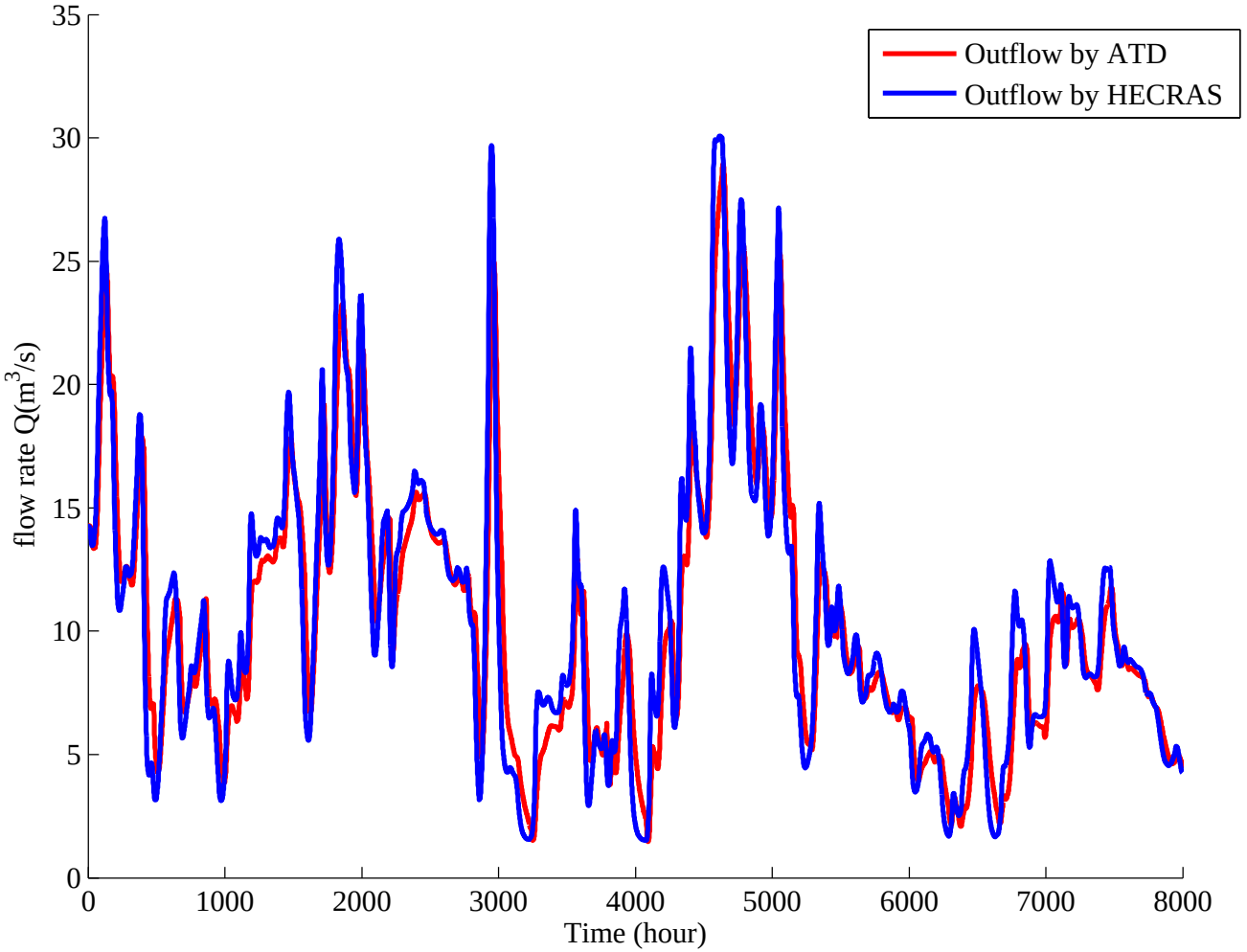

Figure 6.6: Validation of ATD model for a data series of flood event

6.3.2 Optimal control for hydropower cascade

The purpose of this research is to examine the applicability of the ATD model as a internal model of optimization of a hydropower cascade that helps to improve electricity production of the system. The hourly data is used in the optimization to derive hourly operational releases of the reservoirs.

Assumptions

To simplify the optimization for the hydropower cascade, only flow capacity of turbines and water level in dams are considered as a constraint for objective functions. Hence, a few assumptions are made as listed below:

- Overall efficiency of hydropower plants are assigned as 0.9 for both reservoirs;
- The hourly data is used to implement optimal operation;
- Environmental flow and other downstream demand of flow are not taken into account in this study;
- Evaporation from reservoirs is not considered;
- Tail water is defined as function forebay water level of downstream reservoir and discharge of upstream reservoir presented in equation 6.9;
- Release from an upstream reservoirs will be transferred to downstream by ATD model;
- The optimal flow rate through turbines is calculated by considering the discharge capacity of turbines;
- The 40-day data of power capacity will be optimized and compared to current energy production;
- Spill is not considered.

Result of cascade optimization

The reservoir system of Guanyinyan and Hongqi is optimized for 40 days to enhance the energy which is then compared to current energy production.

The tail water level for Guanyinyan and Hongqi stations are calculated by the equation 6.11 and 6.12

$$Z_{tw} = 133.8542 + 0.7766Z_{fb} + 6.0482Q^{0.1376} \tag{6.11}$$

$$Z_{tw} = -177.0298 + 1.3793Z_{fb} + 5.8354Q^{0.0235} \tag{6.12}$$

As shown in figure 6.7, the red curve shows the maximized electricity at every hour. The green line illustrates energy production of the cascade before optimization. The result is also apparently presented in table 6.3. The total current energy production is 845.80 $10^4 KWh$ in which Guanyinyan and Hongqi reservoir accounts for 380.91 $10^4 KWh$ and 464.89 $10^4 KWh$ respectively. After the system is optimized, the Guanyinyan produces 404.53 $10^4 KWh$, whereas the production of Hongqi rises to 493.84 $10^4 KWh$. The total optimal energy of the system reaches 898.24 $10^4 KWh$ which accounts for 6.20% higher than the current situation.

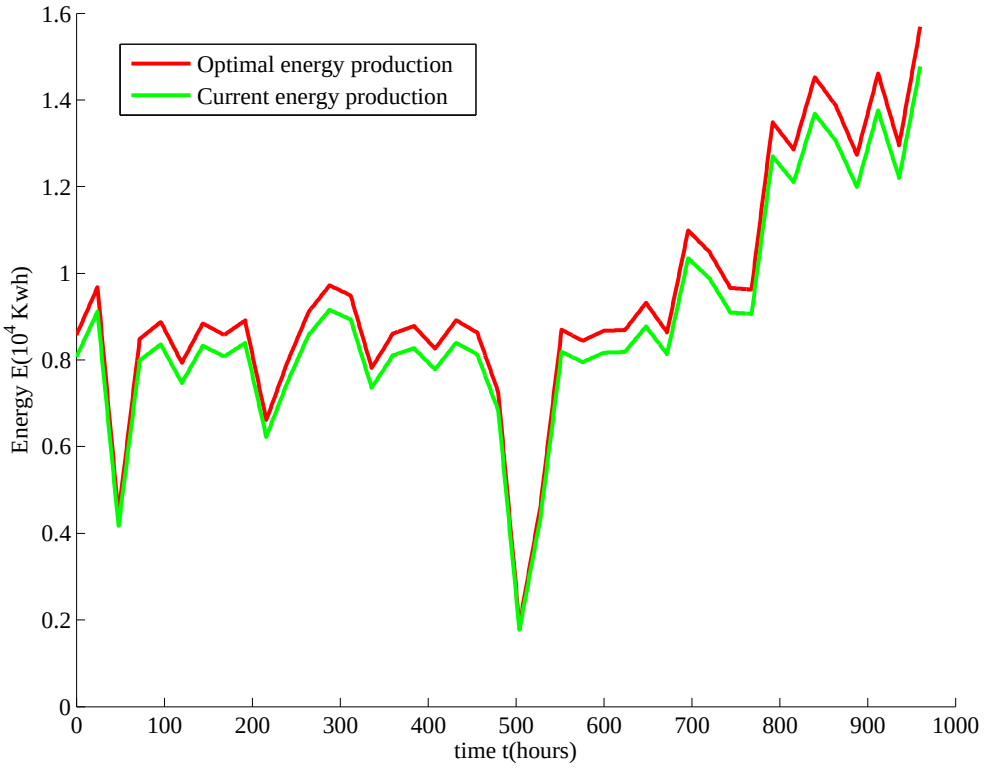

Figure 6.7: Result of energy optimization of the cascade

Table 6.3: Accumulative electricity generation of the cascade

No	Wuyang hydropower cascade		Total E (10^4 KWh)
	Guanyinyan	Hongqi	
Current energy	380.91	464.89	845.80
Optimal energy	404.53	493.71	898.24

To reach the optimal energy production, new operating rules for the cascade have been derived. In case of Guanyinyan dam, the new operation rules are introduced in figure 6.8. The dam releases more water through turbine to enhance the energy to 404.53 $10^4 KWh$. It is obvious in figure 6.8a that the red curves of optimized water level in the reservoir which will goes down 594.0 m from 590.0 much in comparison to the current strategy (cyan curve) from 594.0 m and 590.30 m. In contrast, in figure 6.8b, the flow rate through turbine, see the red line, increases an mount of 5 to 10 percent compared to current discharge. However, the optimal water level and flow rate still satisfy the constraints in table 6.4.

The circumstance is adverse for the Hongqi dam that water level rises to maximize the energy to 493.71 $10^4 KWh$. The release from Guanyinyan and intermediate flow are stored whereas the outflow for turbines does not significantly change. Consequently, the water level goes up from 505.10 m to almost 510.62 m, (see the blue line in figure 6.9a) compared to 505.10 m - 507.20 m for current strategy. Another point is that the discharge of Hongqi slightly declines according to figure 6.9b. The optimal flow in blue curves varies from 2.50 m^3/s to 23.96 m^3/s compared to the range of current flow, (see the line in cyan color), between 6.0 m^3/s - 33.43 m^3/s. In spite of increase of water level, the penalty in table 6.4 is not violated. In general, the power production of a whole system increases as expected. Total computation time is about 303 seconds which is acceptable.

Table 6.4: Flow and stage restrictions of both reservoirs

No	Turbine flow (m^3/s)		Water level (m)	
	Guanyinyan	Hongqi	Guanyinyan	Hongqi
Minimum	0.00	0.00	577	499
Maximum	35.80	55.20	600.5	514

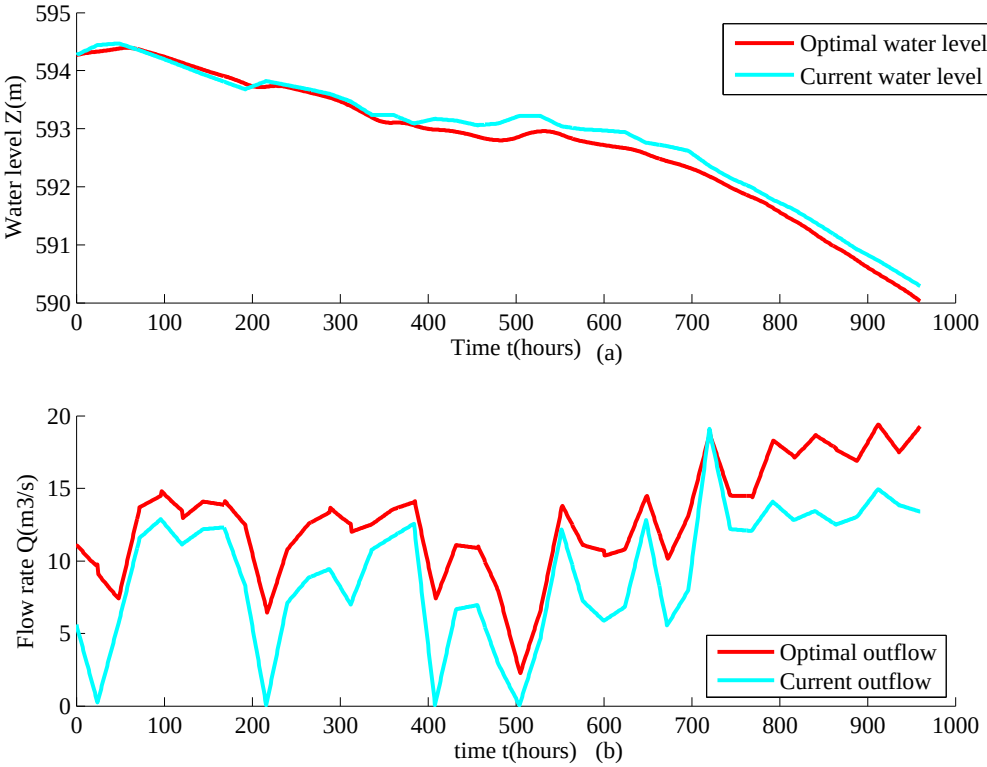

Figure 6.8: Optimal operation rules of Guanyinyan dam

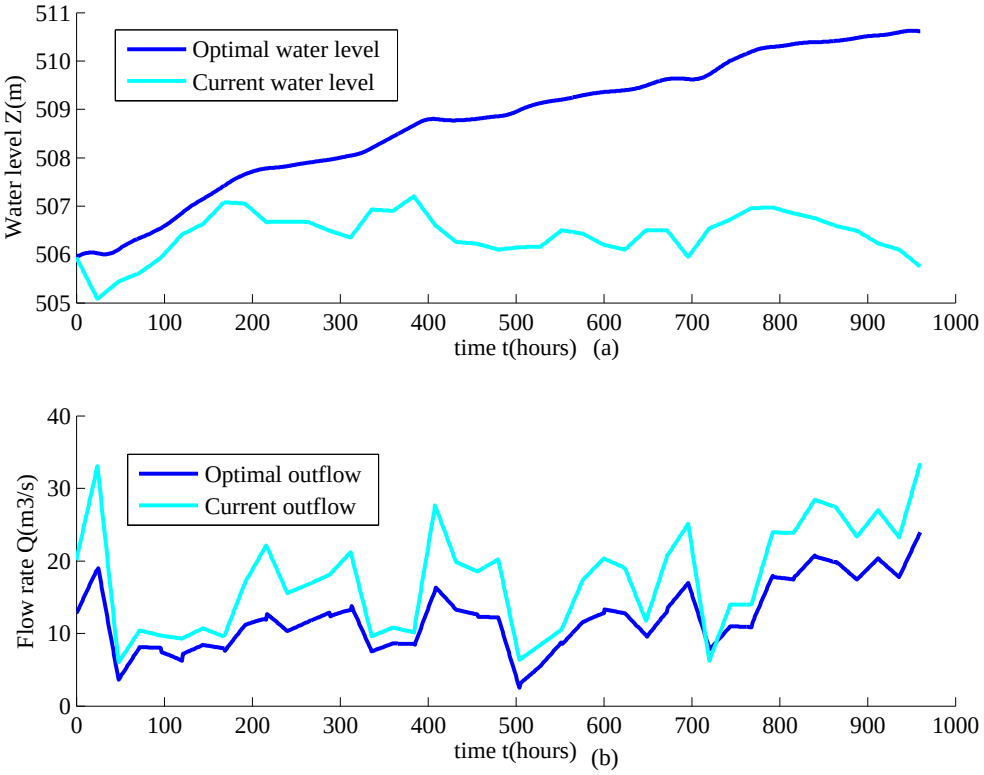

Figure 6.9: Optimal operation rules of Hongqi dam

6.4 Conclusion

This chapter introduces a new approach that utilizes an ATD model in the optimization procedure of a hydropower cascade. The advancement is that the system dynamics are considered during the optimization process while the calculation time is short. The method has been applied to a two reservoir system with promising results (Nguyen et al, 2016a)

Chapter 7

WaterLib toolbox

7.1 Introduction of WaterLib simulation toolbox

The optimal design of an automatic control of water system such as rivers and reservoirs always requires model of their behavior. The MATLAB / Simulink toolbox WaterLib is created for this purpose. Many portable models for typical elements of water systems are stored in the library. From which, a complex hydraulic system can be directly built per drag and drop with the support of a graphic editor. These approaches hence allow to implement and analyze different control strategies for the output of hydrodynamic systems (Pfuetzenreuter and Rauschenbach, 2005; Rauschenbach et al, 1996). Nevertheless, the toolbox is not complete. Therefore, this chapter introduces extensions for the WaterLib toolbox for river modeling realized in the previous chapters of this work, i.e, adaptive the time delay model for different river cross sections, coupled time delay model with backwater effects model. Recently, the module has been continuously extended with a set of simulation tools for complex water surface system. In stead of conducting a detail simulation model with several parameters and enormous computation time, the new elements reduces the workload by using simplified simulation blocks. Up to now most of significant parts of surface water system are integrated, e.g model for a river reach and open channel, models for water works, catchment model as in figure 7.2.

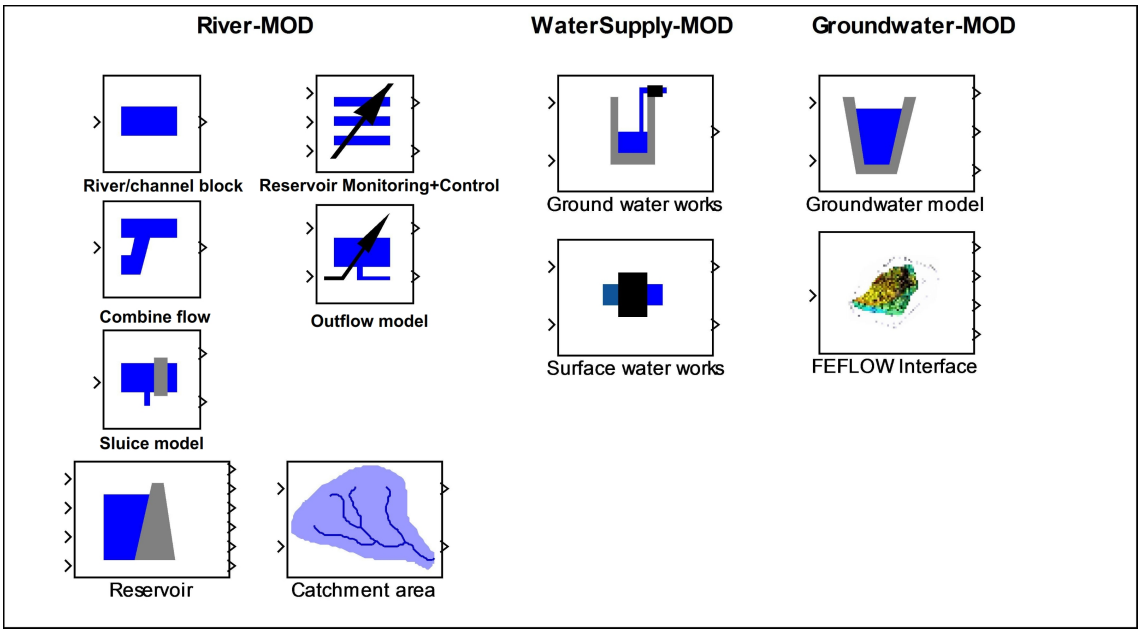

Figure 7.1: Modules of Waterlib

1. The RIVER MOD module includes:

   - Model for rivers and channels is a rough simulation of a simple time constant elements T_c of the first order combined with time delay elements T_d. Hence, the propagation time of flow can be described. The discharge q is then simulated based on these parameters. The following algorithm indicates the first order delay model:

$$\begin{cases} T_c \frac{dq}{dt} + q = Q \\ q = Q\,(t - T_d) \end{cases} \tag{7.1}$$

   - Flow routing element is connection between a river block with other elements of surface water simulation models. These simulation blocks includes: combine flow (for confluences), sluice model (deciding outflow), for confluences, outflow model, and reservoir monitoring and control.

   - Reservoir model presents the storage behavior of dam describe by equation 7.2. The water level and the volume of dammed water are the important parameters of the reservoir. The change of reservoir volume is given to a discrete integrator that computes the resulting water volume at every time step. Then, the water level and surface area are determined by utilizing SIMULINK look up tables of reservoir characteristics (volume

- water level, and volume - surface area). The volume alternation during a time interval k is primary determined by inflow $Q_{in}(k)$, outflow of the reservoir $Q_{out}(k)$, precipitation $Q_p(k)$, evaporation $Q_e(k)$, and infiltration $Q_{infil}(k)$.

$$V(k+1) = V(k) + \Delta V(k) \tag{7.2a}$$

$$\Delta V(k) = Q_{in}(k) - Q_{out}(k) + Q_p(k) + Q_e(k) + Q_{infil}(k) \tag{7.2b}$$

- Catchment area model is designed for long-term forecasting as well as simulation of the flow at outlet of the watershed. According to (Gevers and Maxwell, 1976), the fundamental structure consists of three sub-models: sub-model 1 calculates the net run off from measured rainfall data and the potential evapotranspiration (ETP), sub-model 2 computes surface water flow, and sub-model 3 simulates groundwater flow.

2. The Water Supply-MOD module includes:

- Storage-free surface water works aim at fulfilling the water demand of stakeholders from an available reservoir or water flow (pipeline, channels). The realized flow rate Q_s that must be released for stakeholder demand Q_d can not go beyond the design flow rate of the structure Q_{max}. Moreover, surface waterworks with storage tank has similar algorithm to the storage-free surface structures. Particularly, a storage tank integrated in the system helps to balance the deficit in demand and waterwork inflow. The mathematical algorithm for any waterworks is described by equation 7.3.

$$Q_s = \begin{cases} Q_d, Q_d \leq Q_{\max} \\ Q_{\max}, Q_d > Q_{\max} \end{cases} \tag{7.3}$$

- Groundwater waterworks: water works obtains water from the ground are capable to control their inflow by monitoring the water head in the well. The customer demand is restricted by the maximum supply rate for the waterworks. While the pumping rate of the water works Q_p that

is equal to the outflow to stakholders Q_d is computed as follows:

$$Q_s = \begin{cases} Q_d, Q_d \leq Q_{\max} \\ Q_{\max}, Q_d > Q_{\max} \end{cases} \tag{7.4}$$

$$Q_p = \psi Q_d. \tag{7.5}$$

where ψ is a reduction factor from difference of water head.

3. The Groundwater-MOD consists of

   - Groundwater tool is a reduced model of a complex ground water model FEFFLOW
   - The FEFLOW interface

7.2 Extension of the Waterlib Toolbox

Although modules of WaterLib are able to meet the basic demand in water system simulation some somethings need further attention. Particularly, river/channel simulation, the model is quite simple. The parameter of time delay model can not adapt to the variation in flow rate. Therefore, it can only return a fair good result. In addition, the problem of backwater effect has not been taken into account, consequently, the simulation result is not correct for the river with finite downstream boundary condition. Hence, the new modules developed in the previous chapters are implemented in the Toolbox.

1. ATD model for river channel block

   The model is able to simulate a river with wide range of geometry as well as different boundary conditions. The module is governed by the relationship between flow rate Q, time constant T_c, and time delay T_d is presented in table 7.1

   Two methods are used to determine the curves Q versus T_c, and T_d:

   - According to the Chapter 3 and (Nguyen et al, 2016b), the parameters are designed for a small river with trapezoidal cross section. The param-

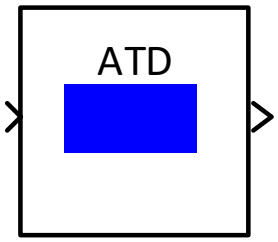

Figure 7.2: A new simulation block for flow routing elements

Table 7.1: Parameters of river/channel simulation block

Parameters	**Description**
Time unit	Unit used for entering constant and delay time values
Flow rate	Q is flow rate at upstream end
Time constant	T_c is time spent for a step response reaching 63% of final value
Time delay	T_d is time spent flowing through conduit

eters T_c, and T_d changes according to alternation of flow rate so that the simulation result is more accurate than the previous model.

- Following the Chapter 5 and (Nguyen et al, 2016c), a nonlinear optimization technique is utilized to estimate T_c, T_d from a travel time and flow rate of an available complex hydraulic model such as HEC-RAS, MIKE 11. Especially, with this approach, the effect of irregular cross sections is also taken into account when generating the curves Q vs T_c, and Q vs T_d.

2. River channel block for backwater effects

   Another upgrade is that a river/channel simulation block with backwater effect has been added to the library which is fundamentally a coupling of the adaptive time delay model and reservoir model (figure 7.3). The algorithm is developed and validated in Chapter 4. In addition, table 7.2 presents significant parameters for implementing the simulation model. With this extension, the flow dynamics in a river reach with different downstream boundaries is able to be precisely simulated.

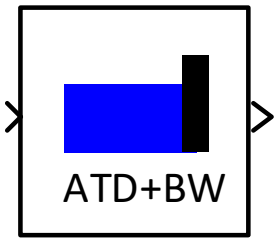

Figure 7.3: A simulation block of river/channel with backwater effect

Table 7.2: Parameters of river/channel simulation block with backwater effect

Parameter	Description
Time unit	Unit used for entering constant and delay time values
Flow rate unit	Unit used for entering flow rate
Reach length unit	Unit used for entering reach length
Water level unit	Unit used for entering water level
Volume unit	Unit used for entering volume
Initialization type	Allows selection of water level or volume
Initialization value	Initial state value of the reservoir
Dead water level	Lowest water level
Maximum water level	Highest possible water level
Lookup table editor	Table of water level, volume, and surface area

7.3 Conclusion

In summary, the MATLAB/Simulink toolbox Waterlib comprising of libraries for modeling water systems has been developed since years. The primary focus is to further develop the library by creating modules which are capable of describing complex hydraulic circumstances and use for controller design. Particularly, a number of models for the water supply network elements (pumping stations, waterworks), for groundwater storage and reuse of treated wastewater are under active investigation (Rauschenbach and Gao, 2005). Nevertheless, the quick approximation of river flow in terms of complex geometry as well as different downstream conditions is particularly strengthened in this work. In addition, the simplified model for controller design is also derived from the available complex river models(HEC-RAS, MIKE 11, and others) which is presented in (Nguyen et al, 2016c). The blocks return results that are accurate as the complex model and faster than the complex ones. These advancements improve the quality in designing control policies for water system.

Chapter 8

Summary, Limitation and Outlook

The dissertation is dedicated to reduced models of the full hydraulic model, the analysis and their applications to optimal control. The simple first order model with delay is selected as a reduced model approach for the SVEs. The algorithm of the model is then extended to analyze the flow dynamics in small rivers with semi-infinite length, a river with backwater effect, a river with complex cross sections, and the application to control of a cascade of reservoirs. Sequentially, the achievements will be summarized and the outlook for further research will also be mentioned.

8.1 Summary

In terms of the reduced model for a small river with infinite downstream length, an adaptive time delay model based on a prismatic trapezoidal geometry is introduced. The nonlinear relation curves of the time constant T_c and the time delay T_d with flow rate Q are derived and used in simulating the outflow for different scenarios which becomes very simple, fast and accurate.

Regarding the model for a river with backwater effect, an ATD model coupling with the back water model to simulate the non-uniformity of flow in rivers/channels is presented. Especially, the uniform flow is considered in unsteady state for flow routing and the computation time is significantly reduced. The approach compensates deficiencies of previous researches by taking into account the backwater effect in routing river flow.

Moreover, a procedure to derive the simplified model directly from the complex

hydrodynamics software is presented. In this case the ATD model that can be used to estimate river flow for irregular geometry. The ATD model is validated in several case studies and it has been shown that the ATD model is suitable for real time flood forecasting and application in designing control policies for water systems.

The application of the ATD model to the optimization procedure of a hydropower cascade is also demonstrated. The method has been applied to a two reservoir system with promising results. The system consists of two hydropwer stations connected by a river reach which are modeled by two reservoir models connected with the ATD model for a river reach. The objective is to maximize the energy production of the system subject to some constrains. This cutting-edge point is that the system dynamics and unsteady flow are considered during the optimization process.

All the above mentioned improvements of the ATD models are implemented in SIMULINK/MATLAB to generate the supplement modules for the WaterLib Toolbox.

8.2 Limitation

Besides the mentioned above advantages, a few limitations of the ATD model are presented as follows

- The ATD model is valid only in the design range of flow. It can be explained that the parameters of the ATD model are obtained from the curves of T_c versus Q and T_d versus Q which are designed for a certain range of flow. If the upstream flow is out of the range, T_c and T_d can not be determined.

- In terms of the coupled ATD model with backwater effects, it is difficult to define the relationship curves of T_c versus Q and T_d versus Q. A reason is that the T_c and T_d are influenced by the upstream flow and the backwater flow. This causes the fluctuation of both backwater part L_b and uniform flow part L_u. Hence, two approaches of the coupling ATD model are introduced in chapter 4. On the one hand, the method presented in the section 4.2 describes the movement of the intersection point of both areas by which the flow dynamics are accurately simulated. However, it consumes much time for the simulation. On other hand, in the section 4.4, the method defines the fixed intersection

point and assumes that the backwater part does not influence the uniform part. This reduces the simulation accuracy but the computation is quick. The selection of the appropriate model should rely on the objectives of the research.

- The accuracy of the ATD model depends significantly on the accuracy of complex hydraulic models (HECRAS, MIKE 11, and SOBEK). It is obvious that the parameters of the ATD model T_c and T_c are derived from the travel time T_M and flow rate Q generated from the complex model. Therefore, it is recommended that the complex hydraulic model must be well validated before using for derivation of the ATD model.

8.3 Outlook

A number of directions are suggested for further research as follows

- The lateral flow is an important factor in hydraulic modeling. The combination of the lateral of flow with the ATD model is recommended for further research. It is suggested that the river reach is separated into several sub-reaches. The ATD model is developed for each reach. The ATD model is connected together at junction where the lateral flow can be integrated.

- The application of the coupled ATD model with backwater model for other downstream conditions such as tidal effect, downstream sluices need to be examined.

- The application of the ATD model for real time forecasting of flooding for water system is proposed because the model can give very good results with low computation effort. Moreover, using the ATD model with ArcGIS in determining flooding area is recommended. For instance, the ATD model is able to describe accurately the water level in the reservoir which is then used by a Geographic Information System (GIS) to defined the upstream inundation area.

- The application of the ATD model for real time control of water system such as hydropower cascade, sluices/tide gate system for flood prevention is also suggested.

Bibliography

Abbott M (1979) Computational hydraulics: Elements of the theory of free surface flows. Pitman, London

Abbott MB (1966) An introduction to the method of characteristics

Abdelmoumène Toudeft PG (1996) Neural and adaptive controllers for a non-minimum phase varying time-delay system. Artificial Intelligence in Engineering 4:431–439

Apollov BA, Kalinin GP, Komarov VD (1964) Hydrological forecasting. Israel Program for Scientific Translations Jerusalem, Israel

Archer D, Foster M, Faulkner D, Mawdsley J (2000) The synthesis of design flood hydrographs. In: Proc. ICE/CIWEM Conf. Flooding–Risks and Reactions. Terrace Dalton, London

Baume JP, Sau J, Malaterre PO (1998) Modelling of irrigation channel dynamics for controller design. In: Systems, Man, and Cybernetics, 1998. 1998 IEEE International Conference on, IEEE, vol 4, pp 3856–3861

Bentura PL, Michel C (1997) Flood routing in a wide channel with a quadratic lag-and-route method. Hydrological Sciences Journal 42(2):169–189

Bhuyan M, Kumar S, Jena J, Bhunya P (2015) Flood hydrograph with synthetic unit hydrograph routing. Water Resources Management 29(15):5765–5782, DOI 10.1007/s11269-015-1145-1

Bolea Y, Martinez-Gonzalez R, Grau A, Martinez-Garcia H (2009) An lpv fractional model for canal control

Bolea Y, Martinez-Gonzalez R, Grau A, Martinez-Garcia H (2010a) An lpv fractional hayami model for canal control. In: Methods and Models in Automation and Robotics (MMAR), 2010 15th International Conference on, pp 329–334, DOI 10.1109/MMAR.2010.5587211

Bolea Y, Martinez-Gonzalez R, Grau A, Martinez-Garcia H (2010b) An lpv fractional hayami model for canal control. In: Methods and Models in Automation and Robotics (MMAR), 2010 15th International Conference on, pp 329–334

Brebbia CA, Dominguez J (1994) Boundary elements: an introductory course. WIT press

Breckpot, Moor D (2012) Control of a single reach with model predictive control. River Flow 2012

Breckpot M, Agudelo OM, De Moor B (2012a) Modelling of a river system with multiple reaches pp 1454–1459

Breckpot M, Oscar MA, Moor BD (2012b) Model predictive control applied to a river system with two reaches

Brunner GW (1995) Hec-ras river analysis system. hydraulic reference manual. version 1.0. Tech. rep., DTIC Document

Camacho E, Bordons C (2004) Model predictive control. Springer, New York

Camacho L, Lees M (1999) Multilinear discrete lag-cascade model for channel routing. Journal of Hydrology 226(1):30–47

Camacho R, Barbosa J (2005) The boundary element method applied to incompressible viscous fluid flow. Journal of the Brazilian Society of Mechanical Sciences and Engineering 27(4):456–462

Cantoni M, Weyer E, Li Y, Ooi SK, Mareels I, Ryan M (2007) Control of large-scale irrigation networks. Proceedings of the IEEE 95(1):75–91

Canuto C, Hussaini MY, Quarteroni AM, Thomas Jr A, et al (2012) Spectral methods in fluid dynamics. Springer Science & Business Media

Catalano P, Wang M, Iaccarino G, Moin P (2003) Numerical simulation of the flow around a circular cylinder at high reynolds numbers. International Journal of Heat and Fluid Flow 24(4):463–469

Chanson H (2004) Hydraulics of open channel flow. Butterworth-Heinemann

Chaudhry MH (2007) Open-channel flow. Springer Science & Business Media

Chow VT (1959) Open channel hydraulics. NY etc: McGraw Hill

Cimorelli L, Cozzolino L, Della Morte R, Pianese D (2013) An improved numerical scheme for the approximate solution of the parabolic wave model. Journal of Hydroinformatics 15(3):913–925

Cimorelli L, Cozzolino L, Della Morte R, Pianese D (2014) Analytical solutions of the linearized parabolic wave accounting for downstream boundary condition and uniform lateral inflows. Advances in Water Resources 63:57–76

Cimorelli L, Cozzolino L, Della Morte R, Pianese D, Singh VP (2015) A new frequency domain analytical solution of a cascade of diffusive channels for flood routing. Water Resources Research 51(4):2393–2411, DOI 10.1002/2014WR016192

Cooley RL, Moin SA (1976) Finite element solution of saint-venant equations. Journal of the Hydraulics Division 102(6):759–775

Corriga G, Sanna S, Usai G (1983) Sub-optimal constant-volume control for open channel networks. Applied Mathematical Modelling 7(4):262–267

Corriga G, Salimbeni D, Sanna S, Usai G (1988) A control method for speeding up response of hydroelectric station power canals. Applied Mathematical Modelling 12(6):627–633

Courant R, Friedrichs K, Lewy H (1967) On the partial difference equations of mathematical physics. IBM journal 11(2):215–234

Cozzolino L, Della Morte R, Covelli C, Del Giudice G, Pianese D (2011) Numerical solution of the discontinuous-bottom shallow-water equations with hydrostatic pressure distribution at the step. Advances in Water Resources 34(11):1413–1426

Cozzolino L, Della Morte R, Del Giudice G, Palumbo A, Pianese D (2012) A well-balanced spectral volume scheme with the wetting–drying property for the shallow-water equations. Journal of Hydroinformatics 14(3):745–760

Cozzolino L, Cimorelli L, Covelli C, Della Morte R, Pianese D (2014a) Boundary conditions in finite volume schemes for the solution of shallow-water equations: The non-submerged broad-crested weir. Journal of Hydroinformatics 16(6):1235–1249

Cozzolino L, Della Morte R, Cimorelli L, Covelli C, Pianese D (2014b) A broad-crested weir boundary condition in finite volume shallow-water numerical models. Procedia Engineering 70:353–362

Cozzolino L, Pepe V, Della Morte R, Cirillo V, D'Aniello A, Cimorelli L, Covelli C, Morlando F, Pianese D (2016) One-dimensional mathematical modelling of debris flow impact on open-check dams. Procedia Earth and Planetary Science 16:5–14

Crossley AJ, Wright NG, Whitlow CD (2003) Local time stepping for modeling open channel flows. Journal of Hydraulic Engineering 129(6):455–462

Crowe DFWBCRJA Clayton T Elger (2009) Engineering fluid mechanics. John Willey & Sons

Cundy TW, Tento SW (1985) Solution to the kinematic wave approach to overland flow routing with rainfall excess given by philip's equation. Water Resources Research 21(8):1132–1140, DOI 10.1029/WR021i008p01132, URL `http://dx.doi.org/10.1029/WR021i008p01132`

Cunge J, Holly F, Verwey A (1980) Practical Aspects of Computational River Hydraulics. Pitman Advanced Publishing Program, London

Cunge JA (1969) On the subject of a flood propagation computation method (muskingum method). Journal of Hydraulic Research 7(2):205–230

D'Aniello A, Cozzolino L, Cimorelli L, Della Morte R, Pianese D (2015) A numerical model for the simulation of debris flow triggering, propagation and arrest. Natural Hazards 75(2):1403–1433

Dooge J, Napiórkowski J, Strupczewski W (1987) Properties of the generalized downstream channel response. Acta Geophysica Polonica 35(4):405–418

Dooge J, Napiórkowski JJ, Strupczewski WG (1988) The linear downstream response of a generalized uniform channel. Acta Geophysica Polonica 35(3):277–291

Elfawal-Mansour H, Georges D, Ohnishi N (1981) Optimal control of an open channel irrigation system based on nonlinear models. In: TENCON 2000. Proceedings, vol 3, pp 308–313 vol.3

Ermolin YA (1992) Study of open-channel dynamics as controlled process. Journal of Hydraulic Engineering 118(1):59–72

Eurén K, Weyer E (2007) System identification of open water channels with undershot and overshot gates. Control Engineering Practice 15(7):813–824

Fan P, Li J (2006) Diffusive wave solutions for open channel flows with uniform and concentrated lateral inflow. Advances in water resources 29(7):1000–1019

Fayaed SS, El-Shafie A, Jaafar O (2013) Reservoir-system simulation and optimization techniques. Stochastic environmental research and risk assessment 27(7):1751–1772

Foo M, Su Ki O, Weyer E (2010) Modelling of river for control design. In: Control Applications (CCA), 2010 IEEE International Conference on, pp 1862–1867

Foo M, Su Ki O, Weyer E (2014) System identification and control of the broken river. Control Systems Technology, IEEE Transactions on 22(2):618–634

Franchini M, Bernini A, Barbetta S, Moramarco T (2011) Forecasting discharges at the downstream end of a river reach through two simple muskingum based procedures. Journal of Hydrology 399(3–4):335 – 352, DOI http://dx.doi.org/10.1016/j.jhydrol.2011.01.009

Fread D (1985) Channel routing. Hydrological forecasting pp 437–503

Garcia R, Kahawita RA (1986) Numerical solution of the st. venant equations with the maccormack finite-difference scheme. International Journal for numerical methods in fluids 6(5):259–274

Gevers M, Maxwell B (1976) Identification of a rainfall-runoff process. In: Identification and system parameter estimation: proceedings of the 4th IFAC Symposium, Tbilisi, USSR, 21-27 September 1976, North-Holland Pub. Co., vol 2, p 735

Haltas I, Kavvas M (2009) Ensemble-averaged flow routing in channel networks: Kinematic wave equation. Journal of Hydrologic Engineering 14(7):655–662

Hamann A, Hug G (2014) Real-time optimization of a hydropower cascade using a linear modeling approach. In: Power Systems Computation Conference (PSCC), 2014, IEEE, pp 1–7

Harley B (1967) Linear routing in uniform channels. M Eng Science Thesis, Department of Civil Engineering National University of Ireland

Hayami S (1951) On the propagation of flood waves

Hofleitner A, Rabbani T, El Ghaoui L, Bayen A (2013) Online homotopy algorithm for a generalization of the lasso. IEEE Transactions on Automatic Control 58(12):3175–3179

Holmes P, JL L, Berkooz G (1998) Turbulence, Coherent Structures, Dynamical Systems and Symmetry. Cambridge University Press, Cambridge, UK

Hughes TJ, Franca LP, Hulbert GM (1989) A new finite element formulation for computational fluid dynamics: Viii. the galerkin/least-squares method for advective-diffusive equations. Computer Methods in Applied Mechanics and Engineering 73(2):173–189

Kalinin G, Milyukov P (1957) O raschete neustanovivshegosya dvizheniya vody v otkrytykh ruslakh [on the computation of unsteady flow in open channels]. Met i Gydrologia Zhurnal 10:10–18

Karamouz M, Houck MH (1987) Comparison of stochastic and deterministic dynamic programming for reservoir operating rule generation1

Karimanzira D, Schwanenberg D, Allen C (2014) Short-term management of hydropower: Definition, assessment and disposal of operational flexibility

Lai C (1986) Numerical modeling of unsteady open-channel flow. Advances in hydroscience 14:161–333

Liggett J (1984) The boundary element method-some fluid applications. Multidimensional Fluid Transients pp 1–8

Litrico X, Fromion V (2004a) Analytical approximation of open-channel flow for controller design. Applied Mathematical Modelling 28(7):677 – 695, DOI http://dx.doi.org/10.1016/j.apm.2003.10.014

Litrico X, Fromion V (2004b) Frequency modeling of open-channel flow. Journal of Hydraulic Engineering 130(8):806–815, DOI 10.1061/(ASCE)0733-9429(2004)130:8(806)

Litrico X, Fromion V (2009) Modeling and control of hydrosystems. Springer Science & Business Media

Litrico X, Georges D (1999) Robust continuous-time and discrete-time flow control of a dam–river system. (i) modelling. Applied Mathematical Modelling 23(11):809–827

Litrico X, Pomet JB, Guinot V (2010) Simplified nonlinear modeling of river flow routing. Advances in Water Resources 33(9):1015 – 1023, DOI http://dx.doi.org/10.1016/j.advwatres.2010.06.004

Liu M, Liu G (2010) Smoothed particle hydrodynamics (sph): an overview and recent developments. Archives of computational methods in engineering 17(1):25–76

Ljung L, Glad T (1994) Modeling of dynamic systems. Prentice-Hall, Inc.

Lundberg KH, Miller HR, Trumper DL (2007) Initial conditions, generalized functions, and the laplace transform troubles at the origin. IEEE control systems 27(1):22–35

Mai D (2009) Development of flood prediction models for the huong and vu gia-thu bon river basins in central vietnam. PhD thesis, Ph. D. thesis, Vrije Universiteit Brussel, Brussels, Belgium

Malaterre PO, Baume JP (1998) Modeling and regulation of irrigation canals: existing applications and ongoing researches. In: Systems, Man, and Cybernetics, 1998. 1998 IEEE International Conference on, vol 4, pp 3850–3855 vol.4

Meijer H (1941) Simplified flood routing. Civil Eng 11:306–307

Monaghan JJ (1992) Smoothed particle hydrodynamics. Annual review of astronomy and astrophysics 30:543–574

Moriasi D, Arnold J, Van Liew M, Bingner R, Harmel R, Veith T (2007) Model evaluation guidelines for systematic quantification of accuracy in watershed simulations. Trans Asabe 50(3):885–900

Moussa R (1996) Analytical hayami solution for the diffusive wave flood routing problem with lateral inflow. Hydrological processes 10(9):1209–1227

Munier S, Litrico X, Belaud G, Malaterre PO (2008) Distributed approximation of open-channel flow routing accounting for backwater effects. Advances in Water Resources 31(12):1590 – 1602, DOI http://dx.doi.org/10.1016/j.advwatres.2008.07.007

Nash J (1957) The form of the instantaneous unit hydrograph. International Association of Scientific Hydrology, Publ 3:114–121

Neelakantan T, Pundarikanthan N (2000) Neural network-based simulation-optimization model for reservoir operation. Journal of water resources planning and management 126(2):57–64

Nguyen LD, Karimanzira D, Rauschenbach T (2016a) Application of adaptive time delay model in optimal control of a hydropower cascade. Procedia Engineering 162:212–220

Nguyen LD, Karimanzira D, Rauschenbach T, Ribbe L (2016b) Design and application of an adaptive time delay model for flow routing in prismatic trapezoidal geometry river reach. Water Resources Management pp 1–12, DOI doi:10.1007/s11269-016-1438-z

Nguyen LD, Karimanzira D, Rauschenbach T, Ribbe L (2016c) A procedure for approximating a complex hydrodynamic model by the adaptive time delay method. In: World Environmental and Water Resources Congress 2016, pp 1–11, DOI 10.1061/9780784479841.001

O'Connor K, Goswami M, Faulkner D (2014) Volume iii hydrograph analysis

Ooi SK, Weyer E (2008) Control design for an irrigation channel from physical data. Control Engineering Practice 16(9):1132–1150

Ooi SK, Foo M, Weyer E (2011) Control of broken river

O'Sullivan J, Ahilan S, Bruen M (2012) A modified muskingum routing approach for floodplain flows: Theory and practice. Journal of Hydrology 470–471:239 – 254, DOI http://dx.doi.org/10.1016/j.jhydrol.2012.09.007

van Overloop P, Miltenburg I, Bombois X, Clemmens A, Strand R, van de Giesen N, Hut R (2010) Identification of resonance waves in open water channels. Control Engineering Practice 18(8):863 – 872, DOI http://dx.doi.org/10.1016/j.conengprac.2010.03.010

van Overloop PJ, Horváth K, Aydin BE (2014) Model predictive control based on an integrator resonance model applied to an open water channel. Control Engineering Practice 27:54 – 60, DOI http://dx.doi.org/10.1016/j.conengprac.2014.03.001

Overloop van PJ, Horváth K, Ekin Aydin B (2014) Model predictive control based on an integrator resonance model applied to an open water channel. Control Engineering Practice 27(0):54–60

Papageorgiou M, Messmer A (1985) Continuous-time and discrete-time design of water flow and water level regulators. Automatica 21(6):649–661

Papageorgiou M, Messmer A (1989) Flow control of a long river stretch. Automatica 25(2):177–183

Perez RR, Batlle VF, Garcia FC, Saez AL (2008) System identification for control of a main irrigation canal pool. IFAC Proceedings Volumes 41(2):9649–9654

Perumal M (1994) Multilinear discrete cascade model for channel routing. Journal of Hydrology 158(1):135–150

Perumal M, Moramarco T, Melone F (2007) A caution about the multilinear discrete lag-cascade model for flood routing. Journal of hydrology 338(3):308–314

Pfuetzenreuter T, Rauschenbach T (2005) Library ilm-river for simulation and optimal control of rivers and hydropower plants. River Basin Management III pp 121–130

Rafiee M, Wu Q, Bayen AM (2009) Kalman filter based estimation of flow states in open channels using lagrangian sensing. In: Decision and Control, 2009 held jointly with the 2009 28th Chinese Control Conference. CDC/CCC 2009. Proceedings of the 48th IEEE Conference on, IEEE, pp 8266–8271

Rafiee M, Tinka A, Thai J, Bayen AM (2011) Combined state-parameter estimation for shallow water equations. In: Proceedings of the 2011 American Control Conference, IEEE, pp 1333–1339

Rafiee Jahromi M (2012) Data assimilation in large-scale networks of open channels

Rauschenbach T (2001) Simulation and optimal control of rivers and hydropower plants. In: Proceedings of the IASTED International Conference on Intelligent Systems and Control (ed. by MH Hamaza), pp 85–89

Rauschenbach T (2005) Optimal co-ordinated control of hydropower plants. IFAC Proceedings Volumes 38(1):291–295

Rauschenbach T, Gao Z (2005) Development of the\"capital water resources allocation decision supporting system" for the city of beijing. WIT Transactions on Ecology and the Environment 83

Rauschenbach T, Hoffmeyer-Zlotnik HJ, Koch M, Wernstedt J, Kopacek P, Allmer H, Schmidt A (1996) Systemtechnische untersuchung zur steuerung oesterreichischer donaustaustufen: Die modellbildung und das steuerkonzept. VDI BERICHTE 1282:259–268

Saint-Venant Ad (1871) 'theorie du mouvement non permanent des eaux, avec application aux crues des rivieres et a l'introduction de marees dans leurs lits.". Comptes rendus des seances de l'Academie des Sciences 36:174–154

Sattari MT, Apaydin H, Ozturk F (2009) Operation analysis of eleviyan irrigation reservoir dam by optimization and stochastic simulation. Stochastic Environmental Research and Risk Assessment 23(8):1187–1201

Schuurmans J, Bosgra O, Brouwer R (1995) Open-channel flow model approximation for controller design. Applied Mathematical Modelling 19(9):525 – 530, DOI http://dx.doi.org/10.1016/0307-904X(95)00053-M

Schuurmans J, A H, Bosgra OH, Brouwer R (1999a) Simple water level controller for irrigation and drainage canals. Journal of irrigation and drainage engineering 125

Schuurmans J, Clemmens AJ, Dijkstra S, Hof A, Brouwer R (1999b) Modeling of irrigation and drainage canals for controller design. Journal of Irrigation and Drainage Engineering 125(6):338–344, DOI 10.1061/(ASCE)0733-9437(1999)125:6(338)

Schwanenberg D, Xu M, Ochterbeck T, Allen C, Karimanzira D (2014) Short-term management of hydropower assets of the federal columbia river power system. Journal of Applied Water Engineering and Research 2(1):25–32

Seddon JA (1900) River hydraulics. In: Proceedings of the American Society of Civil Engineers, ASCE, vol 25, pp 619–669

Sepulveda C, Rodellar J (2005) Irrigation canal system identification for control purposes. Technical report, Polytechnic University of Catalunya

Stoker JJ (1957) Water Waves. Interscience Press, New York

Stoker JJ (2011) Water waves: The mathematical theory with applications, vol 36. John Wiley & Sons

Sturm TW (2010) Open channel hydraulics. McGraw-Hill New York

Szilagyi J (2003) State-space discretization of the kalinin-milyukov-nash-cascade in a sample-data system framework for streamflow forecasting. Journal of Hydrologic Engineering 8(6):339–347, DOI 10.1061/(ASCE)1084-0699(2003)8:6(339)

Szilagyi J (2006) Discrete state-space approximation of the continuous kalinin–milyukov–nash cascade of noninteger storage elements. Journal of Hydrology 328(1–2):132 – 140, DOI http://dx.doi.org/10.1016/j.jhydrol.2005.12.015

Szilagyi J, Laurinyecz P (2012) Accounting for backwater effects in flow routing by the discrete linear cascade model. Journal of Hydrologic Engineering 19(1):69–77

Szilágyi J, Nagy AS (2010) Recursive Streamflow Forecasting: A State Space Approach. CRC Press

Szilagyi J, Balint G, Gauzer B, Bartha P (2005) Flow routing with unknown rating curves using a state-space reservoir-cascade-type formulation. Journal of hydrology 311(1):219–229

Szöllösi-Nagy A (1982) The discretization of the continuous linear cascade by means of state space analysis. Journal of Hydrology 58(3):223–236

Szymkiewicz R (1991) Finite-element method for the solution of the saint venant equations in an open channel network. Journal of Hydrology 122(1–4):275 – 287, DOI http://dx.doi.org/10.1016/0022-1694(91)90182-H

Tosaka N, Kakuda K, Onishi K (1985) Boundary element analysis of steady viscous flows based on puv formulation. In: Boundary Elements VIIth Proceedings, vol 2, pp 71–80

Toudeft A (1995) Neural Control of Nonlinear Non-Minimum Phase Dynamical Systems, Springer Vienna, chap 105, pp 404–407

Versteeg HK, Malalasekera W (2007) An introduction to computational fluid dynamics: the finite volume method. Pearson Education

Violeau D, Issa R (2007) Numerical modelling of complex turbulent free-surface flows with the sph method: an overview. International Journal for Numerical Methods in Fluids 53(2):277–304

Violeau D, Rogers BD (2016) Smoothed particle hydrodynamics (sph) for free-surface flows: past, present and future. Journal of Hydraulic Research pp 1–26

Waltz RA, Morales JL, Nocedal J, Orban D (2006) An interior algorithm for nonlinear optimization that combines line search and trust region steps. Mathematical programming 107(3):391–408

Wang L, Wu JQ, Elliot WJ, Fiedler FR, Lapin S (2014) Linear diffusion-wave channel routing using a discrete hayami convolution method. Journal of Hydrology 509:282 – 294, DOI http://dx.doi.org/10.1016/j.jhydrol.2013.11.046

Wang ZJ (2002) Spectral (finite) volume method for conservation laws on unstructured grids. basic formulation: Basic formulation. Journal of Computational Physics 178(1):210–251

Weyer E (2001) System identification of an open water channel. Control Engineering Practice 9(12):1289–1299

Weyer E (2008) Control of irrigation channels. Control Systems Technology, IEEE Transactions on 16(4):664–675

Xu M (2013) Real-time control of combined water quantity and quality in open channels. Dissertation

Yang K, Zheng J, Yang M, Zhou R, Liu G (2013) Adaptive genetic algorithm for daily optimal operation of cascade reservoirs and its improvement strategy. Water resources management 27(12):4209–4235

Zhou JG, Causon DM, Mingham CG, Ingram DM (2004) Numerical prediction of dam-break flows in general geometries with complex bed topography. Journal of Hydraulic Engineering 130(4):332–340